A Thesis Submitted for the Degree of PhD at the University of Warwick

Permanent WRAP URL:

http://wrap.warwick.ac.uk/176385

warwick.ac.uk/lib-publications

An investigation into

The effects of mould temperature on injection moulded HDPE gear performance.

by

Patrick Zengeya

MSc (Software Development), PgDp (Advanced Manufacturing), BSc (Eng)

A thesis submitted in partial fulfilment of the requirements for the degree of Doctor of Philosophy in Engineering

University of Warwick, School of Engineering

July 2022

Table of Contents

_____

List of Figures

_____

List of Tables

_____

Declaration

_____

I declare that the work published in this thesis is my work under the supervision of Professor Ken Mao and Dr Vannessa Goodship, in the School of Engineering, University of Warwick, between 2018 and July 2022.

Any information derived from the work of others, whether published or not, has been acknowledged and referenced.

This thesis has not been submitted in any form for another degree or diploma at any university or other institution of tertiary education.

Nomenclature and Abbreviations

_____

Nomenclature

A   a constant

C_s Service factor

D   screw diameter [cm]

d   pitch circle diameter

d_p pitch diameter pinion

E   Young's modulus

F   normal force

F_t tangential tooth loading at the pitch line (tangential force)

F_w face width

K   specific wear rate

K temperature (°C)

M   gear module

M_n molecular weight

M_s shot weight [g]

m   speed ratio Ng/Np

n   number of gear teeth

ø   pressure angle

P   pitch circle

P_d diametral pitch

ρ   melt density [g/cm^3]

R   measure dimension

S   sliding distance

S_b bending stress

S_h surface contact stress (Hertzian stress)

T   cycle time [S]

TS   tensile strength

TS_∞ tensile strength at infinity

μ Poisson's ratio

V   wear volume

v   pitch line velocity

W_t transmitted load

Y   Lewis form factor for plastic gears, loaded at the pitch point

Abbreviations

ABS   Acrylonitrile Butadiene Styrene

HDPE   High Density Polyethylene

HPPE   high performance polyethylene

MRT   melt residency time (mins)

PA66   Nylon66

POM   Polyacetylene (Polyoxymethylene)

rpm   revolutions per minute

Publications

_____

The Effects of Cooling Rate on Injection moulded HDPE and PA66 Gears. Proceedings of the Eighth Annual Postgraduate Symposium 2021, School of Engineering, The University of Warwick, UK (first author), Mao K, Goodship V.

PENDING PUPLICATION:

The effects of mould temperature on injection moulded HDPE gear performance. Tribology Internal (Full copy attached with thesis submission)

Acknowledgements

_____

Abstract

_____

Polymers and polymer composite materials are emerging as viable front runner alternatives to metallic gears as they offer distinct advantages, such as good weight to strength ratios, the ability to run without external lubrication, less noise when running, and a lower coefficient of friction. Polymer gears undergo complex microstructural changes such as hysteresis, viscous flow, and elastic deformation which affect their performance capabilities to a greater extent compared to those of metallic gears. These differences mean that the failure of these gears differ to those made from metals. The wear behaviour and performance of polymetric gears has generated much interest from researchers over the past few decades, but to date there has been little focus on understanding the link between the input parameters used during the manufacturing process, and their corresponding physical and performance characteristics. This approach seems peculiar to polymer gears, as metal gears tend to be tested and graded not only by their material type, but also according to their mode of manufacture. Of particular importance during the manufacturing process for both metallic and polymetric gears, is the mould temperature (cooling temperature) of the molten material. Techniques such as quenching, annealing, or tempering, are used in metallic gear production to alter the cooling rate, which in turn alters the internal microstructure of the gear. The main objective in altering the cooling rates in metals is to increase strength, hardness, toughness, machinability, and ductility. Unlike metals, the effects of cooling rates on polymer composites are not well understood and documented. The complex microstructural changes which they undergo right from the manufacturing process to the point of operation, mean that better understanding as to how the input parameters employed during the manufacturing process determine their microstructural construct, and hence physical and performance characteristics.

During this study, HDPE gears were injection moulded using optimised input parameters which were obtained using a robust design of experiments based on the Taguchi method. These parameters were then held constant, while gears were produced at 22°C, 34°C, 50°C, and 65°C. The gears were grouped according to the mould temperature setting at which they were produced. Differential scanning calorimetry (DSC) analysis was carried out for the different temperature settings to ascertain how crystallisation was affected. The results showed lower crystallisation levels for the lower mould temperatures, and higher levels for the higher mould temperatures.

Gears produced at the same mould temperature were then meshed in a uniquely designed gear test rig. Torque loadings of 0.5 Nm, 1 Nm, 2 Nm, 3 Nm, and 4 Nm were applied at 500 and 1000 rpm, and

were run until they failed. A bespoke data logging system was used to record rotational cycles verses wear, and corresponding wear curves were produced. SEM analysis was then carried out to ascertain the topological mode of failure for gears produced at different mould temperatures. The presented results show a direct relationship between the different mould temperatures and the resultant microstructural changes, gear characteristics, and performance. Based on these wear rate responses to the application of varying torque loadings, a Mould to Torque Reference Chart for HDPE is presented.

CHAPTER 1
INTRODUCTION
_____

1.1 Overview

Gears are considered to be one of the oldest equipment known to mankind, with the earliest recordings of their use being in the 3rd century by the Greek mechanics of Alexandria [1]. They saw wide use in the Roman world in heavy-duty machines, such as mills and irrigation wheels, and in small-scale applications such as calendrical instruments and water-clocks. Early gears were made from wood with cylindrical pegs for cogs and were often lubricated with animal fat as grease.

Other early examples of their use can be traced back to China around the 4th century B.C [2], where they were used to lift heavy artifacts, and in water wheel machinery. Fig 1 shows examples of early gears.

There seems to be no literature available detailing any ground-breaking discoveries between the early recordings of gear use until the 17th century when the first attempts were made to provide constant velocity ratios. These attempts utilised the involute curve [3] and were the foundations of subsequent gear theory improvements.

In the 18th century, the industrial revolution in Britain triggered a rapid increase in the use of metal gears, which resulted in a new science of gear design and manufacture rapidly developing. This continued throughout the 19th century where there was greater emphasis on the development of gears capable of transmitting higher power at greater speeds. This led to a desire to understand gear tooth strength and develop a standard method of gear rating. In 1892, Wilfred Lewis [4] developed the Lewis bending equations, which became the basis of gear strength calculations. These equations are still being used today, with some modifications. From the early 20th century, metallurgical improvements increased the useful life of industrial and automotive gears. To date, the most significant developments in the science of gearing are in material developments.

Growing demands for a sustainable environment have increased the need to develop fuel saving solutions in gearing applications such as those found in vehicle and aircraft transmissions. This has led to a general desire for having light weight and energy efficient gearing systems which will help cut the global carbon footprint and save natural resources [5].

Fig 1.1 Examples of early gear artifacts [3]

In the automotive industry, the most favoured gear materials for gear manufacture are steel alloys or cast iron. These materials give the desired qualities, but it also gives them a high weight to strength ratio, which leads to power losses. Power losses in gear systems are associated primarily with tooth friction and lubrication churning losses. Frictional losses not only lead to power losses, but are one of the causes of vibration and noise. The magnitude of the frictional forces experienced in gearing systems are related to the gear design, the reduction ratio, the pressure angle, gear size, and the coefficient of friction. Good gear design and the use of lubricants can mitigate these forces but also tends to introduce other undesirable effects. Increasing the pressure angle, for example, will improve power transmission efficiency, but at the same time will increase gear wear and noise. It will also reduce the load carrying capacity of the gear.

The use of lubricates, on the other hand, will drastically reduce frictional forces, but will introduce churning losses. Churning losses are associated with the peripheral speed of the gears passing through the lubrication fluid used in gearing arrangements, and are dependent on such factors as lubricant viscosity and density. The depth to which the gears are immersed into the lubricant will also influence churning losses, as does the speed of rotation and applied load.

An alternative to metal gears are gears made from polymers or polymer composites. These gears are now positioning themselves as credible alternatives to traditional metal gears in a wide variety of applications. Until recently, the use of polymer gears has been restricted to low load, low torque applications [6], but with the continual improvements in strength and stiffness, polymer gears are now finding their way into applications which require the handling of high torques, high temperatures, and in harsh environments. Commercial publications, such as Engineering Materials [7], are reporting new high strength composite polymers, which can withstand high loads, and high torques. The publication names a composite polymer called polyaryletherketone, which is now being used in the transmission

of an all-terrain stand-on dual Tracked Vehicle (DTV). Another publication [8] names a composite of nylon reinforced with 30% carbon fibre fill, as having a maximum bending torque of 207Nm, which is equal to that of steel, and 1.5 times that of aluminium.

Polymer composites have the following advantages:

- ➢ They have excellent weight to strength ratios
- ➢ They are less noisy
- ➢ They can run without external lubricants
- ➢ They have a low coefficient of friction, which enables them to function without external lubrication
- ➢ They are less expensive to manufacture
- ➢ They have good elasticity which enables them to absorb shock and vibrations
- ➢ Lower inertia

The most popular polymers used in gearing are acetal (POM), acetal resins, nylon, polycarbonate, and polyesters. Within these polymers, there are variations in material formulations which enhance specific performance characteristics.

Various acetals are produced under trade names such as Delrin, Duracon, and Celcon [9]. Each of these brand name includes various formulations which manipulate the product's mechanical properties, such as adding lubrication, or improving their tensile strength. Similarly, there are various trade names for nylon including MC901, MC602ST, Nylaton GSM, and many others. The designation of a nylon type is determined by the number of methyl ethylene (CH_2) atoms on each side of the nitrogen atom in the polyamide chain. The nylons used for gearing are typically type 6, although type 12 is also known to be used [9]. Thus, Nylon 12 has 12 methyl ethylene atoms on each side, which indicates a higher degree of crystallization.

Although polyamides and polyacetals are widely used in gearing applications, other semi-crystalline materials such as polyether ether ketone (PEEK), and high-density polyethylene (HDPE), have shown good surface wear resistance when operating below certain critical loads [10]. HDPE has a relatively low tensile strength, flexural modulus, and melting temperature compared to other semi-crystalline materials, as shown in Table 1.1, but is advantageous to use in low load applications (below 4.6 Nm), due to its low coefficient of friction and low specific density. The low coefficient of friction property of HDPE gears enables them to have high cycles to failure, while their low specific density gives them a distinct weight to surface wear rate advantage.

Table 1.1 Properties of different polymer materials [10]

	HDPE	PC	POM	PA46	PEEK650
Specific density (g/cm^3)	0.96	1.20	1.42	1.18	1.3
Tensile strength (MPa)	23	66	70	105	155
Flexural modulus (MPa)	900	2400	2900	3300	3600
Coefficient of friction	0.1	0.31	0.21	0.28	0.21
Melting temperature (°C)	131	155	178	295	343

Despite these advantages, HDPE is not widely used in gearing applications due to the lack of published research data relating to performance under different environments and load settings. As such, there is hardly any design guidance for those wanting to use these gears. It is therefore important to carry out research which will improve understanding of the performance parameters of HDPE gears.

The development of polymer composites has dramatically increased the strength, toughness, and wear resistance of polymetric gears to levels which are close to those of metallic gears, as shown in Table 1.2.

Table 1.2 Comparisons between polymetric and metallic materials [8]

	Carbon fill	Steel	Aluminium	Glass fill	Nylon
Load capacity (MPa)	369.2	370.2	276.4	142.2	103
Density (g/cm^3)	1.28	7.85	2.7	1.23	1.16
Tensile strength (MPa)	255	660	260	140.2	88.3
Bending elasticity (MPa)	13.2×10^3	190×10^3	68.8×10^3	6.4×10^3	2.9×10^3

Gears made from polymers have different characteristics to those made from metals, such as the way they respond to induced stress at different temperature settings. These characteristics play an important role when considering gear choice. All engineering materials will have viscous, elastic, and plastic responses to stress, but the magnitude of the responses will depend on several factors such as material type, material density, and the rate of stress application. The stress-to-strain ratio (Young's modulus or modulus of elasticity (E)), variation in response to density for polymers, polymer composites, metals, and metal composites, is shown in Fig 1.1 [11]. It can be seen that the Young's modulus for polymer composites overlaps with that of many metals, but at much lower density.
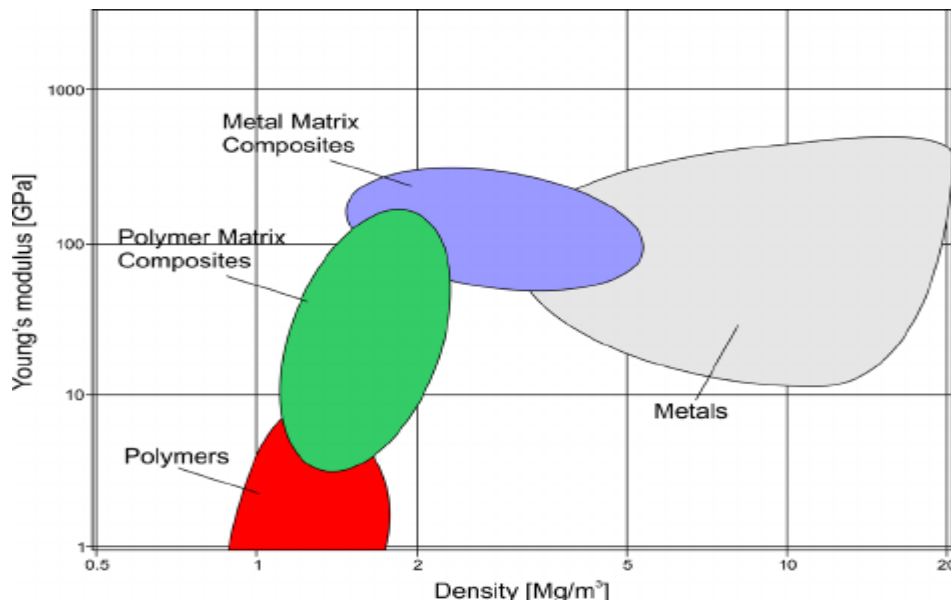
Fig 1.2 Variation of Young's modulus with density [11]

Despite the highlighted advantages, the use of polymetric gears in high power applications is still limited due to several factors, which include:

➢ Lack of in depth understanding of the wear behaviour of polymer gears due to the complex physical changes which they undergo

➢ Limited working temperature range

➢ Low thermal conductivity

➢ Moulded gears cannot hold the same high tolerances that metal gears can

An important hinderance to their use, is the fact that polymers are very sensitive to temperature variations. Their tensile strength, stiffness, and elasticity modulus tends to reduce as the temperature increases. Heat is generated through frictional forces and hysteresis as meshed gears run, but due to low thermal conductivity, this heat is not dissipated efficiently. The building up of heat leads to gear expansion, which in turn results in dimensional instability. Expanding meshed gears introduce transition errors, which have detrimental effects in transmission systems.

The failure of gears made from polymers differs from gears made from steel. An example of this difference is the fact that polymer gears fail through the melting of material, which does not occur with steel gears. It is therefore important to understand the types and nature of these failures to minimize them. This means that the design of polymer gears, must always take into consideration the increase in temperature caused by friction, pressure, and speed.

1.2 Research aim, objectives, and strategies

The aim of this research is to contribute to the understanding of how the mould temperature (cooling temperature) employed in the injection moulding production of HDPE gears affects the crystallization process, and how this in turn affects the physical characteristics of the gears.

To establish this, the objectives are:

- To produce high density polyethylene (HDPE) gears using injection moulding by first establishing optimised input parameters, and holding these constant while varying the cooling rate.
- To investigate the wear, mode of failure, and load handling capabilities of gears produced at differing cooling temperatures.
- To explore a framework/model which can be developed and used as reference to polymer gear qualities, based on mould temperatures used during manufacture.

To achieve this aim and the stated objectives, the research was conducted in two distinct stages.

The first stage was to manufacture the gears using an Engel Victory 60T machine. An elaborate process based on the Taguchi design of experiment was used to ensure that all input parameters were optimised, so that they did not become 'noise' when mould temperatures were varied. The variation of the mould temperatures was achieved through chillers which pump coolant via hoses into the mould cavities. (Covered in Chapter 3).

The second stage of the research involved running tests on gears produced at different mould temperatures, at differing torques and speeds. Torques ranging from 0.5 Nm to 4 Nm, were applied at 500 rpm and 1000 rpm. The testing was done using a novel non-metallic gear test rig developed by the University of Warwick. The rig measures the gear wear rate and performance by applying a constant torque and measuring the resultant displacement. A bespoke data logging software monitors and records the gear wear as a function of time.

To investigate the effects of mould temperature on wear, mode of failure, and torque handling capabilities, the gears were grouped according to the mould temperature employed during their manufacture. Pairs of the same group were then meshed and tested. DSC analysis was carried out before the tests, to determine the level of crystallinity for each group. SEM analysis was then conducted on the worn gears to ascertain the mode of failure at microstructural level.

1.3 Thesis overview

The structure of this thesis consists of seven chapters summarised as follows:

Chapter 1 gives a brief history of gears, and the need for new energy efficient gearing. It highlights the advantages and disadvantages of polymer gears. A table showing a comparison of different material properties is presented.

Chapter 2 starts by introducing the basic gearing principles, before moving onto the injection moulding process. The science behind polymers and polymer composite structures are explained before going into in-depth review of previous work done into polymetric gear wear, and what influences it. The chapter then concludes by critiquing the highlighted work and puts forward the necessity of this research.

Chapter 3 explains the design of experiment (DoE) employed in this work and why it was chosen. The properties of the polymers used are shown and a brief description of why the material was chosen. It then moves into the equipment used to produce, test, and analyse the gears.

Chapter 4 deals with the practical steps taken in producing the gears using injection moulding. Ideal input parameters are obtained using the Taguchi design of experiments, and these are held constant while the mould temperature is varied from 22°C to 65°C. An in-depth discussion of the process and results then follows.

Chapter 5 is an explanation of the processes involved in wear testing of HDPE gears. Gears are tested for wear at different torque loadings and rotational speeds. The wear test results are then presented.

SEM results showing the mechanisms of failure according to differing cooling temperatures are also presented.

Chapter 6 is an in-depth compilation and analysis of the test rig wear rates and SEM results are presented in this chapter.

In Chapter 7, conclusions are drawn as to what effects cooling rates employed in the injection moulding process have on wear rates for HDPE. Recommendations for future work are then given.

CHAPTER 2

LITERATURE REVIEW

_____

2.1 Introduction

As mentioned in the introduction section, polymer gears offer distinct advantages over their metal counterparts, and this has caused a growing interest in the science behind polymers and their performance parameters. Published work has so far mainly focused on understanding the following factors:

• The effects of injection moulding input parameters on the characteristics of produced products

• The wear behaviour of meshed polymer gears

• The effects of temperature changes

• Modes of failure

• The effects of varying loads and speeds on gear arrangements

• The introduction of external lubricants

It is difficult to obtain accurate figures relating to the exact number of published material relating to polymetric gearing, but Singh et al [12] reported a steady increase since 2000, with an average of 5 papers being published between that year and 2016.

2.2 Gear Principles

A gear is a toothed wheel which works in conjunction with other toothed wheels, to transmit motion or power, by altering the relation between the speed of a driving mechanism (such as an engine), and the speed of the driven parts (such as wheels). They give mechanical advantage to power producing units. Other methods of power transmission include belt, chain, or rope drives.

Power transmission drives can be classified in several ways, such as engagement drive, friction drive, or flexible drive [12]. In engagement drives, power is transmitted by means of successive engagements

and disengagements, as is the case in gear and chain drives. In friction drives, power is transmitted by means of friction force between two mating parts, as is the case in belt and rope drives. Flexible drives consist of an intermediate flexible element between the driving and driven shafts, such as in belt, chain, or rope drives.

Mechanical drives can also be classified according to whether they provide constant velocity ratio [13]. A constant velocity ratio is achieved when there is no slip, creep, or polygonal effects between the driving and driven shafts. This is referred to as a positive drive. Only gear drives satisfy these conditions, and as a result, they have higher transmission efficiency (usually above 99%), higher transmission speeds, higher power transmission, and higher service life [13].

Gears need to have high tensile strength to prevent failure against static loads, high endurance strength to withstand dynamic loads, low coefficient of friction, and ease of manufacture.

There are many different types of gears such as spur, helical, bevel, hypoid, worm, rank and pinion, sprockets, and harmonic gears. The easiest way of categorising them is through the way the gear axes intersect. If the gears are to operate on parallel axes, then spur or helical gears are required. If the axes are intersecting at right angles, then bevel and worm gears are used. If the axes are both nonintersecting and nonparallel, then crossed-axis helical worm gears, hypoid, and spiroid gears are used [13].

The most common types of gears are spur, helical, and worm gears [14]. Spur gears are cylindrical in shape, with the flank of the gear tooth parallel to the gear axis. Fig 2.1 shows the interaction of two spur gears, and the nomenclature used in gear design. The mentioned terminologies will be used throughout this work. Each pair of test gears will have a driving and driven gear, with a 1:1 ratio.

Spur gears impose only radial loads on their bearings, and will operate on a variety of centre distances, making them relatively easy to mount.

If the teeth of a spur gear point away from the axis, the gear is an external spur gear, and if they point towards the axis, the gear is an internal spur Fig 2.2(a).
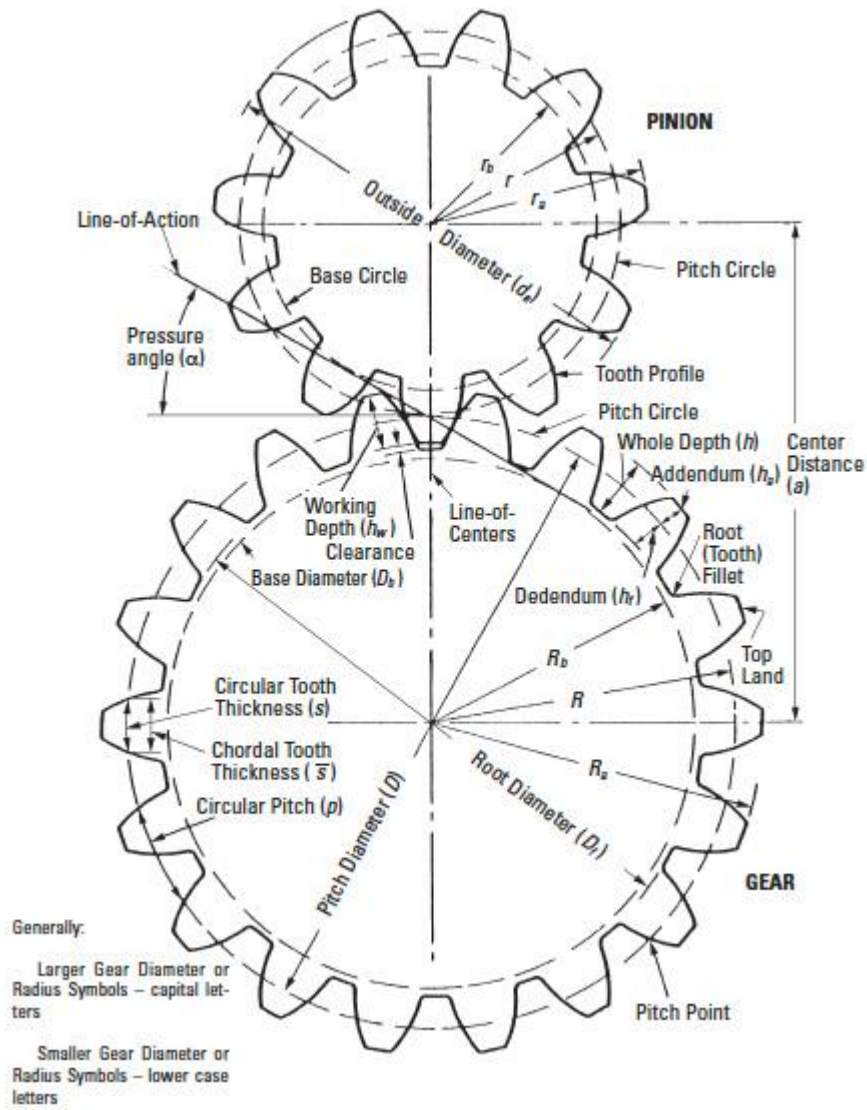
Fig 2.1 Spur Gear geometry [14]

(a)   (b)
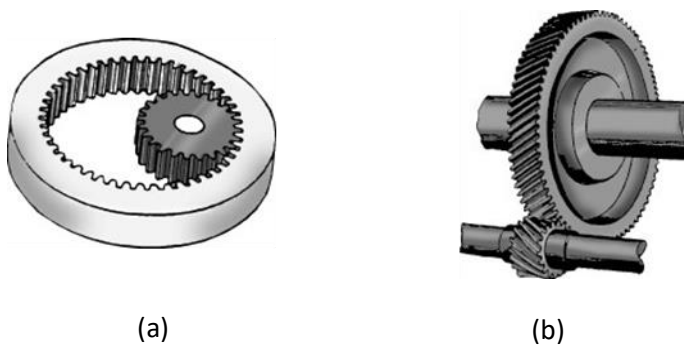
Fig 2.2 (a) Internal Spur Gear (b) Helical Gear

A helical gear is similar to a spur gear, but the tooth flank is at an angle to the axis of the gear, Fig 2(b). Helical gears are used when both high speed, and high loads are involved, but they impose both radial and thrust loads. They do, however, run quieter and smoother than spur gears.

2.3 Gear design analysis

The most important part of a gear are the teeth. The teeth determine the gear module (M):

$$M = d/n \hspace{4cm} (2.1)$$

where: d = pitch circle diameter; n = number of teeth.

To have a smooth and continuous tooth action, one pair of teeth must cease contact as succeeding pair of teeth come into engagement. Increasing this overlap improves gear performance as it distributes the load to adjacent teeth and the load experienced per tooth is reduced [15]. The amount of overlap is the contact ratio. Good gear design dictates that a minimum contact ratio of 1.2 should be maintained [16].

The pitch circle, P, is a theoretical cycle which intersects with a meshing gear pitch circle at a point referred to as a pitch point.

$$P = \pi d/n \hspace{4cm} (2.2)$$

Tooth profile which is located outside the pitch circle is called the addendum, while the inside part of the tooth is called the dedendum.

Gear teeth incline at an angle called the pressure angle. The pressure angle is the angle between the line of action and the line tangent to the pitch circles of mating gears [17], as shown in Fig 2.3. Most designers use a 20° pressure angle [18], but 22.5° and 25° are also common. Pressure angles above 20° give higher load capacity and good wear resistance characteristics, but do not run as smoothly or as quietly.
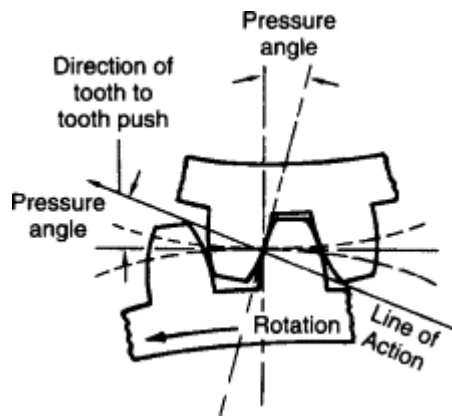
Fig 2.3 Relationship of the pressure angle to the line of action [17]

Meshing gears experience two main forces: bending and contact stress.

2.3.1 Bending stress

The tooth of any gear is, in effect, a cantilever beam supported on one end. The contact tries to bend and shear the beam from the rest of the material. These bending forces lead to failures through tooth breakage due to static loading or fatigue action.

The bending stress on a gear tooth of a standard tooth form loaded at the pitch line can be calculated using the Lewis Equation [19, 20]:

$$S_b = \frac{FP_d}{fy} \qquad\qquad (2.3)$$

where S_b = bending stress; F = tangential tooth loading at the pitch line; P_d = diametral pitch; f = face width; y = Lewis form factor for plastic gears, loaded at the pitch point.

The Lewis bend equation can be modified to consider other variables, such as in the incorporation of the pitch line velocity and service factor.

$$S_b = \frac{HP55(600+v)P_d Cs}{fyv} \qquad\qquad (2.4)$$

where HP = Horsepower; C_s = Service factor; v = pitch line velocity.

2.3.2 Contact stress

The next set of forces acting on the tooth surface are contact forces. Contact between interacting surfaces mainly occurs through two ways: conformal contact, and non-conformal contact [21]. Conformal contact occurs when contact is over an extended area, such as between discs. The test pieces are shaped accordingly to allow full-face contact. Non-conformal or counter-formal occurs when contact is made nominally at a point or along a line. It must be noted, however, that extended wear can lead to conformal contact.

When gear teeth are in mesh, non-conformal line contact is made. This results in the generation of frictional forces along the line of contact, which in turn induce stress. This non-conformal contact can be split into two components: rolling and sliding contact. The magnitude of each component varies throughout the cycle and is different for the driving and driven gear.

The slip ratio is the ratio of sliding velocity to average rolling velocity and is often used to describe contact conditions at the point of contact.

Beginning of contact

(a)

End of contact

(b)
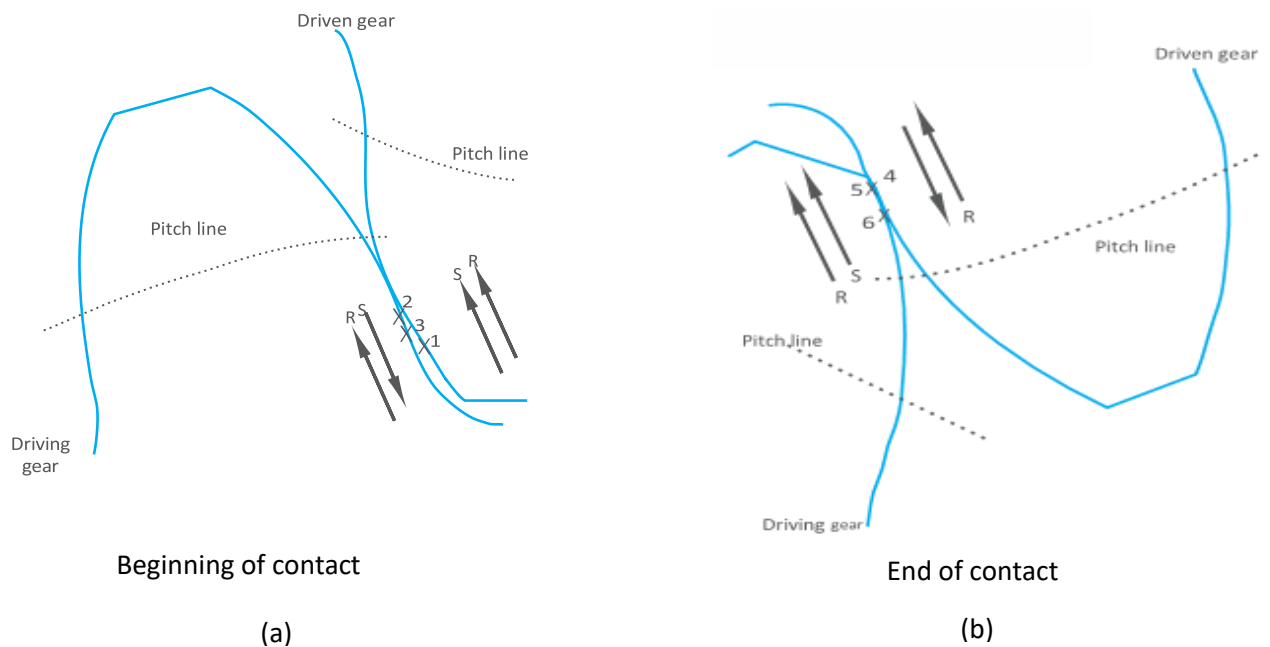
Fig 2.4 Gear teeth interaction

As the teeth first come into contact, there is an initial contact loading. Using Fig 2.4(a), point 1 on the driving gear is under compression from the rolling action towards the pitch point, and under tension due to frictional resistance to the sliding motion away from the pitch point. The arrows marked R show

the direction of rolling and the arrows marked S show the direction of sliding. This combination of forces cause surface cracking, surface fatigue, and heat build up. As the gears continue to move, the sliding forces change direction at the pitch line, and at this point, there is no sliding Fig 2.4(b). This is the point of highest loading for the tooth, and as result, is a point of high fatigue failure, severe surface deterioration, and heat build-up [14].

The surface contact stress enduced by the meshing teeth can be calculated by employing modified notation into an equation first proposed by Hertz et al [22].

$$S_h = \sqrt{\frac{W_t}{f d_p} \cdot \frac{1}{\pi \left(\frac{1-\mu^2_p}{E_p} + \frac{1-\mu^2_g}{E_g} \right)} \cdot \frac{1}{\frac{\cos\varnothing \sin\varnothing}{2} \cdot \frac{m_g}{m_g+1}}} \qquad (2.5)$$

where: S_h = surface contact stress (Hertzian stress); W_t = transmitted load; d_p = pitch   diameter pinion; μ = Poisson's ratio; E = modulus of elasticity; $\varnothing$ = pressure angle; m = speed ratio, Ng/Np; n = number of teeth;

Gupta et al, [23], argues that the contact stress produced in mating gears, is one of the most important factors in the design of gears, as it determines the dimensions of the gear teeth, or gear module. In spur metal gears, a high module is the best choice for transmitting large power between parallel shafts. This is because tooth root strength increases (due to an increase in width) as the module increases. In polymer gears, it is the polymer type used which determines whether it is desirable to have a high module, or a high contact ratio. Gupta et al [23], discovered that for polymers which are deemed less strong, such as elastic thermoplastics, a small module is preferred (contact ratio increased, and several teeth engage simultaneously). For hard thermoplastics, a larger module is preferred.

2.4 Fundamental Law of Gear-Tooth action

The velocity (speed) at which the process described above occurs, is of particular importance to this research, as it is varied and the corresponding change in polymer gear wear is assessed.

Referring to Fig 2.5, the driving gear has a velocity, V_1, and the driven gear, V_2, at point K. The surface tangent velocity component for the driving gear is V_{1t}, and that for the driven is V_{2t}. The difference

between V_{1t} and V_{2t} (V_{1t} - V_{2t}) gives the sliding velocity direction, which is tangential to the surface contact [14]. It is constantly changing, and is maximum at the beginning and end of contact. It is zero at the pitch point.

V_1 and V_2 are equal in both magnitude and direction along N_1N_2 otherwise the two profiles would separate.

$$O_1N_1 . w_1 = O_2N_2 . w_2 \qquad\qquad (2.6)$$

which can be rearranged to:

$$\frac{w_1}{w_2} = \frac{O_2N_2}{O_1N_1} \qquad\qquad (2.7)$$

At the intersection of tangent N_1N_2 and O_1O_2 is point P (pitch point):

$$\Delta O_1N_1P \sim \Delta O_2N_2P$$

The relationship between the angular velocities of the driving gear and driven gear, or velocity ratio, of a pair of mating teeth is:

$$\frac{w_1}{w_2} = \frac{O_2P}{O_1P} \qquad\qquad (2.8)$$
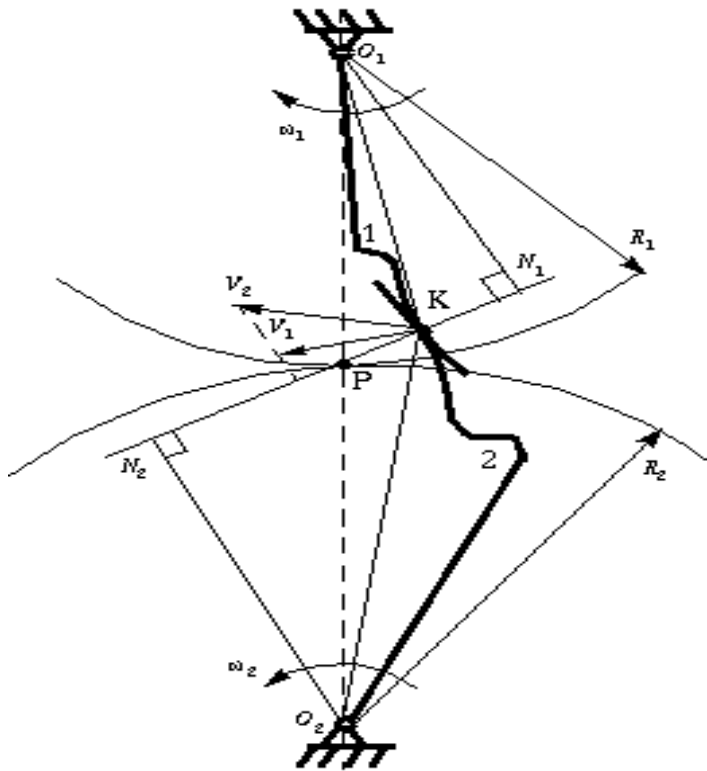
Fig 2.5 Meshing teeth profile [24]

The pitch point, P, is very important, and the Fundamental law of gear-tooth action [25] states that:

> "The common normal to the tooth profiles at the point of contact must always pass through a fixed point (the pitch point) on the line of centres".

2.5 Polymers and their classification

A Polymer (or plastic) is a substance which contains many molecules called monomers. These monomers join in a reaping way to form long chains which are held together by covalent bonds [26]. A polymer formed from a single type of monomer is referred to as a homopolymer, while that formed of a mixture of two or more monomers of suitably reactivity, are referred to as copolymers [27]. This linking up of monomers happens through a process called polymerisation. Polymerisation occurs through two major processes: condensation and addition polymerisation. In condensation polymerisation, the molecular linking process results in the elimination of smaller molecules such as H_2O or CH_3OH. In addition polymerisation, the polymer is formed without the loss of other molecules.

Both processes of polymerisation will cause the monomers to form links which can be classified as linked, branched, or cross-linked polymer chains. These polymer chains influence the characteristics of the resultant polymer. Depending on the type of link, polymers can be classified as thermoplastics, thermosets, or elastomers. Fig 2.6.

Monomers

↓

Polymerisation

↓

Polymers
(Resins)

Rubbers   Textiles

Adhesives   Paints

Plastics
$(E\sim I - 10GN\ m^{-2})$

Thermosets   Thermoplastics   Elastomers
(Crosslinked, rigid)   (Uncrosslinked, heat reversible)

Semi-   Crystalline   Amorphous
crystalline
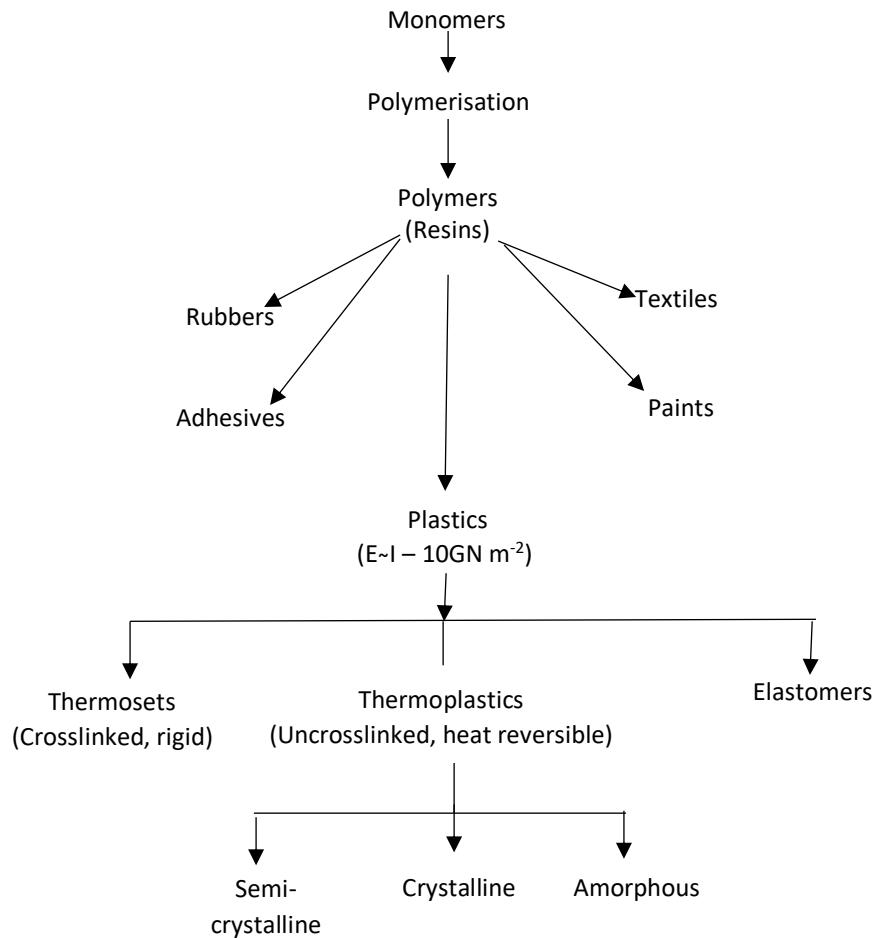
Fig 2.6 Polymer classification

2.5.1 Elastomers

Elastomers have molecular chains with a low degree of crosslinking. This gives them the ability to deform substantially through stretching, compression, or torsion, and then return to their original shape after the removal of the force causing the deformation. Examples of elastomers include silicone, natural rubbers, polyurethanes, and polybutadiene.

2.5.2 Thermoplastics

Thermoplastics are formed by long chains of monomers which are not crosslinked and held together by weak van der Waal forces. This allows them to soften, and eventually melt when subjected to high temperatures. Depending on how tightly packed joined-up monomers are, polymers can be referred to as crystalline, semi-crystalline or amorphous polymers [28].

In crystalline polymers, the molecules pack together tightly. The resulting polymers are rigid, have high melting points, and are affected less by solvent penetration. Crystallinity makes a polymer strong, but also lowers their impact resistance.

Polymers can also be classified as being amorphous. In these types, the molecules form branches or irregular independent groups which do not act together regularly to form crystals. Amorphous polymers are softer, have lower melting points, and are penetrated more by solvents, than their crystalline counterparts. Polymers can also be classified as being semi-crystalline. These polymers have both crystalline and amorphous regions. Semi-crystallinity is a desirable property for most plastic applications, as they combine the strength of crystalline polymers with the flexibility of amorphous. Semi-crystalline polymers can be tough with an ability to bend without breaking.

2.5.3 Thermosets

Thermoset monomers have a high cross-linked structure which is joined together by covalent bonds. This structure makes them resistant to heat softening and gives them higher mechanical and physical strength in comparison to thermoplastic materials. An important characteristic of a thermoset material is the gel point. The gel point represents the temperature at which the irreversible viscous-liquid state changes to a solid state during the curing process. Past the gel point, the material stops flowing and cannot be formed again.

Both thermoplastics and thermosets are used in gears, but thermoplastics are by far the most used [16].

2.6 Polymer Composites

A composite material is a material which is made up of two or more distinct materials [29]. Fibre-reinforced polymers (FRP), or Fibre-reinforced plastics are composite materials made from polymer matrix reinforced with fibres, or other particles. The fibres used are usually glass, carbon,

thermoplastic or thermosetting resin, and aramid. Other fibres such as asbestos, wood, or paper have sometimes been used [27]. The polymer is the matrix and the fibres or particles dispersed within it are referred to as the reinforcement. The reinforcement is usually stiffer than the matrix, thus stiffening the composite material. This reinforcement mechanically enhances the strength and elasticity of the polymer, depending on the mechanical properties of the fibre and matrix, their volume relative to one another, fibre length and orientation with the matrix [30]. Table 2.1 shows how different attributes of nylon 66 (PA66) are affected by different fibre reinforcements.

Table 2.1 Comparison of reinforcing fibres in a nylon 66 matrix [31]

Property	Units	Unfilled	30% glass fibre	30% Carbon fibre	15% Aramid fibre
Shrinkage	% (flow/trans)	1.5/1.8	0.40/1.5	0.08/0.56	0.02/0.03
Tensile strength	psi/MPa	12000/83	24000/165	38600/266	1400/97
Flexural modulus	ksi/GPa	410/2.8	1370/9.4	2720/18.8	560/3.9
Coefficient of friction	Static/dynamic	0.55/0.65	0.57/0.11	0.30/0.32	0.75/0.73
Wear factor	10-10in5-min ft.-lb.-hr..	200	75	36	19

The tensile and compressional properties of reinforced polymers are mainly influenced by interfacial adhesion between the matrix and the fibres [32]. Lack of adhesion between the matrix and fibre can lead to undesirable properties, such as weakening of the composite. Ku et al [32] points out that it is sometimes necessary to modify the fibre surface by employing chemical modifications to improve the adhesion between fibre and matrix. In their published paper, the authors noted that the tensile strength of fibre reinforced polymer composites increased with fibre content, up to a maximum, or optimal value. After this point, the strength drops. They also found that the Young's modulus of the fibre reinforced polymer composites increased with increasing fibre loading. It is therefore important to select an optimum level of reinforcement which corresponds to specific demands for which the composite material is required to fulfil.

In addition to being able to select the optimum level of reinforcement, Senthilvelan et al [33] noted that the type of material used in the reinforcement of polymers, and the process of manufacture directly affects the way they fail. In their research, the authors investigated the various types of

failures exhibited by unreinforced, and fibre reinforced Nylon 66 gears. They discovered that reinforced gears exhibited longer life compared to unreinforced gears. The reinforcement affected the strength, ductility, thermal conductivity, and creep resistance of the composite. Furthermore, the amount of reinforcement fibre, the fibre orientation, aspect ratio, and the fibre/matrix interphase strength also influence the failure mechanism of the polymer composite.

Pogacnik [34] studied gears produced from PA6 and reinforced PA-GF30, and was able to show that glass reinforcement improved robustness of the gears. PA-GF30 gears exhibited a lower gear bulk temperature as a result of lower heat generation of the sliding surfaces and better heat dissipation. However, at high loads, the advantages gained by reinforcement are lost if it is in a pair with tribologically incompatible reinforced material, in this case PA6-GF30/PA6-GF30. The reduced lifespan was due to a high coefficient of friction generated by higher temperatures. This improvement in performance was also noted by the work done by Mahsenzaden et al [35], who analysed the mechanical and gear performance of POM reinforced with 3% nano-$CaCO_3$ and reported a 61% drop in the wear rate compared with the unreinforced POM.

Mao et al [36], conducted experimental investigations into the wear performance of non-reinforced POM and 28% glass fibre reinforced (GFR) POM, and noted a 50% increase in the load carrying capacity of 28% GFR compared to the non-reinforced. The crystallinity of the non-reinforced POM was initially higher than that of the 28% GFR but showed a 20% drop during the tests. The reinforced POM crystallinity was unchanged. It can be inferred from this observation that reinforcement of POM produces stable morphology, which in turn leads to better performance.

An alternative to conventional fibre reinforcements such as glass, aramid, or carbon, are natural fibres. Natural fibres are categorised as being either animal-based, or plant-based [37]. An example of animal fibre is wool or silk, while those for plant-based include sisal, coir, ramic, jute and bamboo. Natural fibres are attractive due to their low cost, high specific strength, non-abrasive, eco-friendly, and bio-degradable qualities [32]. They possess long aspect ratios which results in efficient stress transfer, and some qualities of their mechanical properties are comparable to existing inorganic glass fibres [38]. Studies have shown that natural fibres such as sisal fibre, kenaf fibres [39], and hemp fibres [40], show a marked improvement in thermal stability, increase tensile strength, elastic modulus, and flexural strength compared to nonreinforced polymers. Work done by Nishino et al [41] showed that the mechanical strength and thermal properties of kenaf composites are superior to other types of natural fibre polymer composites. This makes it suitable for high performance applications, and there have been suggestions that it can eventually supplement, and substitute petroleum based composite materials in many of the known industrial applications [42, 43].

Natural fibres, however, have several disadvantages, such as higher degrees of moisture absorption, lower impact resistance, and poor fibre/matrix interfacial adhesion [44, 45, 46], but these can be overcome through chemical treatments or compatibilizers, which amend the adhesion between fibre and matrix, or through hybridization with natural or synthetic fibres [47].

2.7 Polymer gear manufacture

Polymer composite gears can be manufactured through a variety of processes, such as casting, forging, extrusion, powder metallurgy, injection moulding, and blanking. Each process of manufacture will produce unique final products, and so it is important to understand the science behind the production.

In this research, injection moulding was used to manufacture high density polyethylene (HDPE) gears. An analysis of the process follows below.

2.8 Injection Moulding

Injection moulding is one of the most common methods of polymer manufacture. It accounts for around a quarter of all plastic production and processing in the UK, and about a third globally [48].

Injection moulding is regarded as having the highest efficiency, largest yield, and highest dimensional accuracy among all the processing methods [49]. It is cost effective and is used to produce complex-shaped parts quickly and at high volumes [18]. Agrawal et al [50], argues that one of the main reasons why injection moulding has become so popular is because it is a dynamic as well as a cyclic process. It is dynamic because the output (product) condition, determine the input variables in a time cumulative manner. It is cyclic because of the repetitive nature of the process.

Since the 1960's, several authors [18, 51, 52, 53, 54, 55] have studied injection moulding and its associated processing parameters. Although Bryce [55] identified over 200 processing parameters which can influence the injection process, these can be grouped into four major categories using a concept outlined by Ishikawa [56]. In general, these processing parameters can be grouped into four basic categories: temperature, pressure, time, and distance, as shown in the Ishikawa diagram in Fig 2.7.
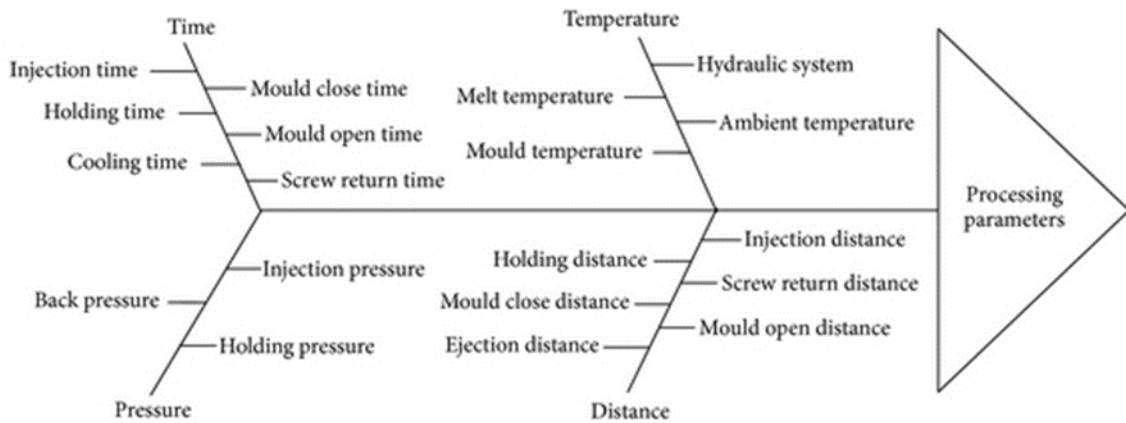
Fig 2.7 Ishikawa diagram of processing parameters in injection moulding [56]

2.8.1 Injection moulding process

Injection moulding involves the feeding of raw material through a hopper, which is attached to a heating barrel. The heating softens (plasticises) the material into a molten state before injecting it into a mould cavity, where it cools and hardens to produce the desired shape.

There are several design types of injection moulding machines [57, 58], and they are primarily classified by the type of driving system they use. The main driving system can either be hydraulic, mechanical, electrical, or hybrid. Hybrid type machines are most widely used as they take advantage of best features of both the hydraulic and electric.

A typical hybrid injection moulding machine can be split into two main units: the clamping unit, and the injection unit, Fig 2.8.
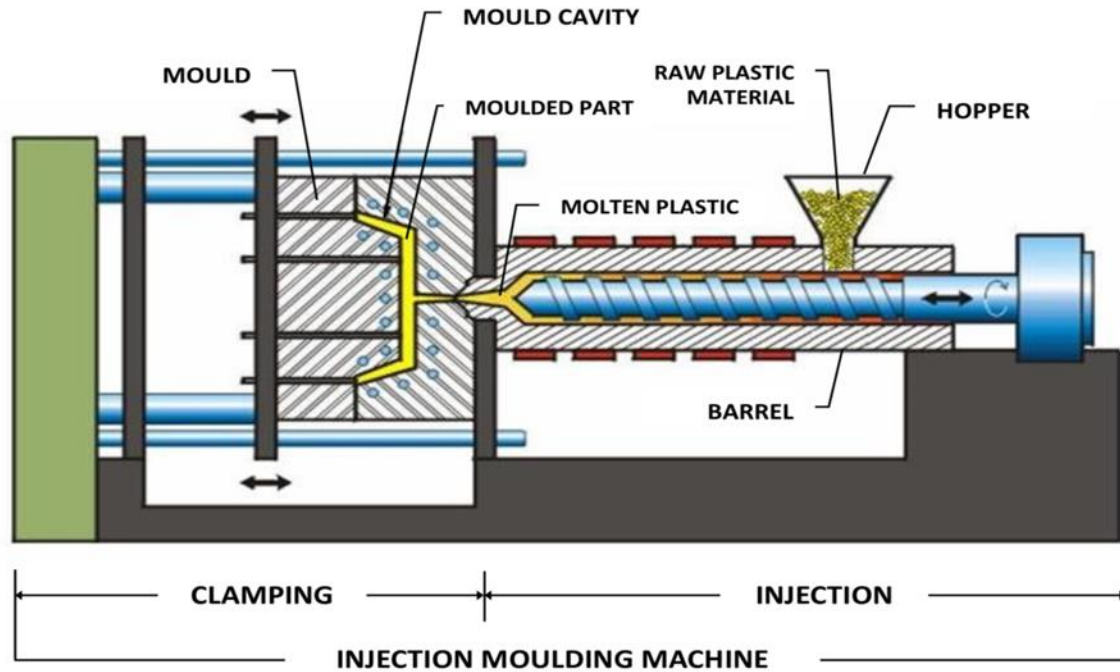
Fig 2.8 Typical injection machine [59]

The clamping unit carries the mould and performs the following functions:

➢ Holds the mould halves securely and in accurate alignment

➢ Opens and closes the mould quickly in a controlled manner

➢ Exerts enough clamping force to ensure that the mould remains closed as the molten material is injected

➢ Ejects the moulded component once the mould opens

There are several forms of clamp units which are in widespread use, but the two most common systems are the direct hydraulic clamp unit, and the toggle lock system [54]. The direct hydraulic system has a large hydraulic cylinder which is directly attached to the moving platen on which one half of the mould is mounted. The other half is attached to the fixed platen. The fixed and moving platens are linked by moving tie bars which provide the support and alignment between them.

The injection unit assembly consists of:

➢ A hopper to feed in raw material

➢ A plasticising unit, which consists of an Archimedean screw to convey and heat the material. Plasticising units can either be single stage plunger units, two stage screw-plunger units, or in-line screw reciprocating units

➢ A method of rotating the screw, to give adequate torque to convert the plastic into its molten state

➢ A method of injecting the molten plastic material into the mould

The injection unit must be capable of:

➢ Advancing and retracting the carriage to bring the nozzle in contact with the sprue bush of the mould

➢ Generating pressure between the nozzle and sprue brushing

➢ Rotating the screw during the feeding stage

➢ Allowing axial motion of the screw or plunger during injection

➢ Build up hold pressure

The injection moulding process can be divided into five main stages: loading and plasticisation, injection, clamping, holding and solidification, and ejection [60].

Stage 1: *Loading and plasticisation*

Raw material is loaded through the hopper and is driven through the heated barrel by a rotating screw. Frictional forces produced by the rotating screw also increase the melt temperature.

State 2: *Injection*

During this stage, the melt is forced into the mould as a result of the screw being forced forward by a hydraulic ramp action. The volume of material which is injected is called the 'shot', and the injection time/fill time is finished when 95-99% of the mould is filled. The injection pressure usually ranges from 35-140 MPa.

Stage 3: *Clamping*

This is the process in which the two halves of the mould are closed together before melt is injected into it. The clamp force must be sufficient to hold together the two halves of the mould as melt is

injected. Injection moulding machines are often classified by the maximum clamping force which the machine can provide.

Stage 4: *Holding and solidification*

With the completion of the injection stroke, pressure is maintained by the screw to compensate for material shrinkage as cooling of the material occurs, until the gate freezes. The applied pressure is referred to as the hold pressure, and the length of time it is held is called the hold time. The wall thickness of the part and the thermodynamic properties of the plastic determine the cooling time.

Stage 5: *Ejection*

This is the last stage of the process in which the moulded part is ejected by the opening of the mould.

2.9 The effects of input parameters during the injection moulding process

Material selection, mould designs, and processing parameters, all interact to determine the quality of the product during the injection moulding process [61]. It is therefore important to ensure that careful consideration of these factors is made, otherwise numerous production problems such as high scrappage rates and long lead times, could reduce the highlighted benefits offered by injection moulding.

The Ishikawa diagram shown in Fig 2.7 has grouped all identified input parameters into four main categories of temperature, time, pressure, and distance.

2.9.1 Temperature

Temperature is an important variable in injection moulding. Each stage of the process requires different temperature values. Of importance is the barrel temperature, melt temperature, nozzle temperature, and the mould temperature.

2.9.1.1 Melt temperature

Melt temperature is the actual temperature of the polymer as it exits the nozzle and enters the mould. Melt temperature is one of the most fundamental variables in the injection moulding process [52] and needs to be continuously controlled and held to a specific level. Bozzelli [62] points out that too high

a melt temperature may destroy the UV or antioxidant stabilizers used in polymer manufacture, whereas too low a temperature could cause damage to the screw tip, or unmelts may flow through the barrel and mould.

Speke [52], states that a change in the melt temperature affects several variables such as melt flow rate, the nozzle pressure, the cavity pressure, the final molecular weight, and the quality of the produced product. He conducted an experiment involving parts moulded in polypropylene using different melt temperatures. He discovered that parts produced at a melt temperature of 204°C had a measurably higher average molecular weight than parts produced at 249°C. This translated into better impact resistance as well as lower energy consumption in moulding and a shorter cycle time.

2.9.1.2 Mould temperature

The mould temperature (cooling temperature) has a direct influence on resultant physical characteristics of polymer products. Cartledge et al [63], carried out experimental investigations into the effects of thermal processing on microstructures of glass filled PA6 composites. Results showed that crystallinity increased as the cooling rate was increased from fast to slow. This observation was subsequently collaborated by the work done by Apichartpattanasiri et al [64], who carried out an investigation into the wear behaviour of injection moulded PA66 discs using different mould temperatures ranging from 30°C to 90°C. He observed that different microstructures were obtained by altering the mould temperature. A cross section of the discs showed a non-spherulitic skin followed by a transition region spherulite core. They observed that the spherulite size at a given distance from the skin was depended on the mould temperature, and that in general, the higher the mould wall temperature, the bigger the spherulites. The discs were then examined for wear at different slip ratios, Fig. 2.9. At low slip ratios (0-4%), both the wear rates and friction coefficient for 30°C and 90°C specimens were not different. At higher slip ratio (8.5%), the authors observed that there was an initial 5 times higher wear rate for discs produced at 90°C mould wall temperature compared to those produced at 30°C. The difference in wear rate, however, decreased with time and became stable in the final stages. At this stage, there were no significant differences observed between wear rates for different mould temperature. Using SEM, the authors conducted topological studies which suggested that delamination and surface cracking were the wear mechanisms at 0 and 4% slip ratio, while at 8.5% slip ratio, the wear mechanism changed from surface cracking initially to adhesion in the final period.
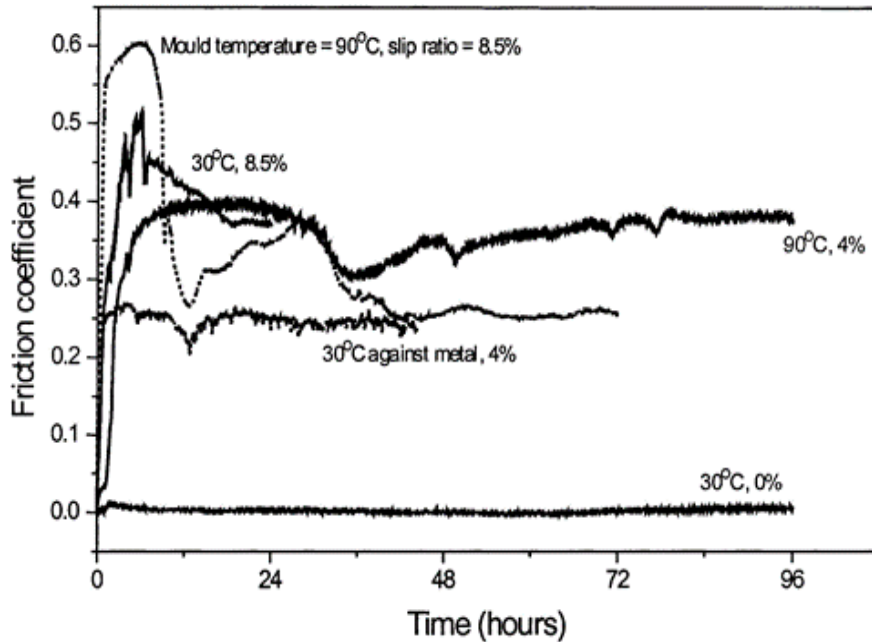
Fig 2.9 Friction coefficient against time and at different slip ratios [64].

The work done by Apichartpattanasiri et al [64], is supported by the findings of Russell et al [50], who carried out a number of studies on injection moulded PA66, and found that an increase in mould temperature increased crystallinity and established a skin-core morphology which increased with mould temperature. This led to an increase in yield strength, but a reduction in toughness. They were able to show that the strain-rate within the crystals was responsible for the slight increase in yield strength, but for a significant decrease in toughness. This finding mirrors that of Woodward [66], as shown in Fig 2.10.
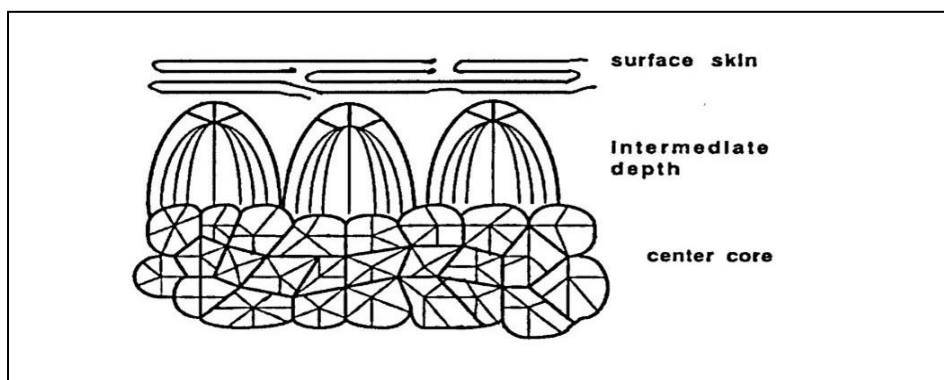
Fig 2.10 Microstructure of crystalline injection moulding [66]

27

Zhuang et al [67] showed that varying the mould temperature of PEEK during the injection moulding process produced glassy or crystalline parts. In general, cold moulds produce glossy parts, and hot moulds, crystalline parts.

Further work which was carried out by Speke [52], noted that mould temperatures had profound effects on the final properties of different polymers. In amorphous polymers such as acrylonitrile butadiene styrene (ABS), and polycarbonate, higher mould temperatures produced lower levels of moulded-in stress, and consequently better impact resistance, stress-crack resistance, and fatigue performance. Additionally, Speke found that in semi-crystalline materials, the mould temperature was an important factor in determining the degree of crystallinity in the polymer. The degree of crystallinity governs many performance parameters, including creep resistance, fatigue resistance, wear resistance, and dimensional stability at elevated temperatures. Crystals can form at temperatures below the melting point, but not above the glass-transition temperature (Tg) of the polymer. Speke adds that when moulding semi-crystalline materials, the ideal mould temperature should be above the Tg, in order to give the polymer adequate time to crystallize.
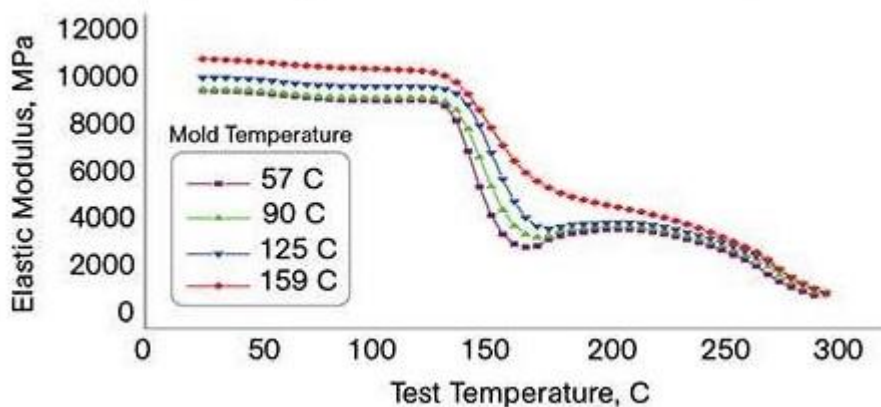
Fig 2.11 Effects of mould temperature on Modulus Vs Temperature for PA (51)

Fig. 2.11 shows the results of Speke's experiments as he compares the behaviour of a high-temperature nylon (PA), when moulded at the right mould temperature, and at the lower mould temperatures. It shows that as the mould temperature increases, the stiffness of the material at room temperature also increases. The most significant difference between the samples moulded at the proper temperature and at lower mould temperatures can be seen at elevated test temperatures. As the material approaches the glass-transition region at 130°C to 140°C, the modulus begins to decline in material moulded at lower temperatures and falls further and faster at even lower mould

temperatures. Speke concludes by stating that the best results are obtained when higher mould temperatures are combined with lower melt temperatures. This behaviour is characteristic of all polymers. Unfortunately, this is the opposite of what is usually found on the production floor, where, typically, melt temperatures are running higher than is ideal because melt temperature is often considered to be the only available tool for reducing the melt viscosity. Higher melt temperatures increase energy consumption, degrade the polymer, and extend the cooling time needed to create a dimensionally stable product.

2.9.2 Pressure

The main pressures in the injection moulding process can broadly be classified as back pressure, injection pressure, holding pressure, and clamping pressure.

The injection pressure is the force applied by the reciprocating screw to push molten plastic into the mould cavity up to about 95% of capacity. Injection pressure is a function of the injection speed, or injection rate. Johannaber [68] noted that an increase in the injection rate resulted in an increase in the shearing of melt, which increased the melt temperature and injection pressure, while Bright et al [69] noted that an increase in injection rate gave an increase in the gloss appearance of finished materials. Increasing the injection rate therefore plays an important role in determining the quality of the product, especially in composite materials where fibre alignment is important.

Holding pressure has an influence on features such as weight, dimensional accuracy, shrinkage, and internal structure of the part [70]. A holding pressure which is too low leads to defective products which show insufficient material formation, whereas excessive holding pressure may increase internal residual stresses [71].

Back pressure is the pressure exerted by the melt on the screw head as it winds back after injecting melt into the mould. According to Pye [72], this pressure is used for better mixing of the plastic, removing small amounts of trapped air, and controlling the weight of the short by maintaining an accurate density of a given volume of melt. He suggests that the back pressure should be kept as low as possible and should not go over 20% of the machine's maximum rated injection moulding pressure. Some back pressure is required to stop the screw pushing itself (auguring) too easily out of the barrel. As the rpm of the screw is increased, the melt temperature increases, together with the backpressure.

2.9.3 Pressure vs Temperature

According to Bozzelli [61], both temperature and pressure have a great influence on moulded parts. His work revealed that as the temperature was lowered, a higher pressure is needed to deliver the polymer melt into the cavity, Fig 2.12. If the temperature is too high, there's an increased risk of causing material degradation. If the injection pressure is too low, a short shot could result. If the pressure is too high, then flash could occur in the mould.
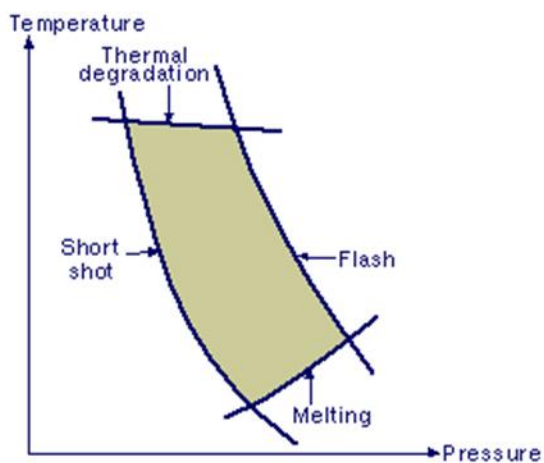
Fig 2.12 The Influence of Pressure vs Temperature [61]

2.9.4 Injection volume

The injection volume or shot size, is the amount of molten material which is injected into the mould. To produce high quality products, the amount of injected material should sufficiently fill the mould and assume the shape of the mould entirely. The amount injected into the mould is dependent on:

- ➢ The density of the material

- ➢ The volume of the mould

- ➢ The melt temperature

- ➢ The mould temperature

It is important to constantly ensure that the correct injection volume is metered into the mould as the injection process proceeds. If the injection volume is too small, the following will occur [66]:

i.   Raw material will not plasticise completely. This will reduce the viscosity of the melt, which would introduce shear stresses in the final product.

ii.   Un-melted material would be injected into the mould.

iii.   The final product would show deformities due to insufficient material.

On the other hand, if the injection volume is too high, then the injected material would be forced through mould mating surfaces, leading to what is referred as 'flash'.

2.9.5 Viscosity

One of the most important properties to be considered during the injection moulding process is the viscosity of the melt. Viscosity is defined as the resistance to flow of a liquid or melt. Plastics are non-Newtonian, meaning they all change viscosity with changes in temperature and injection rate. The higher the viscosity of the melt, the higher will be the injection pressure required during filling. A low viscosity, on the other hand, might present problems of flashing. It is therefore desirable to keep the viscosity variations to a minimum. Direct measurement of viscosity is very difficult and various models to measure it have been put forward by different authors. Haynes et al [73] put forward a model which uses melt fluidity as a measure of viscosity. He employed a Rate Sampling Transmitter (RST) to provide a signal proportional to the melt fluidity.

Ma [74], used the nozzle pressure as a viscosity indicator since the shear rate is proportional to the injection rate (speed), and the shear stress is proportional to the nozzle melt pressure. Viscosity is then the ratio of nozzle pressure to injection rate, which under the assumption of constant injection rate is proportional to nozzle pressure.

Typical Viscosity Curve for a Nominal Wall Part
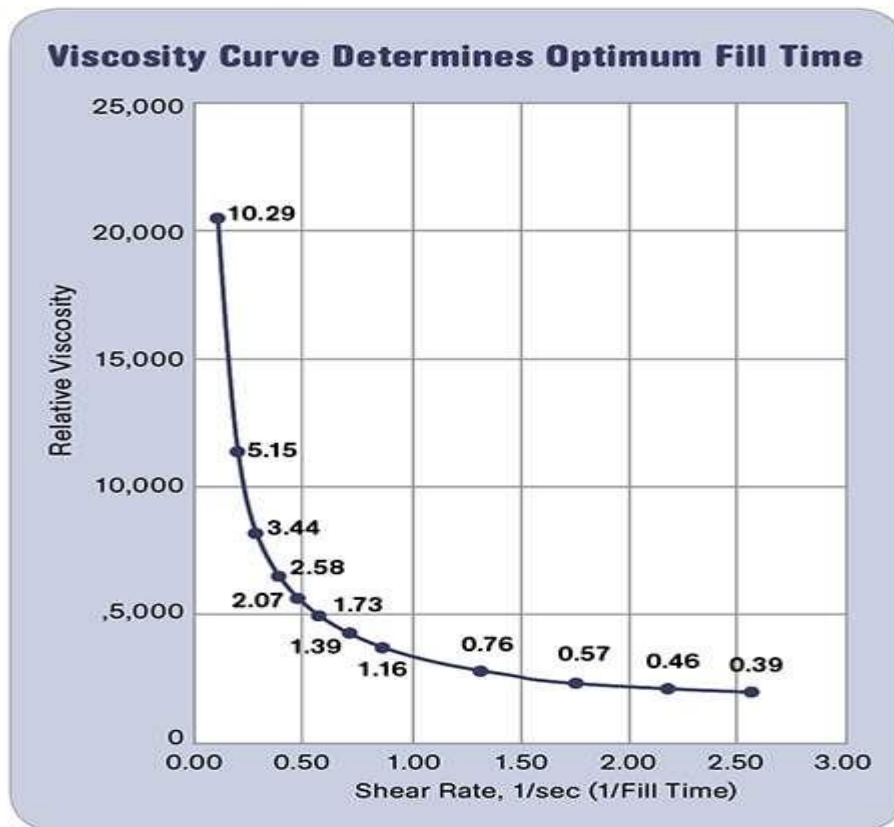
Fig 2.13 Typical viscosity curve for a nominal wall part [74]

2.9.6 Time

Cooling time is the time it takes for the injected melt to cool to a solid state which is strong enough to be able to be ejected from the mould. The wall thickness of the part and the thermodynamic properties of the plastic determine the cooling time. Bryce [55] argues that this is the most important time in the injection process. Longer cooling time increases dimensional stability as a result of better crystal formation.

Fill time is important in injection moulding. Fill time is defined as the time from the start of the injection to when the screw reaches the transfer position, filling 90-99.9% of the part by volume. According to Agrawal et al [70], the important output variables to be controlled during this phase are the melt temperature, rate of filling (injection speed), and the melt viscosity. The fill time is related to the melt molecular orientation which in turn affects the final product quality. It can also influence common problems such as flashing and short shot. Bozzelli [62], states that the fill time is important because the viscosity of plastics changes as a result of temperature variations during the production

cycle. As the viscosity changes, the flow pattern and balance to fill the mould will need to be changed to produce consistent parts. The Fill Time is related to the injection speed. High injection speeds introduce shear stresses in moulded parts. Bozzelli states that shear has a larger impact on resin (reinforcement) viscosity than temperature, and therefore needs to be kept to a minimum. He suggests that to make consistently identical parts, you need to keep fill time constant.

2.10 Stress-strain behaviour of polymers

As is the case of metals, polymers can be classified according to their strength, toughness, modulus of elasticity, or tensile strength [29]. Fig 2.14 shows how a generalised stress-strain curve can used as a simple way of categorising polymer mechanical parameters [75]. This relationship is dependent on temperature. At temperatures which are below the glass transition temperature T_g, brittle polymers (green curve) show very little elongation as strain is applied before breaking. The orange curve represents tough and strong plastic or polymetric material deformation behaviour. Initially, there is linear elastic deformation. As further strain is applied, there is a peak, referred to as the yield strength, as the material transitions from elastic to plastic deformation. At yield point, the polymetric material undergoes strong irreversible plastic deformation, followed by necking. Further application of strain will cause breakage. The point at which fracture occurs is referred to as the polymer tensile strength. The tensile strength can be greater than, equal to, or less than the yield strength.
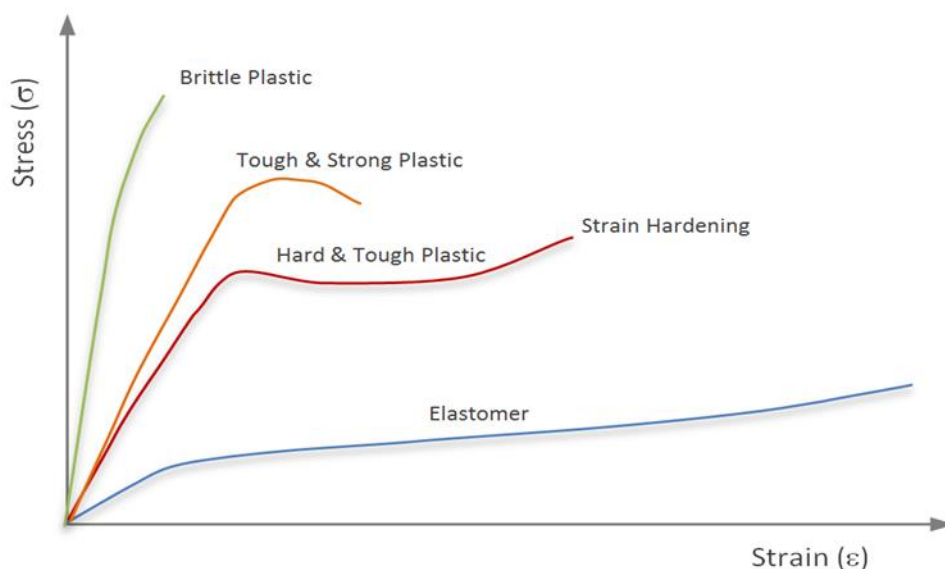
Fig 2.14 Stress-Strain behaviour of polymers [75]

The blue curve represents elastomers. These materials exhibit rubber-like elasticity and will return to their original shape and form unless they are extended to the point of fracture.

The modulus of elasticity (Young's modus) is a measure of the stress-strain curve within the elastic deformation region [29].

$$E \ (Modulus \ of \ elasticity) = \frac{Stress \ (\delta)}{Strain \ (\varepsilon)} \qquad\qquad (2.9)$$

2.11 Mechanical properties of polymers

The mechanical properties of polymers, such as strength and modulus, are influenced by molecular weight, degree of crystallinity, strain rate and temperature [29, 75].

 ➢ Molecular weight

 The tensile strength of polymetric materials increase with molecular weight [29]. According to Callister [48], this can mathematically be expressed as:

$$TS = \ TS\infty - \frac{A}{M_n} \qquad\qquad (2.10)$$

 where TS is tensile strength, TS_∞ is tensile strength at infinity, M_n is molecular weight, A is a constant.

 ➢ Degree of crystallinity

 Highly crystalline materials have high strength, are tougher, and exhibit higher tensile modulus [48]. They also tend to be more brittle.

 ➢ Strain rate

 At low strain (rate), the deformation of most polymetric materials is elastic, and after removal of the deforming load, will return to their original size and shape. In meshing gears, this translates to a flexural movement of the gear teeth. In this region of low strain rate, the stress (δ) is proportional to the strain (ε), (Hooke's Law)

 ➢ Temperature

 The characteristics of a polymer greatly depends on temperature [29]. At temperatures well below T_g brittle failure at low strain rate occurs. If the temperature is increased, the material

changes from brittle to ductile (yielding) behaviour in deformation and fracture. This temperature is referred to as the brittle-ductile transition temperature, T_β.

2.12 Polymer gear standards and classification

The rating standards of metal gears according to strength, toughness, wear, and other characteristics are well established. These standards include BS 436, AGMA 218, and ISO 6336 [76]. The Lewis bending and Hertzian contact equations are used as the fundamental equations in the ratings, albeit with modifications of different correction factors to take into account stress concentrations, dynamic and load distribution effects [77]. As will be discussed in section 2.13, one of the most important factors influencing polymer gear performance is temperature. Small temperature increases in polymer gears have a much greater influence on polymeric gears than on metal gears, as these affect their mechanical properties such as elastic modulus, tensile strength, and creep limit. The Lewis bending and Hertzian contact equations do not take into consideration these factors, and so their use for ratings produces inaccuracies in ratings. Another limitation to the Lewis bending and Hertzian contact equation is that the gear strength determined are only valid under the assumption that the load is constant along the line of contact. Finite element analytical techniques used by Karimpour et al [78], showed that polymer gear teeth experience larger tooth deflections as a result of lower stiffness values compared to metals. These larger tooth deflections extend the path of contact at the beginning and end of the meshing cycle, thereby negating the constant line of contact assumptions made in the Hertzian contact equation.

The current polymer gear design methods are based on the British Standard 6168 [127], the German VDI 2736 [76], and the Polypenco rating method [79]. These standards make an effort to take gear surface temperature, as first suggested by Hackman and Strickle [80], but according to the work done by Hooke et al [81], the BS 6168 estimates and the actual practical values differ appreciably.

The limited information provided by both the British and German standards are mainly based on tests done on steel/polymer gear pairing. Studies, such as that conducted by Mao et al [82], show that polymer/polymer and metal/polymer pairing produce significant differences in wear rates. This makes quoted values differ from actual test results.

The large variety of polymeric material has led to a reliance on manufacturers to provide material design data for their products. Different manufacturers use different strategies to grade their material. This has made it difficult to have consistent information relating to mechanical and tribological properties of different materials.

Wright et al [21] conducted wear tests on polymetric gears and compared their results with those provided by the supplier. There was little correlation between the author's results and those of the supplier, Fig 2.15. They put these disparities down to the fact that most suppliers provide wear data obtained from pin-on-disc or roll/slide on steel techniques.
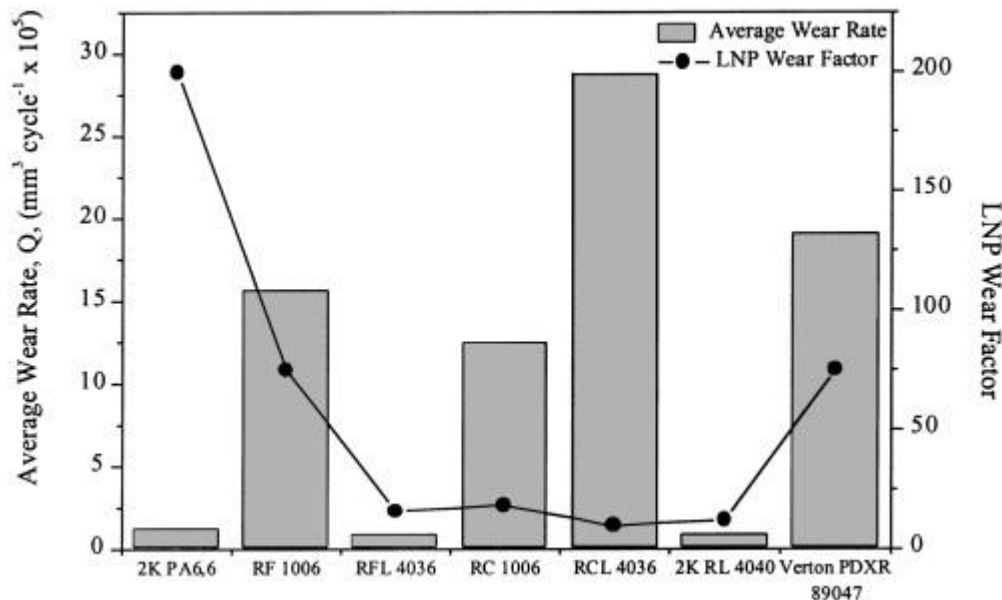
Fig 2.15 Supplier pin-on-disc wear coefficients compared to actual wear rates [21]

The lack of standardised information is a challenge in attempting to interpolate these values from values from readily available information. In his published paper, Zhang [83], proposed the development of a model based on existing experimental data, which would predict material properties. He calls this model Artificial Neural Network (ANN). He argues that this model will standardize the correlation between the wear properties and the characteristic parameters. To date, there are different databases, such as CAMPUS, which seek to list the properties of plastics with an aim of standardising plastic properties. Consequently, the prediction of wear for a particular gear set is a convoluted, ill-defined process. Commercially available design data are given in the form of wear coefficients, but these must be used with caution, as data is usually correlated experimentally and does not necessarily recreate the complex kinematics (loading, deformations and simultaneous rolling and sliding motions which change direction during a cycle) experienced by the gear teeth during a typical meshing cycle. To this effect, Wright [21], carried out comparative tests to compare catalogue coefficients given by a particular manufacturer (LNP Ltd), and actual wear rates obtained in laboratory conditions. He found that there was a weak correlation between the sets of data, indicating that

catalogue data is suitable for comparative purposes only, and as such should not be used as the principle means of selecting a material for a gearing application.

2.13 Polymer gear test methods

There are no universally agreed methodologies and philosophies for testing polymer gear strength [53]. This makes it difficult to grade polymers according to strength. The American Society for Testing Materials (ASTM), and the International Organisation for Standardisation (ISO), are the primary organisations which set general testing standards. Although these organisations do not always agree on exact testing standards, the tests they specify and develop are generally accepted [84].

One reason why it is difficult to have universal test methods is that there is a wide variety of polymetric materials with differing properties and characteristics. Each material type will have unique operating conditions under different geometrical arrangements. The vast number of different types of polymers and polymer composites makes it extremely difficult to come up with a universal way of testing these types of gears. Lifetime gear testing for each material involves performing tests at constant load and speed and measuring wear. Several load/speed combinations would have to be tested. Although this type of testing enables collection of wear data which can accurately provide a correlation between load levels and cycles to failure, it is time consuming and expensive. To decrease test times, researchers sometimes use a highly accelerated life testing method (HALT). This method involves testing at high stresses for a short period of time [85, 86].

An alternative to HALT testing is step-stress accelerated life testing (SSALT) [53, 87]. Using this strategy, stress levels can be increased or decreased several times during the test.

Different researchers have used different methods to test gear strength/wear. Pogacnik et al [34] used an open-loop gear testing machine, shown in Fig 2.16, to conduct wear tests on POM and PA6 gears, by employing a SSALT strategy (where torque was increased) and lifetime tests (where different speeds and torques were used). The authors conclude that the use of this approach is a pragmatic approach to obtain material data through optimised gear testing.
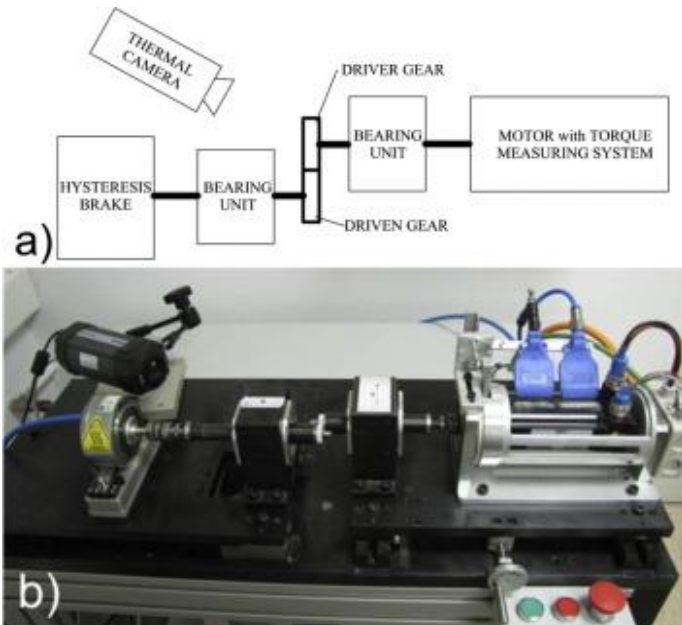
Fig 2.16 Open-loop gear testing machine used by Poganick [34]

Mao [15] used a test rig which employed a back-to-back test configuration where the test gears were meshed in a bearing block which was made to pivot against a loading arm with adjustable weight, Fig 2.17. As an electric motor ran, the reactive forces between the test gears balance the externally applied torque. This results in a balance between the bearing block and the loading arm, thereby maintaining a constant torque on the test gears regardless of tooth wear (covered in Chapter 3). As the test gears wear, there is a proportional rotation of the loading arm about the pivot. This rotation is measured and represents wear. Using this design, wear, torque, speed, and time to failure of the test gears can be recorded.

1. Motor	12. Weight
2. Pulley	13. Controller
3. Gear box	14. Thermal cut-off
4. Conical clutch	15. Bridge Amplifier
5. Driving shaft	16. A/D converter
6. Driven shaft	17. Computer
7. Four universal couplings	18. Micro switch
8. Pivot block assembly	19. Micro switch block
9. CDT Transducer	20. Stop block
10. Test gears	21. Four spaces
11. loading bar	22. Pivot
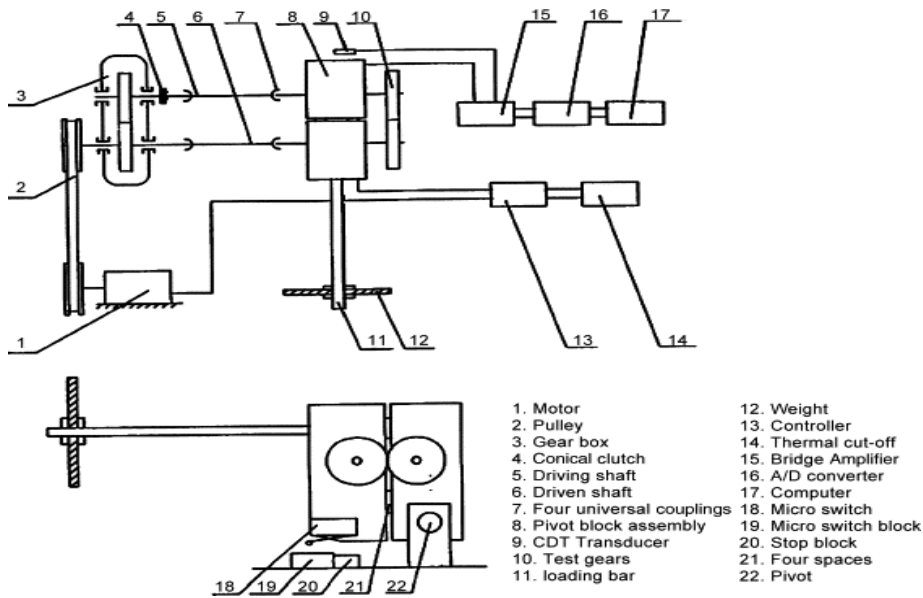
Fig 2.17 Gear test rig used by Mao [15]

Kurokawa et al [18] used a gear test rig which absorbed power through a powder clutch to measure the wear of carbon fibre reinforced polyamide 12 (PA12). In this arrangement, powder is conveyed to the clutch/brake as the gears wear, Fig 2.18. The gear load capability is calculated from the time it takes for the powder to stop from being conveyed due to fatigue, or wear failure.
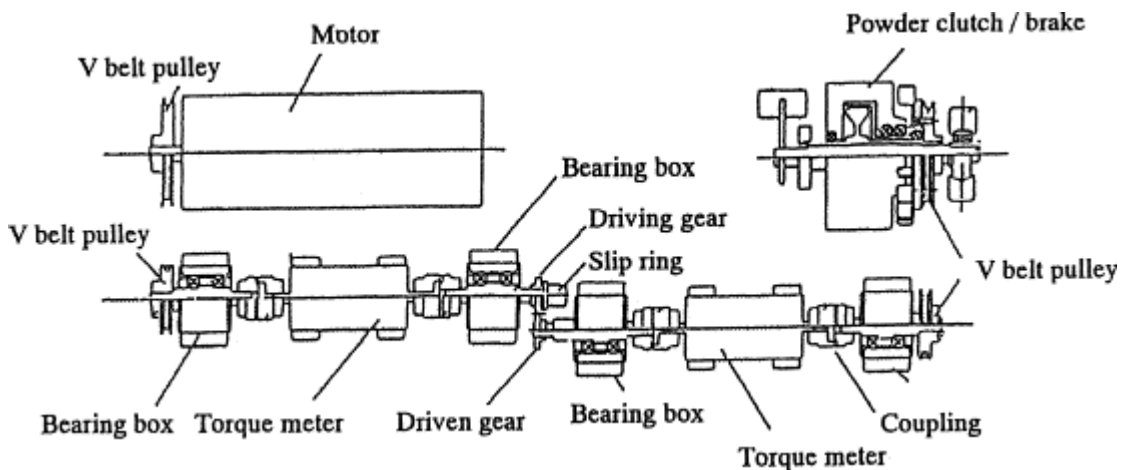
Fig 2.18 Gear test rig used by Kurokawa [18]

Wright et al [21] used a test rig where torque was applied to the test gears through the application of an axial load to one of three meshing helical steel gears mounted on the same shafts as the test

gears. The action of these helical gears converted the axial load to a torque in the test gears. The relative angular displacement of the driving gear to the driven gear is determined by measuring the axial displacement of the driving saft. A schematic diagram of this arrangement is shown in Fig 2.19.
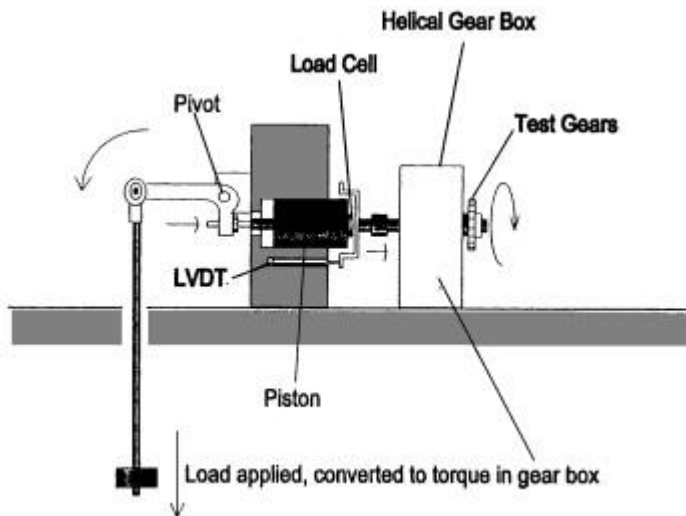
Fig 2.19 Gear test rig used by Wright [21]

2.14 Failure mechanisms of polymer gears

Polymetric gears experience complex operating conditions and fail through different mechanisms compared to metallic gears. Their mode of failure is dependent on operating conditions, type of material, and material pairing [89]. It is therefore important to understand these failures to minimize them.

Literature has revealed that different authors have identified different types of polymer gear failures, but these can generally be grouped into [90]:

➢ Cracking at the root, caused by bending fatigue
➢ Cracking at pitch circle, caused by contact fatigue
➢ Wear
➢ Pitting
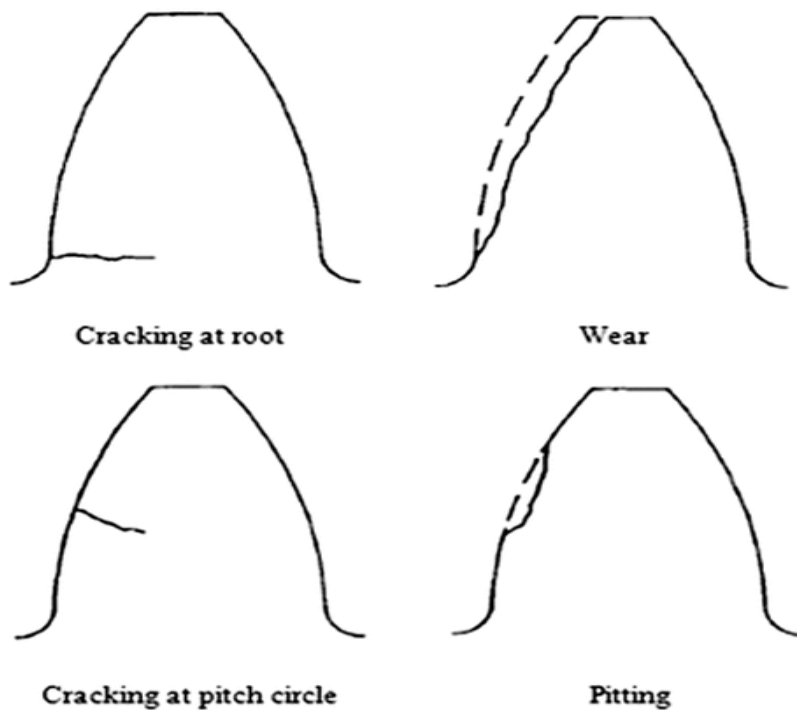
Fig 2.20 Polymer gear teeth failure mechanism [90]

2.14.1 Cracking at the root

This happens at the root of the tooth as a result of repeated alternating torque forces acting on it. It happens when the fatigue limit is reached.

2.14.2 Cracking at pitch circle

Pitch circle cracking is unique to polymer gears. According to Hacman et al [53], this is due to the decrease in strength caused by high local temperature at that point. This initiates a shear-type failure. Tukamoto et al [91] showed that this type of failure mainly occurs in unlubricated gears.

2.14.3 Pitting

Pitting is defined as a surface fatigue failure which occurs when the endurance limit of a material is exceeded. It is most pronounced in the pitch line area when the loads are high enough and the stress

cycles are repeated often enough, resulting in the removal of micro parts from the tooth surface [15]. The removed material leaves behind a pit, which tends to widen over time.

2.14.4 Plastic flow

Plastic flow is a yielding of surface and subsurface material caused by high contact stresses and the rolling and sliding action of gears in mesh.

2.14.5 Wear

Gear teeth wear is a process in which material is removed from the surface of contacting teeth. It is an undesirable consequence of friction occurring on the surface. The wear rate can be defined as the volume of surface material removed per rolling cycle [92]. It is dependent on variable such as material type, applied torque, operating temperature, slip ratio, and rotational speed. It can be expressed as:

$$K = \frac{V}{F.S} \qquad\qquad (2.11)$$

where K is the wear rate, V is removed volume, F is normal force, and S is the total cycles.

Ghazali [93], observed that polymer gear wear occurred in three stages: running-in; linear and final rapid wear:

Running-in occurs at the start of operation for a short time, but the amount of wear is high.

Linear wear: low amount of wear can be seen but is progressive.

Final rapid wear: high wear rate, but small amounts of debris, indicating thermal wear

Wear can occur through abrasion, adhesion, surface fatigue, corrosion, and plastic flow [L103].

Adhesive (normal) wear

This is wear which is caused by the intermittent welding and tearing of small areas of the opposing wear surfaces. It is referred to as normal wear if only microscopic welding occurs.

Abrasive wear

This type of wear occurs under two main conditions:

➢ Two body abrasion – This occurs when one of the gears has a harder or rougher surface than the other. Particles are removed from the softer material.

➢ Three body abrasion – This is caused by a hard particle being present between the contact surfaces. The particle could be dirt from the environment, or wear debris from one of the gears.

2.14.6 Fatigue wear

Surface fatigue wear is a consequence of friction being generated between mating surfaces. It occurs when the applied load becomes higher than the strength of the material. Tooth bending stresses result in some hysteresis heating which lead to a rise in tooth surface temperature. This temperature rise can lower the strength of the material leading to pitch line deformation failure (tooth fold over). This can also be referred to as thermal cyclic fatigue.

Surface fatigue can also be a result of pitting.

2.15 The wear behaviour of meshed polymer gears

The importance of the science of interacting surfaces (tribology), has led many researchers to study the wear behaviour of different meshing polymers and polymer composites [11, 15, 21, 34, 64]. Research has been carried out on the wear behaviour of several polymer gears coupled together in differing combinations of materials such as steel and glass-fibre reinforced polymer matrixes. Comparisons have revealed that wear factors vary over several orders of magnitude for different polymers [94]. Similarly, the coefficients of friction of polymers also vary with different polymers [95]. In their research, Vaziri M et al [89] showed that when several polymers were slid against steel, the wear decreased with sliding distance. For glass-fibre reinforcing matrix, Friedrich K [96], showed that the process of material wear in dry sliding is dominated by four wear mechanisms: matrix wear, fibre sliding wear, fibre fracture and interfacial de-bonding.

 Mao et al, [82], investigated the friction and wear between meshed acetal and nylon gears, and observed that there were significant differences in wear behaviour when running acetal against nylon gears. The driver and driven material play a key role in the wear performance. When nylon was used as the driver, the acetal gear failed due to thermal wear in a similar way as observed when acetal gears were run against acetal gears. However, when acetal was used as the driver, the wear rate was significantly lower. The author also concluded that nylon gear friction and wear performances are

completely different when compared to those of acetal gears. The gear failures are mainly root and pitch fractures, instead of surface wear. This finding outlines the need to choose polymer combinations accurately to enhance efficiency and the longevity of meshing gear arrangements.

The findings of Mao et al are supported in the paper published by Wood [97]. He investigated the wear rates of different polymer/polymer, polymer/steel, steel/steel gear combinations, and noted that there was a marked increase in the tooth surface wear rate when polymer gears ran against steel gears. The wear rate improved when polymer gears of similar material were meshed. Further work into this phenomenon was carried out by Takashi et al [98] who concluded that wear resulting from temperature increase was greatly influenced by whether polymer-on-polymer or polymer-on-metal gear combinations were used. His observation was that the increase in meshing teeth temperature was lower for the metal-plastic gear pair than that for the polymer-polymer. He puts this difference to that fact that the thermal conductivity of the metal is much higher than that of the polymer.
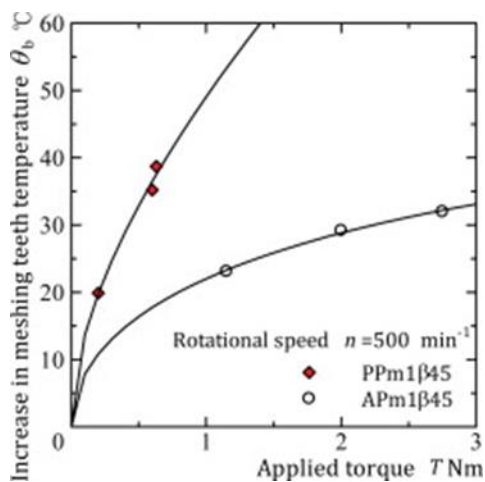
APm1β45 – metal on polymer gear pair
PPm1β45 – polymer on polymer gear pair

Fig 2.21 Effects of gear material on the increase in meshing teeth temperature [98]

In continuation of the work done by Mao et al [82], Duhovnik [99], carried out testing on the wear characteristics of two different polymer gears of the same size. Polyacetal (POM) was used for the driver gear, and PA6 (Nylon 6), for the driven gear. He made several important observations:

• Different moment loads on polymer gears cause different types of failures. These failures are failures due to fractures (cracked flank surfaces and fractures in the root); and failures due to material softening (mainly caused by heat)

• An increased moment load increased both the contact stress between the tooth flanks and tooth deformation, followed by an increase in temperature because of friction and hysteresis effects. Hysteresis is a consequence of internal friction in the material which occurs as result of large deflections of the gear teeth. When a polymer material heats up beyond the temperature of the glass transition (sometimes referred to as the flash temperature), the material softens, causing severe plastic deformations of the teeth.

• He also noted that fatigue defects appear at lower loads, while higher loads cause temperature-induced defects. During the transition from low to high loading, a combination of temperature and fatigue defects occur i.e., plastic deformation in combination with tooth fracture.

• The gears heated up during operation, thereby causing thermal expansion. This expansion meant that the centre distance of the gears changed. A changed centre distance introduced transmission Errors (TE), and an increase in backlash. Both factors significantly affected the lifetime of the gears through tooth deformation.

Earlier work by Rhee [100] had shown that not only does material combinations affect wear mechanisms, but that these mechanisms also depend on the conditions of sliding, such as load, speed, and time. If the meshed system does not reach a steady system but goes through a transient state such as rising temperature due to friction, the relative contribution to the total wear of the individual wear mechanisms may vary with temperature. Because of such factors, Rhee argued that the prediction of wear of material under such conditions becomes extremely difficult, and as such he believed that there were no satisfactory universal wear equations in existence before his work. Through his experiments, he goes on to propose an equation which he described as being satisfactory in the prediction of polymer-matrix friction material.

Hoskins T.J et al [101], investigated the rolling-sliding wear behaviour of two poly-ether-ether-ketone (PEEK) discs running against each other. His conclusion was that the wear and friction mechanisms were closely related to surface morphology, with changes in crystallinity correlating to the operating conditions such as load, speed, and temperature. The observed failure mechanisms were also related to the structure of the contact surfaces and included surface melting and contact fatigue. He observed that generally, discs could run at low slip ratios for both low and high loads. Their performance reduced with an increase of the slip ratio.

Polymers have a low modulus of elasticity, and this results in gears made of polymers having higher tooth flank deflections. Melick [102], studied the influence of stiffness of a gear material on the bending of gear teeth. He compared the deflections of steel-steel gear teeth against those of steel-

polymer, and polymer-polymer. He discovered that polymer-polymer gear teeth deflected more under load, thereby sharing the load with more teeth. The tooth bending of polymer gears results in an increase in the contact path length and in a considerable change in load sharing. For steel-steel, and polymer-polymer gear pairs, the load sharing is symmetrical around the pitch, while for a steel-plastic gear pair, it becomes skewed, and the teeth face the most severe loading in the last part of the meshing cycle.

Singh [12], investigated the potential of Acrylonitrile Butadiene Styrene (ABS), High Density Polyethylene (HDPE), and Polyoxymethylene (POM), to be used in plastic gearing applications. The thermal and wear behaviours of these gears were examined at different torque levels, along with different rotational speeds. He then carried out steady state analysis of the gears at a specific torque and rotational speed setting, to measure the reduction in the gear tooth, durability, and failure modes occurring. Just as in the Hooke et al [95] investigation, he discovered that each material failed through different modes. ABS gears failed due to excessive wear of the teeth at 0.5 million cycles, whereas HDPE gear failures were caused by the cracking at the root of the gear teeth at 1.1 million cycles. POM, on the other hand, completed 2 million cycles without any failures.

Donald [103] used an experimental program to evaluate and compare characteristics of six different polymers operating under identical conditions. These were high performance polyethylene (HPPE), Polytetrafluoroethylene (PTFE), Tetrafluoroethylene, Acetal, PVC, and Fluoropolymer. The wear testing was conducted on two pin-on-disc machines, using a variety of polymers as pins on two different steel rotating counter faces. His analysis confirmed previous studies [100] that the wear volume is affected by the load, sliding speed, sliding length (test duration), and counter face roughness. He made the following important conclusions:

•   The measured coefficient of friction is not related to the resistance to wear for the conditions he had applied in his research

•   As the counter face roughness increased, the coefficient of friction was found to decrease, but with a resulting increase in wear volume.

•   An increase in the operating variables had no effect on the wear of acetal, PVC and fluoropolymer, whereas the wear factors varied for HPPE, PTFE, and tetrafluoroethylene

•   During sliding, the polymers were seen to load up the counter face profile, but no changes in counter face roughness were detectable

•   There did not appear to be a generalised wear behaviour for all the polymers he tested

2.16 The effects of temperature on polymer gears

In general, polymers have a higher temperature coefficient compared with metals. This means that they experience higher dimensional change (dR) per given change in temperature (dT). This relationship can be mathematically expressed as:

$$\frac{dR}{R} = \frac{dT}{K}$$
(2.12)

where R is measure dimension before change, K is temperature

Consequently, the mechanical properties of polymetric materials depend to a much greater extent on temperature than those of metals [52]. According to Kono [132], the thermal conductivity of Nylon 66 is approximately 1/80th of steel, and the thermal expansion coefficient is 11 times larger than that of steel. As the temperature of the environment in which they are operating rises, their performance falls. Within a given range of temperatures, metals have a level of certainty where temperature-dependant behaviour is concerned, which polymers do not provide. Speke [52], states that when approaching melting point, even a relatively low-performing metal such as aluminium, can retain up to 80% of its room temperature strength. That is not the case with polymers. The lack of thermal stability with rising temperature gives rise to a phenomenon where changes in temperature will greatly influence the mechanical properties of these materials.
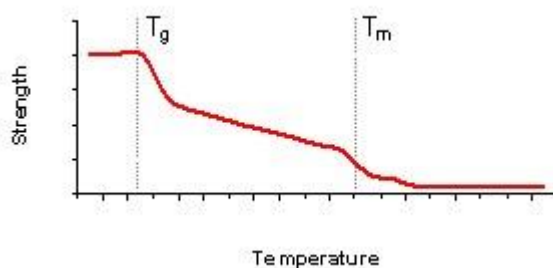
Fig 2.22 Effects of temperature rise on polymers [52]

Given the importance of temperature on polymer gears, several papers looking at how temperature changes affect different polymers, have been published. Unfortunately, the results of such work lack consistency. Kalin [104], noted that, although temperature has a critical influence on all polymers, the results from different tests and different loads which are not temperature controlled, cannot be directly compared. This is because temperatures (even for the same load and velocity), vary greatly

with testing devises, gear sizes and shapes, and surrounding environments. He concludes that without controlling the external environmental temperature in which the experiment is being run, it is very difficult to obtain consistent results for the same gear arrangements run at different times. In the same research, he observed that temperature affects the efficiency of the gear system. When he ran gears under a controlled root temperature, the average efficiency decreased by 6% as the torque increased from 0.1 to 1.4 Nm. The decrease in efficiency with torque increase became more pronounced at elevated temperatures i.e., by 11% at 70°C. He, however, concedes that the efficiency change is not only due to temperature, but also due to a change in the coefficient of friction, gear thinning, and gear-teeth deformations. These combined factors brought about an overall change in meshing conditions, which in turn introduced transmission errors.

In his follow up work, Kalim, investigated the effects of temperature on polymer gear arrangements and noted that an increase in temperature at a given load/torque setting dramatically reduces the fatigue life. In his study, this was up four times at 70°C and up to two times at 50°C, as compared to 30°C. Furthermore, the author was able prove that by keeping the temperature at 30°C, there was no tooth deflection on POM (Polyacetal) gears after running at 1.4Nm for 300×10^3 and 600×10^3 cycles, while at uncontrolled or high temperature (50°C, 70°C), tooth deflection is obvious. Another observation by the author was that the polymer gear temperature never stabilised during 2 million cycles but continued to increase. This resulted in an accumulation of heat, which cannot be removed from the gears via natural cooling. This increase in root temperature is also dependent on the torque.

Mao [105], reported a substantially reduced torque at which the transition from low to high wear occurs as a response to increased ambient temperature. He refers to this temperature as the flash temperature. In his research, he points out that polymer gear teeth temperature can be divided into three components: ambient, bulk, and flash temperature. He notes that it is difficult to accurately predict a rise in the tooth temperature of a polymer gear meshing using Blok's equation since the heat build-up is unsteady and changes in intensity as the velocity of the meshing gears changes. He introduces a numerical method for polymer composite gear flash temperature prediction and the heat partition between gear teeth.

In his follow up work, Mao et al [124], noted that the wear rate on acetal gears increased dramatically when the load placed on them reached a critical value for a specific geometry and running speed. He points out that the reason for the sudden increase in wear rate is due to the gear operating temperature reaching the material melting point under the critical load condition. Through his experimental investigations and modelling on gear surface temperature variations, he was able to

show that there is a relationship between gear surface temperature and gear load capacity. He then goes on to propose an approach for acetal gear transition torque prediction.

Hooke et al, [106] performed an experimental study on the wear behaviour of three typical gear materials. He found that the wear behaviour differed greatly for each material, and was associated with the maximum surface temperature of the gear reaching its melting point. From his study, he was able to present a numerical model to simulate bulk temperature.

Nakamae [107], examined the temperature dependence of the elastic modulus, E, of the crystalline regions in the direction parallel to the chain axis of various polyoxymethanes (POM), by using x-ray diffraction. He discovered that the elastic moduli of each POM material were dependent on temperature, but the dependency was unique to a particular POM. In general, E values decreased with increasing temperature until it reached a plateau at a certain temperature. This plateau temperature is different for different POM materials. Knowledge of the elastic modulus, E, of the crystalline regions of a polymer is of importance because it gives us an indication of the mechanical strength of each POM material.

2.17 Ways of improving gear efficiency

The efficiency of a gear system is given by:

[output shaft power/input shaft power] x 100

To achieve greater efficiency, it is important to reduce power losses. This process is well understood for metallic gears and has been outlined in section 2.2. Polymetric gears, on the other hand, experience more complex processes while in mesh, and therefore require different approaches to achieve better efficiency. These approaches include:

•   Gear teeth modification
•   Cooling holes embedded in polymer gears
•   The use of external lubrication

2.17.1 Gear teeth modification

An obvious way to increase gear strength would be to increase gear teeth size. This approach is discussed in the research done by Imrek [109]. He investigated the effects of tooth width modification on Nylon 6 spur gears in comparison to their unmodified counterparts. The modification was made to the width of a gear tooth up to a maximum tooth width. He noted that there was a maximum tooth

width, beyond which negative factors would reduce strength. The increment of gear teeth did not alter the contact ratio, and the sliding velocity. He made the following important conclusions:

•   A 10 – 15°C reduction in surface temperature was achieved when the gear width was increased.

•   Tooth width modifications help in the reduction of wear rates on tooth profiles

•   Tooth breakages occur around the pitch area of unmodified Nylon 6, whereas these breakages appear near the tooth roots in the modified gears.

•   The decrease in heat generation and the increase of heat dissipation because of teeth width enlargement in the modified gears prevented premature failures and led to increased gear life.

•   Modified spur gears show longer life performance than unmodified gears

•   Width modification can be applied to increase the life of Nylon 6 gears.

Duzcukoglu [110] research mirrored that of Imrek [109]. The aim of his study was to delay the formation of thermal damage in the region of single tooth meshing by decreasing the Hertzian surface pressure through the increase of tooth width. His results are consistent with those of Imrek. He points out that rather than producing gears with the maximum tooth width size to decrease the Hertzian surface pressure in the single tooth contact region, increasing the single tooth contact region would save production costs during the injection moulding process.

2.17.2 The use of cooling holes embedded in polymer gears

Due to the poor thermal conductivity of most polymers, different researchers have investigated how cooling holes could be used to reduce the build-up of heat during operation. Koffi et al [111] notes that these cooling hole tend to promote increased stress and tooth deflection, thus exerting a negative effect. He carried a numerical study to determine the best methods for reducing thermal damage through cooling holes. This was done by analysing 5 different gear-hole configurations. Fig 2.23 is a pictorial representation of his results when a stress greater than 50% of the maximum strength of the gear material was applied to each of them.
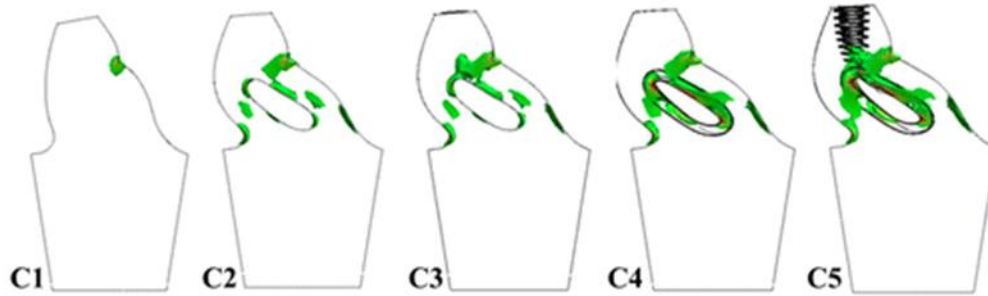
Fig 2.23 Mechanical Failure Response of a polymer to stress after cooling holes have been drilled [111]

His conclusion was that the orientation of the applied holes has an effect of overall decrease in strength of each gear, but the application of tapped holes, as shown in C4 and C5 was the best trade-off between heat dissipation and strength reduction.

In a similar study, Duzcukoglu [110] drilled holes in different locations on the teeth of a polymer gear to encourage the dissipation of heat. He again noted that the thermal damage caused by the effects of heat accumulation on the tooth was reduced. In the operational tests he carried out, he was able to conclude that the tooth temperature was significantly reduced when the air hole was drilled in the vicinity of the pitch diameter, and the temperature reduction was primarily at the regions where the cooling holes were perpendicular to the tooth axis.

2.17.3 Use of external lubricants

One of the main advantage of polymers is their ability to have lubricants, such as polytetrafluoroethylene (PTFE) power or silicon fluid, added to them during the manufacturing process. This enables them to run without external lubrication. The addition of external lubrication to meshed gear pairs would be advantageous, as this would be an effective way of further reducing frictional forces and aid in the cooling process by moving the heat away from teeth surfaces. The choice of the type of lubricant is an important fact in determining whether to use them. Fluid based lubricants introduce churning losses, while reducing the power transmission efficiency of the gears. They also add to the total weight of the assembly as leak proof casing would need to be installed.

2.18 Summary

The studied literature has revealed the immense progress which has been achieved regarding the understanding of principles which underpin gearing. The current focus is on the development of light weight material which will reduce energy losses, and hence carbon emissions. Polymers and polymer composite materials are emerging as front runners as viable alternatives to metallic gears, but the complex microstructural changes which they undergo right from the manufacturing process to the point of operation, mean that different approaches to those of their metal counterparts need to be employed.

The lack of standardised gear testing methodologies and gear ratings for polymers makes it difficult for designers to fully explore the potential which polymer gears offer. As has been highlighted by the work done by Wright et al [21], the reliance on manufacturers to provide material ratings leads to an overstating of their material capabilities.

Temperature has been shown to be of major significance in the both the injection manufacturing process, and in the performance capabilities of polymers. During manufacture, it needs to be kept within a range which is specific to the polymer, and any deviation will result in products which do not have desired qualities. During operation, temperature rises adversely affect gear performance, and ultimately lead to gear failure.

Literature has also revealed that the link between the many input parameters, such as mould temperatures, employed during the manufacturing process, and the resulting physical properties and performance, still need to be fully investigated. Techniques, such as annealing or quenching, are fully understood when used in metallic gears, but not so well in polymer gear manufacture. This research attempts to help to understand how such processes directly affect the wear rates and performance characteristics of polymetric gears.

Chapter 3 explains the methodologies and equipment used in achieving the stated objectives.

CHAPTER 3
RESEARCH METHODOLOGY
_____

3.1 Introduction

The reviewed literature in Chapter 2 shows that there is a clear need to focus research efforts on understanding the link between the input parameters used during the manufacturing process of polymer gears, and their corresponding physical characteristics. Most of the work carried out so far has focused on the different performance aspects of gears, with little regard to the input parameters employed during the manufacturing process. This approach seems peculiar to polymer gears, as metal gears tend to be tested and graded according to their mode of manufacture. Techniques such as annealing and quenching enable metallic gears to be accurately graded according to strength, wear rates, and impact resistance [112].

To better understand what processing parameters, such as the mould temperature (cooling rate or cooling temperature), have on polymers, injection moulding was used to produce HDPE gears at differing mould temperatures ranging from 22°C to 65°C. This range of temperature was chosen as it represents a marked deviation from the recommended mould temperatures of the materials (as stated in the manufacturer's datasheet), and as such, the expectation was that the microstructural and physical influence of the mould temperature would be more pronounced. Another contributing factor for the choice was the limitations imposed by the equipment used.

During the manufacturing process, average gear diameter and weight measurements were taken for each temperature setting. The gears were then subjected to DSC analysis to ascertain how crystallinity was affected. Once the analysis was completed, the gears were subjected to wear tests using a uniquely designed gear test rig. Further analysis was conducted using SEM to investigate the nature of gear failure for gears produced at different temperature settings, by subjecting them to different torque loadings and speeds.

To achieve the objectives of this research, four distinct methodologies were employed covering the injection moulding process, DSC analysis, gear testing, and SEM analysis, as shown in Fig 3.1.

Injection Moulding

➢ Produce gears using different input values for melt temperature, injection volume, hold pressure, and cooling temperature. Measure resultant mass, diameter.

➢ Determine deviation of mass and diameter from expected values, and identify optimum input values

➢ Vary the cooling temperature while holding the optimum values constant

DSC analysis

➢ Analyse changes in crystal formations at different cooling temperatures

Gear Testing

➢ Use different load settings and rotational speeds on gears produced at different cooling rates

➢ Analyse gear wear characteristics for each group

SEM analysis

➢ Analyse modes of failure at microstructural level

RESULTS

Fig 3.1 Methodological approach used in research.

3.2 Injection moulding methodology

Injection moulding was used to produce the gears used in this research because of the advantages it offers, as outlined in Chapter 2.

3.2.1 Injection Moulding Machine

The injection moulding machine used for this project was an Engel Victory 60T moulding machine (Engel U.K. Ltd, UK), with a clamping force of 60T, and a maximum injection volume of 113cm^3. It is a

hybrid type, consisting of both hydraulic and electric driving systems. It offers computer-integrated manufacturing with flexible automation. The full machine specifications are shown in Table 3.1, and Fig 3.2 shows the machine.

The Engel Victory 60T has four distinct segments: hopper, heating cylinder, mould, and a clamping mechanism. An integrated LCD touch screen enables user interface.

Hydraulic clamping unit   Electric injection unit
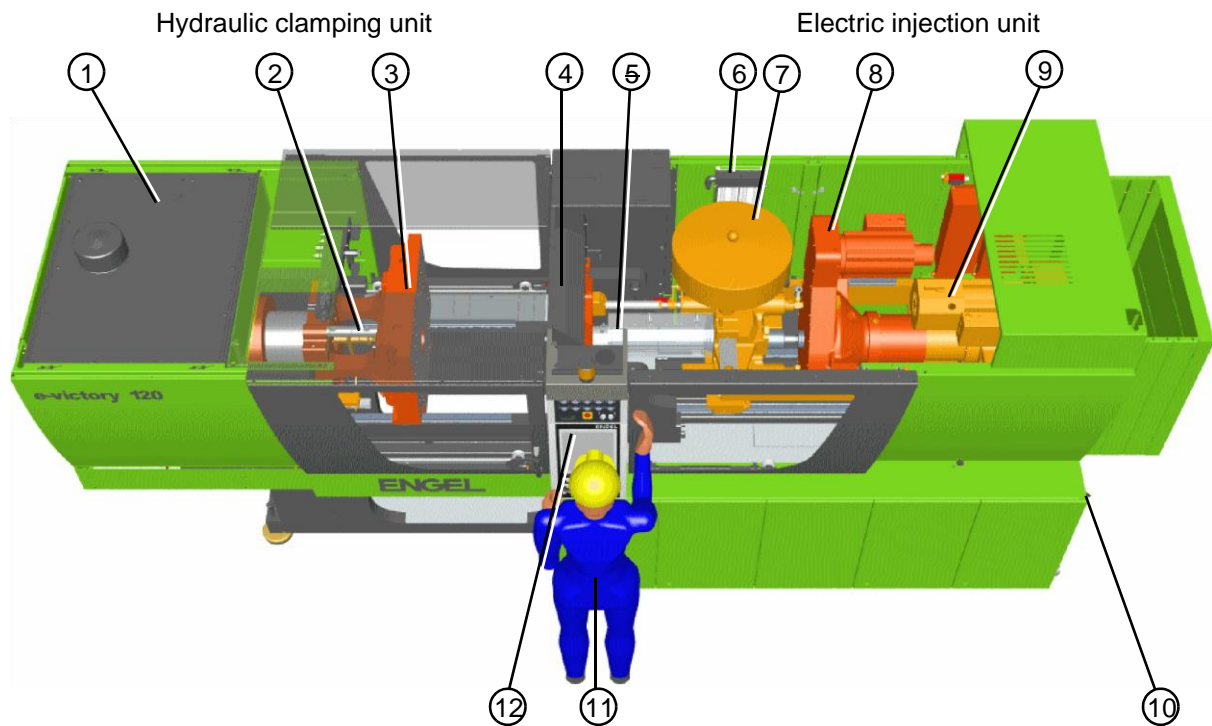
[1]   Hydraulic oil tank
[2]   Hydraulic ejector
[3]   Stationary platen
[4]   Barrel with nozzle
[5]   Cooling water manifold
[6]   Material hopper
[7]   Screw drive for plasticizing
[8]   Injection drive
[9]   Main switch and machine type plate
[10] Operator workplace

[12] Switch panel with screen

Fig. 3.2 Engel Victory 60T Injection Moulding Machine [113]

Table 3.1 Engel Victory 60T Injection Moulder Specifications

Clamping force	kN	600
Opening stroke	mm	457
Ejector stroke	mm	100
Ejector force	kN	39.8
Screw diameter	mm	30
Max swept volume	Cm^3	113
Max screw speed	r/min	420
Injection rate	Cm^3/s	157
Injection pressure	bar	2400
Nozzle stroke	mm	290
Nozzle cont. pressure	kN	40.6

3.2.2 Hopper

This is where the prepared polymer pellets are loaded into the machine. It is designed to hold approximately 2 hours cycle time of raw material. A transparent perplex screen situated on the side allows the user to see the material as it reaches low levels. A magnetic lining is used to remove any metal swarf which could damage the injector or barrel.

3.2.3 Heating cylinder

This section consists of a cylinder, surrounded by four heating zones, each with its own heater bands. Zone 3 is next to the hopper and is the coolest part of the barrel. The temperature is set so that the plasticization process of the pellets can begin. In zone 2, the polymer pellets will transition through glass transition temperature (Tg) into a molten state, and this process will continue into Zone 1. Zone 0 represents the melt temperature as it exits the barrel and is injected into the mould.
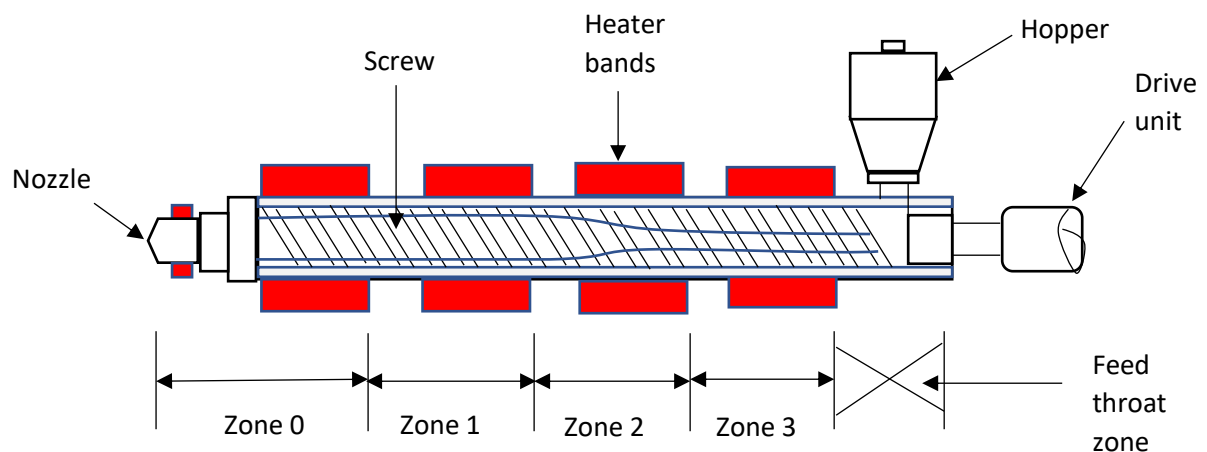
 Fig 3.3 Schematic diagram of Heating barrel

Inside the cylinder, is a screw rod with a one-way valve at its tip next to the injection nozzle. As the screw is rotated, it drives the pellets from the hopper towards the nozzle. The solid pellets are heated by the heating elements and turn into melt.

The amount of time which the melt stays in the heating barrel is referred to as the melt residence time (MRT) and needs to be controlled, otherwise the material will start to decompose if allowed to remain within the heated zones for too long. The melt residence time for HDPE, was calculated using equation 3.1:

$$\text{MRT} = \frac{\pi D^3_\rho}{m} \; x \; \frac{t}{60} \qquad\qquad (3.1)$$

where:

MRT is melt residency time (mins), D is the screw diameter [cm], ρ is melt density [g/cm^3], m is shot weight [g], t is cycle time [S].

Since density (ρ) is given by:

$$\rho = \frac{Mass\ (m)}{Volume\ (v)} \qquad\qquad (3.2)$$

Substituting equation 3.2 into equation 3.1, gives

$$\text{MRT} = \frac{\pi D^3}{v} \; x \; \frac{t}{60} \qquad\qquad (3.3)$$

3.2.4 Mould

The mould is a confining cavity or matrix which gives the injected melt its final shape as a finished article. The design of the mould is important because it has an influence on the strength, durability, shape, and size of the final part. It is sturdy and can withstand the pressures involved during the injection process.

The gear mould used in this experiment is of a 2-half-split design, with a centre gate in one half, through which the melt is injected into the mould as shown in Fig 3.4. Table 3.2 shows the gear mould specifications.

Table 3.2 Gear Mould Specifications

Module (mm)	2
Tooth number	30
Pressure angle (°)	20
Face width (mm)	15
Thickness (mm)	3.14
Contact ratio	1.67

The gate is centred, thereby ensuring that the injected melt flows uniformly in all directions of the mould, while allowing good heat transfer to control the cooling process. Uniform flow helps eliminate the influence of differences in material density along the gear. Such differences in density would affect gear wear performance. The other half of the mould is mounted onto a moving mount, which acts as the clamping half. It has 6 ejector pins, which protrude and force off the gear once the mould is retracted.

The keyway and two-pin holes used for gear installation are not created on the mould directly to reduce the plastic turbulence during the injection moulding process. These are created through a separate operation using a 16mm reamer and a 6mm drill bit.
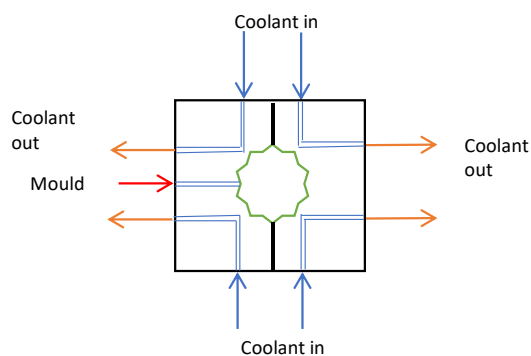
(a)
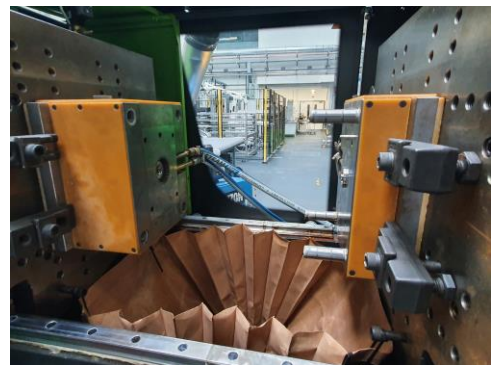
(b)
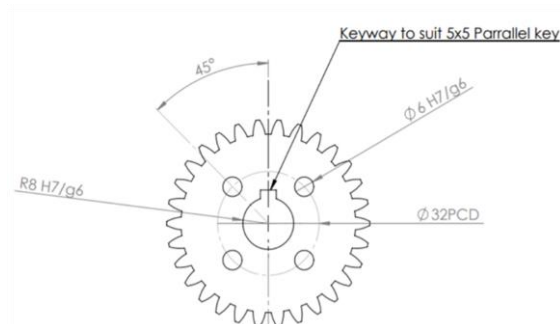
(c)

Fig 3.4 (a) Schematic of gear mould design (b) Gear mould (c) Gear produced using mould.

3.2.5 Chillers

Mould cooling is achieved through a pair of independent chillers manufactured by PL Machinery Ltd (Bedfordshire UK). An interface enables the user to select a desired mould temperature, and coolant is pumped via connecting hoses to the two halves of the mould.

Fig 3.5 Cooling chillers

The temperature selection range of these machines is from 0°C to 120°C.

3.3 High density polyethylene (HDPE)

To analyse the response to varying cooling temperatures on polymetric gears, an unfilled material called high density polyethylene (HDPE), was used. All materials have different responses to variations in temperature, which are dependent on factors such as molecular weight, density, and moisture content. Polymer composites are made up of reinforcement materials, fillers, and other bonding compounds, which will have direct influence on gear characteristics. An investigation into temperature response to a composite material would reveal an aggregate response to all materials within the compound.

The decision to use an unfilled polymer enables a single material response to mould temperature variations to be analysed, thereby giving an accurate determination of how a particular polymer grade is affected by such changes.
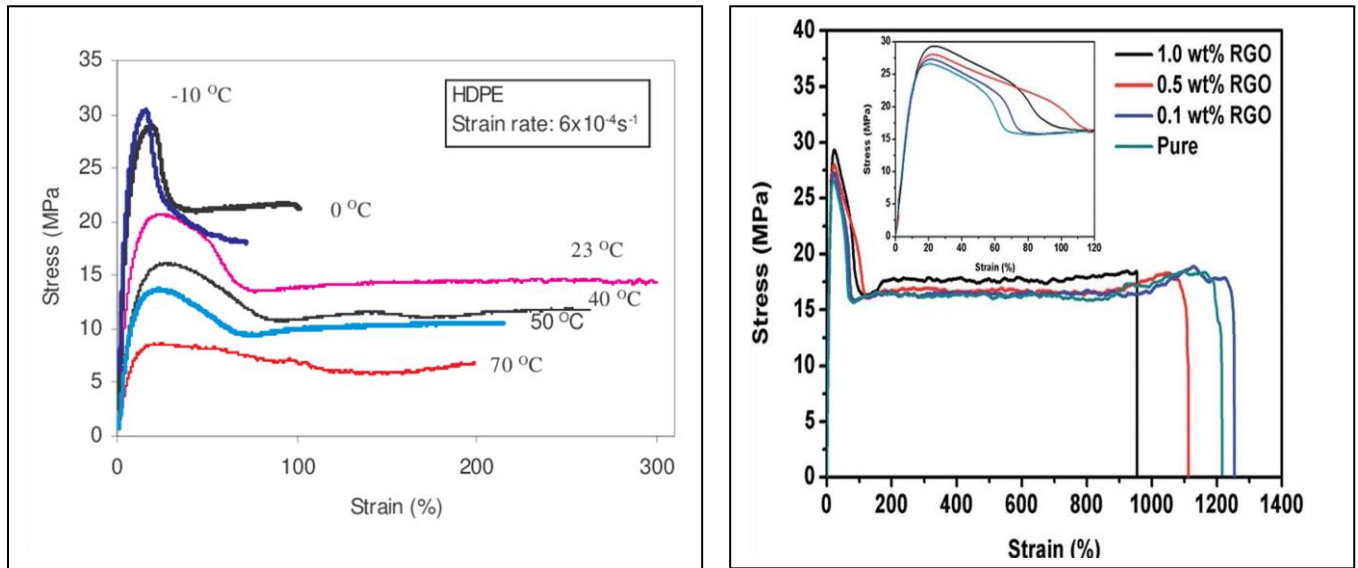
(a)

(b)

Fig 3.6   (a) Stress-strain rate HPDE at different temperature
(b) Stress-strain comparison curves of pure HDPE and its nanocomposites with various RGO contents [133]

Fig 3.6(a) [133], shows the stress-strain rates for HDPE at different temperatures. It can be seen that an increase in temperature produces a decrease in elastic modulus, a reduction in tensile strength, and an improvement in ductility. Fig 3.6(b) shows comparisons to stress-strain responses between unfilled and filled HDPE at different temperatures.

3.3.1 High Density Polyethylene – HDPE

High Density Polyethylene (DHPE) is a widely used versatile, semi-crystalline thermoplastic polymer made from the ethylene monomer. It has a chemical formula of $(C_2H_2)_n$, and its chemical structure representation is:

60
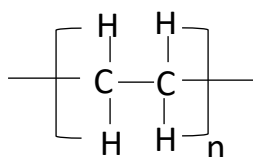
It is one of the most widely used polymers, with applications in bottles, containers, water pipes, and a variety of consumer goods. Its main properties are listed in Table 3.3.

HDPE was primarily chosen because of its ability to exhibit variable crystallinity structures. This is important for this research as it enables clearer analysis of crystal formations with varying cooling temperatures. Other advantages of HDPE include:

➢ A high tensile and strength-to-density ratio
➢ High impact resistance
➢ Good corrosion resistance
➢ It can easily be recycled

The ability for HDPE to be easily recyclable is an important factor as to why it was selected for this project. According to a test carried out by ESE World B.V (Maastricht, Netherlands) [114], HDPE can be recycled up to ten times without adversely altering the material properties. This means gears made from HDPE can be recycled many times, thereby increasing the availability of the material and at the same time reducing waste to the environment.

Table 3.3 HDPE properties [115]

Material/Properties	Method	HDPE
Commercial name		Hostalen GC 7260
Melting temperature (°C)	Internal method DSC	140
Injection melt temperature (°C)	ISO 8302	180 - 225
Injection pressure (MPa)	ISO 9001	80
Mould temperature (°C)	ISO 10724 – 1	30
Glass transition temperature (°C)	ASTM E1356	111
Density (g/cm^3)	ISO 1183 – 2	0.94g/cm3
Flexural modulus (MPa)	ISO 178	1400
Tensile strength (MPa)	ISO 527 - 3	20 – 29.5
Melt mass flow rate (g/10mins)	ISO 1133 – 1	0.2 – 3.0
Hold pressure range (MPa)	ISO	65 - 70
Mould shrinkage (%)	ISO 294-4	2.4 – 4
Cooling time (Sec)	10724 – 2	30
Coefficient of friction	ASTM D1894	0.25 – 0.3
Picture of actual gear		

3.4 Design of Experiment (DoE)

The rationale of having a DoE, is to have a systematic method of determining the relationship between factors affecting a process and the output of that process. In other words, it is used to find cause-and-effect relationships.

The techniques employed in this experiment seek to meet the 3 main principles of Design of Experiments (DoE), which are:

➢ Validity,

➢ Reliability, and

➢ Replicability.

3.5 Factorial design of experiment

Factors (or parameters) are the different input variables which determine the functionality or performance of a product or system, and these are highlighted in the Ishikawa diagram, as shown in Fig 2.7. Each polymer comes with a manufacturer's data sheet, which gives a range of recommended input values for each factor. In order to analyse what an individual input factor has on the final product, it is necessary to ensure that other factors do not interfere with the result as the chosen factor is varied. To isolate the effects of cooling temperature, the experiment was carried out in two phases:

Phase 1 involves an optimisation process.

Phase 2 involves using the optimised input values and keeping them constant, while varying the mould temperature (cooling rate).

The range of input values given in the datasheet for each material can be classified as high (representing the highest recommended value), medium, and low (representing the lowest recommended value). This means each factor has three levels. The large number of input factors makes it impractical to consider them individually, and so only 4 factors are considered and optimised. A median value for all other factors is used.

The following factors were selected for optimisation:

- Melt temperature

- Injection volume

- Hold pressure

- Hold time

This makes the 1st stage of the experiment a 4-factor, 3-level experiment.

According to Fisher [116], to obtain optimum combinations, a full factorial design which works on all possible combinations extruded from preselected sets of factors would have to be performed.

The full fractional design consists of K experiments, where

K = number of levels of factors (3 in this case)

n = number of factors (4)

This would mean that:

$K^n = 3^4 = 81$ experiments would need to be done.

During production, ten gears are produced in each experimental run (Chapter 4), meaning a total number of gears 810 would need to be made. Using the full factorial design would therefore make the experiment costly and time consuming. Rao, et al [117], notes that, although fractional factorial design is well known, it is too complex and there are no general guidelines for its application, or the analysis of results obtained by performing the experiments.

To overcome these problems, the Taguchi method was chosen.

3.6 Taguchi design of experiments and processing sequence

In Phase 1, the gears are produced by altering the chosen factors through the different levels, while keeping all other factors constant. This is the optimization process, and it involves taking each factor in turn, and changing the given values from the median, to the highest, and then to the lowest, while keeping the values of all other factors at the mean value of the given range. During each run, measurements of the corresponding change in gear diameter and gear mass are taken. The target gear diameter is the gear specification of the mould tool. The input parameter value which produces a gear diameter which is closest to that of specification, will be the ideal value for that parameter. The experiment is continued until all ideal values for each parameter are achieved.

To achieve an accurate and methodical approach, a Design of Experiment (DoE) called the Taguchi method is used. This method gives a robust design which attempts to ensure that the physical measurements of the produced gears (Output), will not only stay within specifications, but will always be centred at the target (Mean), which in this case is the mould tool specification, regardless of uncontrollable factors (noise). This makes this method a dynamic response design, Fig 3.6.

To effectively use the Taguchi design of experiment, the following steps needed to be taken:

➢ Selection of output target parameter.
➢ Identification of the input parameters.

➢   Identification of the number of level settings for each input parameter.

The parameter design of the Taguchi method utilizes orthogonal arrays (OA), signal-to-noise (S/N) ratios, main effects, and analysis of variance (ANOVA).
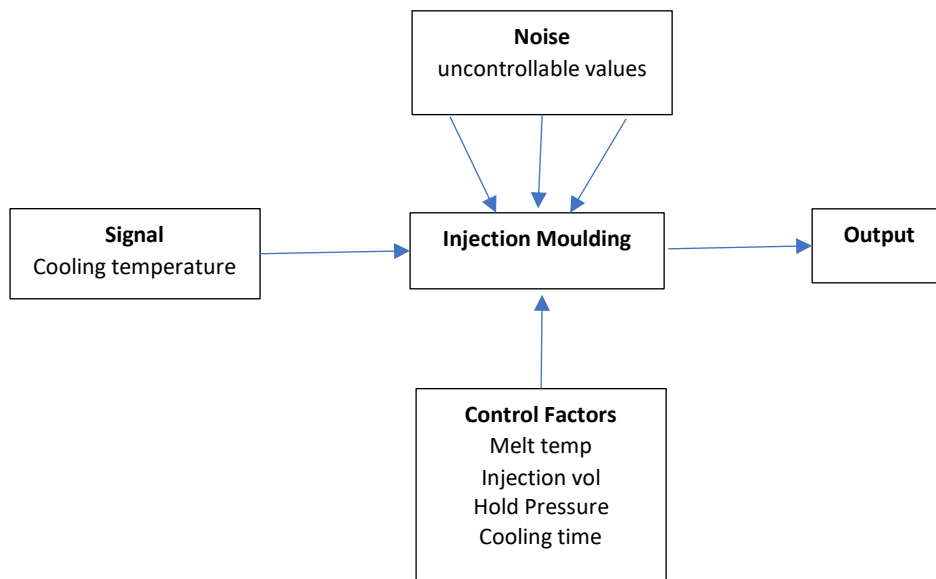
Fig 3.6 A robust dynamic response methodology

Noise

The Taguchi method not only aims at modelling the controllable factors, as in conventional DoE, but also the 'noise' (uncontrollable) factors. In this experiment, the noise factors have been identified as:

-    Polymer quality

-    Machine discrepancy

-    Unverifiable parameters such as barrel temperature, hold pressure, and injection volume

-    Ambient temperature

Although noise is present, it will have minimal effect on the output. The primary aim of the Taguchi method is, therefore, to minimize variations in output, even though noise is present in the process. The process is then said to have become robust.

In phase 2 of the experiment, gears are produced by employing the optimised parameter values, and keeping them constant, while varying the cooling temperature.

The outputs for phases 1 and 2 are shown in Fig 3.7 and 3.8.

Controlled input factors   **Process**   **Response/output measures**

Melt temperature
Injection volume
Holding Pressure
Cooling time
Median values for all
other factors

Injection Moulding

Change in gear diameter
Change in gear strength
Change in weight
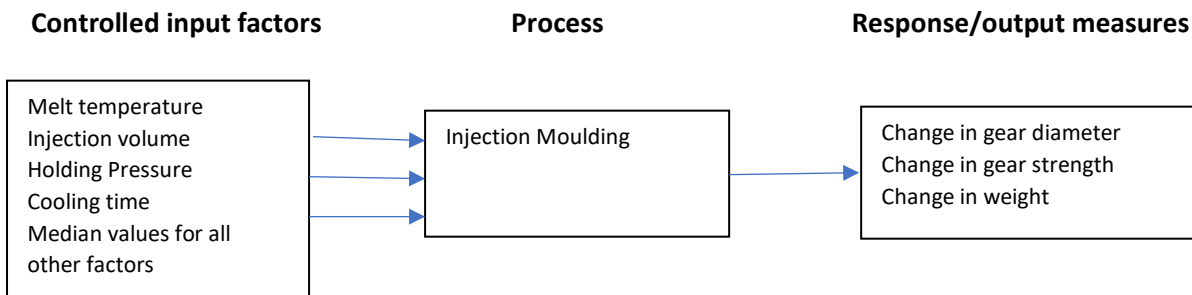
Fig 3.7 Phase 1: Determination of optimum parameter values

Controlled input factors   **Process**   **Response/output measures**

Cooling Temperature

Injection Moulding

Change in gear diameter
Change in gear strength
Change in weight

Optimised melt temperature
Optimised injection volume
Optimised hold pressure
Optimised cooling time
Median values for all other
factors

Unchanged input factors
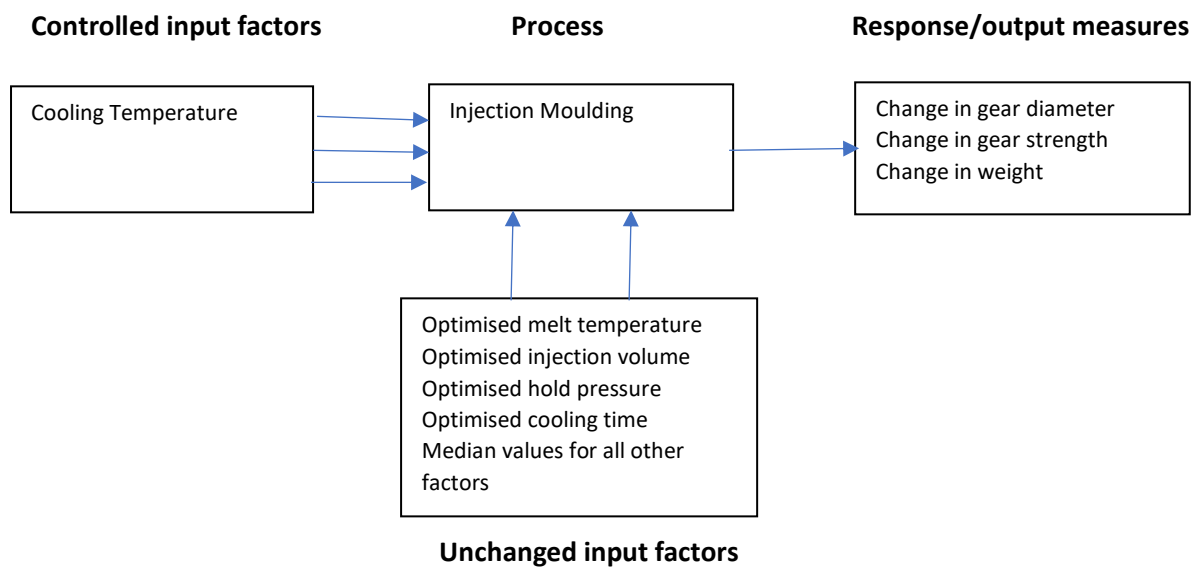
Fig 3.8 Phase 2: Optimised parameters held constant

3.7 Signal/Noise Ratios

This is used to determine the quality of the produced gears. The S/N ratio is a logarithmic function which can be defined as an inverse of variance. The S/N ratio characteristics can be divided into three categories: the smaller the better, the larger the better, nominal the best.

In this experiment, the noise should be as low as possible, and so, the larger the better, is chosen. The logarithmic function is:

$$S/N = -10\log\left[\frac{1}{n}\sum_{i=1}^{n}\frac{1}{y_i^2}\right]$$

(3.4)

where:

y_i = nth observation of response variable

3.8 Assumptions made

Most of the factors highlighted in the Ishikawa diagram (Fig 2.7) can affect the injection moulding process. In this study, the following assumptions have been made:

i.   Only the effects of melt temperature, injection volume (shot volume), hold pressure, and hold time are considered.

ii.   The two halves of the mould are assumed to have uniformity of temperature. The layout of the cooling channels is assumed to maintain a constant temperature everywhere within the mould.

iii. The purity and quality of the used material is neglected.

iv.   Research conducted by different researchers [118, 119], has shown that shrinkage of injection moulded products changes along the flow path and can show different values when measured in the flow or across flow directions. For the purposes of this study, these differences are ignored as they are relatively small.

v.   The room temperature in which the experiment is conducted is 22°C

3.9 Quality Control

It is important to ensure that the stated input parameters are accurate so that credible results can be obtained. To achieve this, both an infrared and a contact type thermometer are used to verify the mould cavity temperature, at the tip of the injection barrel. Unfortunately, the actual temperatures of the melt within the heating barrel cannot be independently verified as it is encased in an insulated barrel. This means that the readings displayed on the LCD screen of the machine are assumed to be correct. For the cavity, the temperature read by the independent thermometer is taken as the correct cooling temperature.

3.10 Gear property measurements

3.10.1 Mass

In injection moulding, the mass of a product is normally used as a part quality indicator. Changes in mass can be linked to input factors such as melt temperature injection volume and holding pressure. The mass of each gear, including the sprue, was measured using a standing mass balance, and noted against variation of each input value.

3.10.2 Diameter

All polymetric materials shrink as they cool from molten to solid state. This shrinkage is affected by material properties, mould design, and processing parameters at the filling, packaging, and cooling stages, as described in Chapter 2. Jansen et al [120] points out that there are three types of shrinkages in injection moulding: in-mould shrinkage (this is the shrinkage which occurs during processing); as-mould shrinkage (this happens just after mould opening and is sometimes referred to as 'mould shrinkage'); and post-shrinkage (this happens over a period of time as the material ages). In this study, the term 'shrinkage' is solely used to refer to in-mould shrinkage.

Radial diameter measurements were taken using a digital vernier callipers, as shown in Fig 3.9

Gear diameter measurement
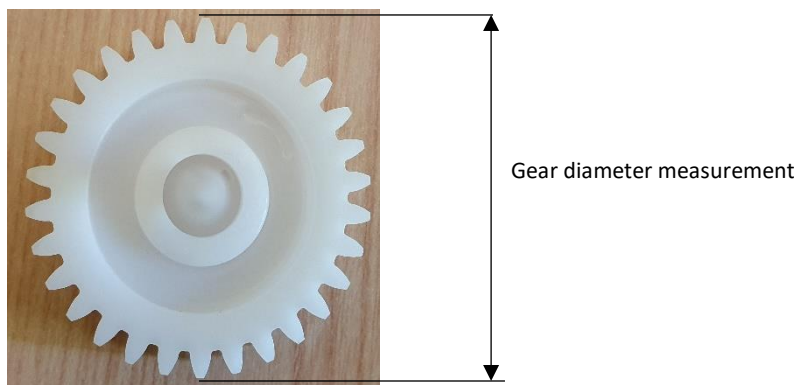
Fig 3.9 Measurement of gear radial diameter

To determine the shrinkage as a percentage of the cavity dimensions, a mathematical formula defined by ISO 294-4 [M26] was used. This is expressed as:

$$R = L/L_o \times 100 \qquad (3.5)$$

Where R is the shrinkage, L_o is the mould cavity dimensions, and L is the measure gear diameter.

3.10.3 Visual inspections

A continuous visual inspection regime was adopted during the produced gears to monitor any unexpected imperfections such as distortion, burn marks, or 'flash'.

3.11 Crystallinity

Polymer properties such as the glass transition (T_g) temperature, melting point, tensile strength, and stiffness, are influenced by the degree of crystallinity.

Differential Scanning Calorimetry (DSC) was used to determine changes in crystallinity of the gears. It is a thermo-analytical technique in which the difference in the amount of heat required to raise, lower, or isothermally hold the temperature of a sample, and an empty reference are measured as a function of temperature or time. The measured signal is the energy absorbed or released by the sample in milliwatts. This can be used to analyse several characteristics such as the glass transition temperature (T_g), melting behaviour, reaction enthalpies, detection of endothermic and exothermic effects, determination of specific heat capacity, and the influence of reinforcement fillers. A shift in T_g between samples of the same material indicates a difference in crystallisation. A lower T_g represents lower crystallisation.

A Mettler Toledo HP DSC 1 machine (Mettler-Toledo Ltd, Leicester, UK), which uses STARe software, was used for this analysis, as shown in Fig 3.10.
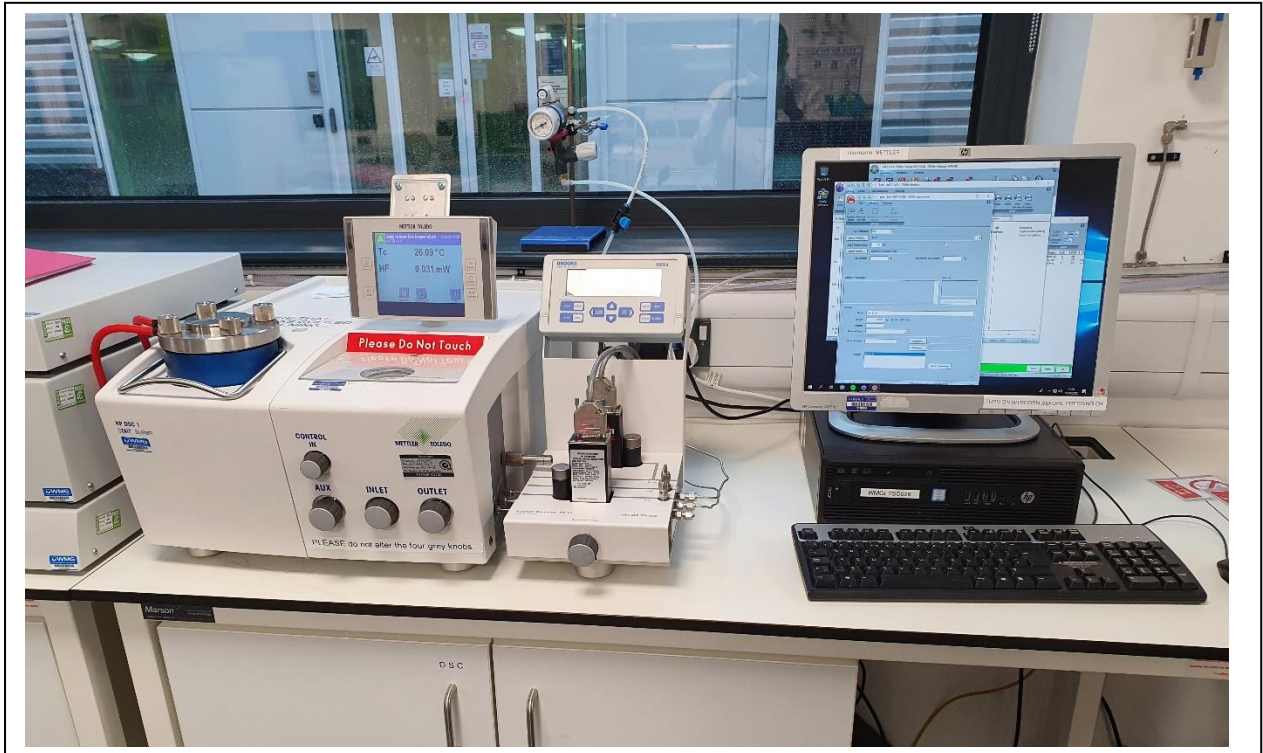
Fig 3.10 Mettler Toledo HP DSC 1

The HP DSC1 has the following features [121]

➢ a small furnace made of pure silver with electrical flat heater, and can be pressurised up to 10MPa

➢ Pt100 temperature sensor (A resistor made of platinum wire with electrical resistance of 100Ω at 0°C)

➢ Heat sensors (FRS5 and HSS7) with a star-shaped arrangement of thermocouples underneath the crucible

➢ Positions which measure the difference between the two heat flows

➢ Various cooling options
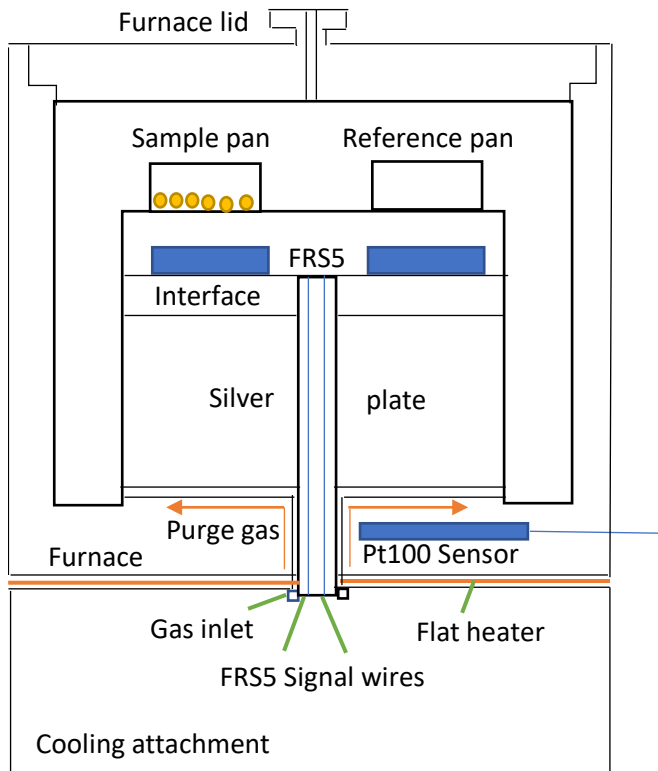
Fig 3.11 Simplified cross-section of a DSC measuring cell equipped with a FRS5 sensor [121]

3.11.1 Heat Flow Measurement

Fig 3.11 shows the schematic diagram of the DSC measuring cell equipped with an FRS5 sensor. As an electric current is passed through the resistor, with resistance R_{th}, it heats up and there is a heat flow, $\emptyset_1$, form it.

Ohm's law states:

$$V = IR \qquad\qquad (3.6)$$

Where:

V is potential difference. In this case, it is expressed as a temperature difference, T_s, T_c.

I is current flow. In this case it is expressed as heat flow, $\emptyset_1$

R is resistance. In this case it is expressed as the resistance of the FRS5 resistance, R_{th}

Substituting into equation (3.6), heat flow to the crucible, $\emptyset_1$, becomes:

$$\emptyset_1 = \frac{Ts - Tc}{Rth} \qquad (3.7)$$

Similarly, the heat flow to the empty reference crucible, $\emptyset_r$

$$\emptyset_r = \frac{Tr - Tc}{Rth} \qquad (3.8)$$

The heat flow to the sample, $\emptyset$, corresponds to the difference between the two heat flows. This is the DSC signal.

$$\emptyset = \emptyset_1 - \emptyset_r = \frac{Ts - Tc}{Rth} = \frac{Tr - Tc}{Rth} = \frac{Ts - Tc}{Rth} \qquad (3.9)$$

The thermal resistance on the left and right sides are identical due to the symmetrical arrangement. This is also true for Tc. The equation for the determination of the DSC signal can therefore be simplified to:

$$\emptyset = \frac{Ts - Tr}{Rth} \qquad (3.10)$$

The temperature differences are measured using thermocouples which rely on differences in voltage as the temperature changes (ΔT). This ability is referred to as the sensitivity of a thermocouple, S.

$$S = \frac{V}{\Delta T} \qquad (3.11)$$

Where V is the thermoelectric voltage.

3.11.2 DSC analysis procedures

There are six main steps involved in carrying out an effective DSC analysis using the Mettler Toledo HP DSC1 machine:

1. Identification of points on the gear structure to analyse. The gear tooth surface was chosen, and a sample of between 4g and 6g was removed, as shown in Fig 3.12.

Fig 3.12 Point where test sample for DSC analysis is taken form.

The following assumptions were made during the preparation of the sample:

- The test specimen is representative of all tooth surfaces of the gear
- No major mechanical or thermal stresses were introduced to the test specimen during cutting
- A mass of between 4 and 6g of the test specimen, regardless of its geometry, is sufficient to produce good accuracy

2. Sample calibration. Weight measurements of the empty reference crucible and the crucible containing the sample are taken.

Fig 3.13 Aluminium crucible in which test samples are placed.

3. Setting up of the STARe software. A four-step method step up must be followed

4. Choosing the environment. Nitrogen was used to provide an inert environment

5. Running the tests

6. Evaluation of the results

3.11.3 Method setting for STARe software

Before commencement, a common method for sample analysis had to be determined. This enables the same testing conditions to be applied to all samples, by simply 'calling the method' every time an analysis is to be done. A multi-segment approach consisting of dynamic and isothermal activities was chosen. During the dynamic segment, the sample is either being heated or cooled. A rate of 20K/min was used as it provided good resolution. An isothermal segment is one where the temperature is held constant.

The crucible insertion temperature was 50°C. The sample and reference crucibles are then heated to 160°C, and held at that temperature for 2 minutes, after which the temperature is raised to 240°C, before being cooled back to the insertion temperature. Fig 3.14. The length of each segment is determined by the initial and final temperature of that segment.
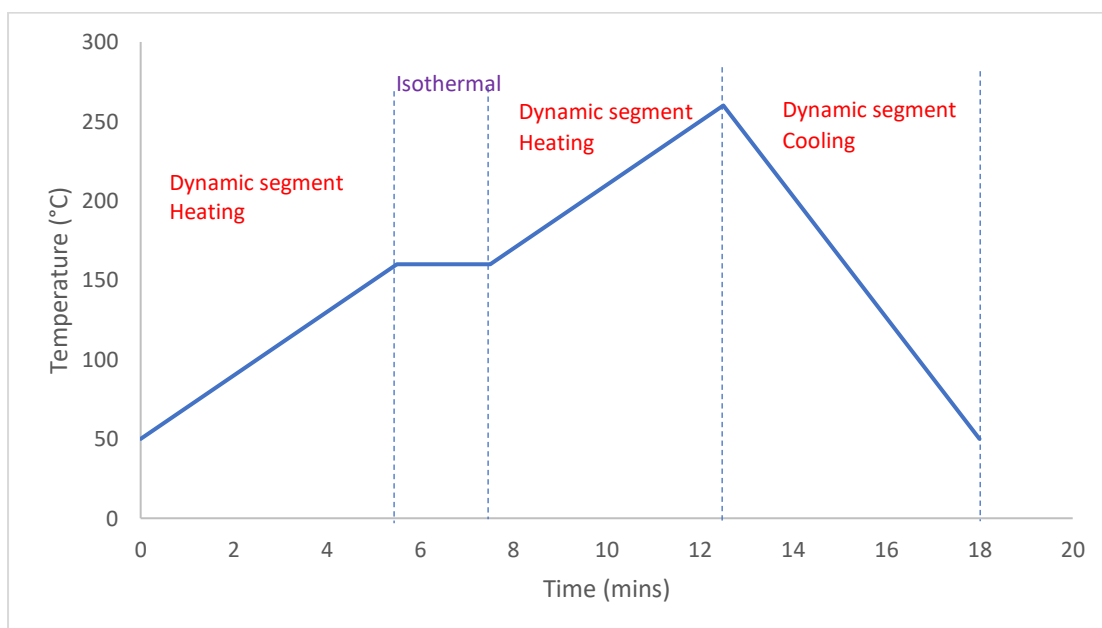
Fig 3.14 Method for HDPE analysis using STARe software.

3.12 Polymer Gear Testing

The reviewed literature has shown that the study of interacting surfaces in relative motion (tribology) has been covered by several authors [15, 21, 34, 88, 92, 95, 103]. The principle behind these studies involved meshing gears and employing a back-to-back, or closed loop testing configuration as a means of measuring the interactions. There are no universally agreed ways of testing polymer gears, but the general concepts involved are the same as those used in metallic gear testing. To investigate the tribology of HDPE gears, a new and novel gear test rig, which was developed at the University of Warwick, was used [123]. The test rig continuously measures gear wear while a constant load is applied.

3.13 Non-metallic gear test rig design concept

The design of the test rig is modelled on a back-to-back, 'four-square' design. It consists of an electric driving motor, gearbox, a pivoted bearing and test gear mounting block, and a loading bar. A Linear Vertical Displacement Transformer (LVDT) translates the linear displacement of the loading arm due to wear as an electric signal. This signal is interpreted by LabView software. A flowchart of this arrangement is shown in Fig. 3.15.
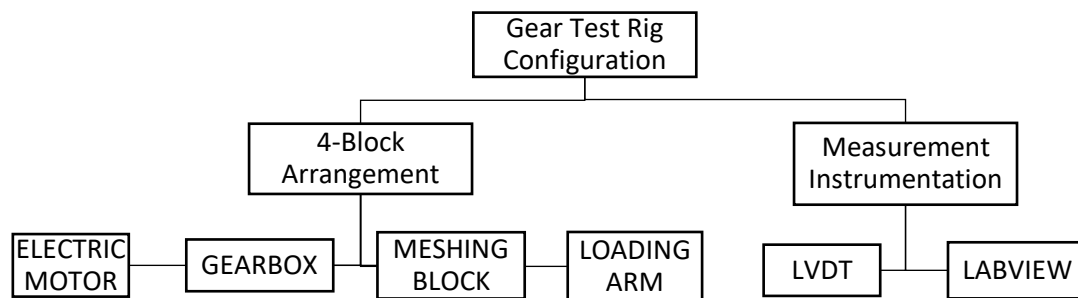
Fig. 3.15 Gear test rig configuration

A CAD and pictorial diagram of the gear test rig is shown in Fig 3.17, and 3.18, respectively.

The electric motor is a TEC single-phase and can provide a maximum power of 0.55 kW at 1500 RPM. It is attached to the gearbox through belt-driven toothed-pulleys, which can be changed to provide speeds of 500, 1000, 1500 and 2000 RPM. Fig 3.15 shows the different types of belts which were used to alter the drive speeds.

Fig 3.16 Different types of drivebelts used to alter speed.

The gearbox contains two identical metal meshing gears, which are immersed in lubricating oil. These metal gears have the same dimensional specifications as the test polymer gears. A pair of shafts with universal couplings, link the gearbox with the test gears via a pivoted bearing and test gear mounting block, thereby forming a closed circuit. This arrangement enables the electric motor to only transmit the power needed to overcome frictional resistance in the gears and bearings.

The pivoted bearing and test gear mounting block is the where the gears to be tested are meshed. The two shafts from the gearbox are supported by bearings in the block and the gears are mounted onto each shaft. The mounting block is made in two halves so that the centre distances between gear pairs can be adjusted by using different sized shims as spacers, and then clamped together. The optimum centre distance for each gear pair is obtained by measuring the induced backlash. This was done by using vernier callipers.

An important and distinct advantage of this design is that it allows polymer gears to be geometrically misaligned in the axial, radial, yaw, and pitch axes. Misalignment was not introduced in this research, but has been covered in previous studies [125, 126].
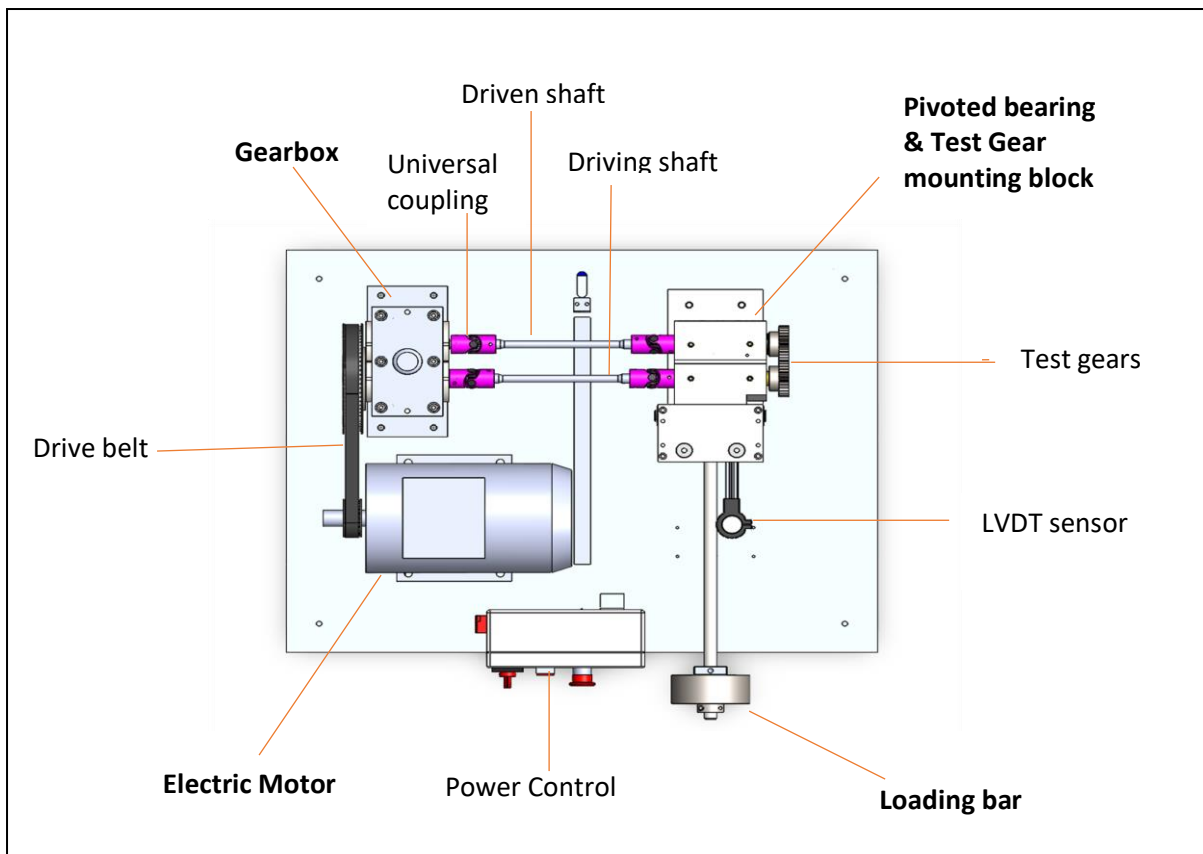
Fig 3.17 CAD diagram of non-metallic gear test rig.

Fig 3.18 Non-metallic gear test rig.

The loading arm is attached to the block at the pivot arm, and a dead-weight load can be placed along its length. As the gear teeth wear, the arm rotates from the initial equilibrium position, while maintaining a constant torque on the tested gears. Fig 19 shows movement of the pivot block as wear occurs.
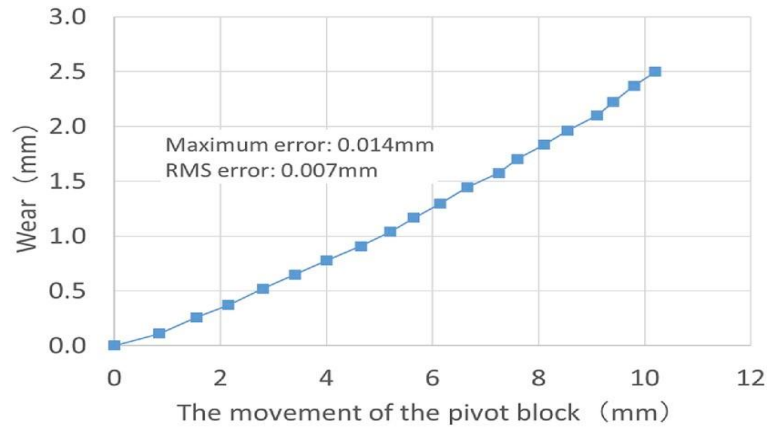
Fig 3.19 Movement of the pivot block in response to wear [123].

This rotation is measured as a linear movement at a defined point on the arm by a Linear Variable Differential Transformer (LVDT) sensor. The LVDT is covered in detail in section 3.14.

An important characteristic of this new test rig is that the load is not affected by the rotation of the arm as the gears wear. This load stability gives an accurate load to wear rate of the tested gears.

Table 3.11 Gear test rig specifications

Attributes	Value	Description
Motor rating	0.55kW	At 1500 RPM
Speed range	500 – 2000 RPM	With 1% precision
Load torque	1 – 50Nm	Stable to 1%
Maximum wear	1.6mm	Stable to 1% of 0.002mm
Temperature range	20 – 200°C	At tooth surface
Gear	1:1	Identical driving and driven gears

3.13.1 Backlash adjustment

The tested gears were produced at differing cooling temperatures, which resulted in differing outer diameters due to shrinkage. There was an average difference in diameter of 0.4mm between gears produced at 22°C and those produced at 65°C. To achieve a uniform amount of backlash between the different production temperatures, centre distance adjustments had to be made by placing different sized shims, as described in section 3.10.
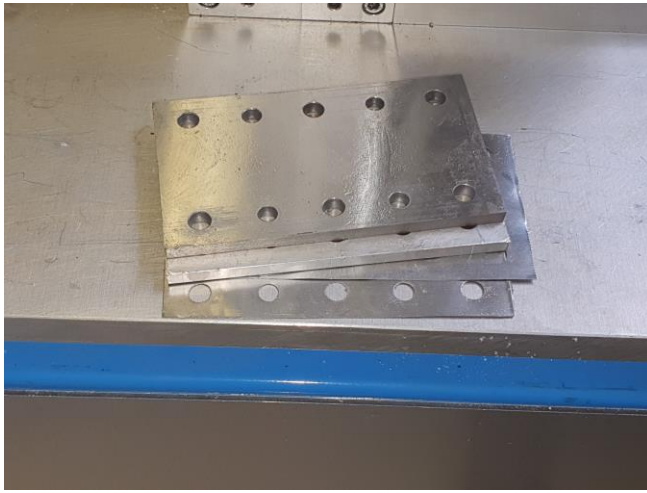
Fig 3.20 Shim plates used to adjust backlash.

3.13.2 Torque loading

Fig. 3.10.2 shows the gear loading schematic of the gear test rig. The underlying principle of this arrangement is, at equilibrium, the dead-weight (W) attached at distance L, on one side of the pivot, must be balance by an opposing force induced by the torques of the two shafts, $T1$ and $T2$.

$$WL = T1 + T2 \qquad (3.12)$$

Equation (3.12) makes the following assumptions: there's negligeable friction at the pivot; the frictional torque in the two shafts is equal; and the variation in the true dead weight due to the slight rotation, is negligeable.

Rearranging (3.12)

$$WL = 2T$$

$$T = WL/2 \qquad\qquad (3.13)$$

During the experiments, each torque setting is determined by placing weights at a particular distance from the pivot and attaching a high-quality spring balance at the end of the arm to record W. This distance is 0.5m.

Equation (3.13) becomes:

$$T = (W \times 0.5)/2 = W/4 \qquad\qquad (3.14)$$

Therefore, to determine the torque applied on the gears, W is simply divided by 4.
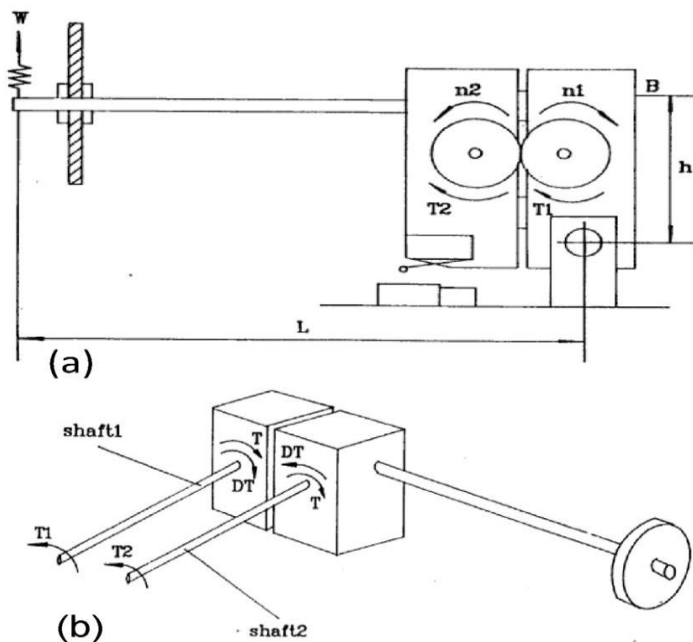
Fig 3.21 Gear loading schematic

3.14 Principles behind wear measurement technique

Meshed polymer gears experience both creep and viscoelastic deformation which contribute to 'wear'. The wear measurements, T_w, taken in this experiment is the sum of all different types of wear. Since the measured wear is for a pair of meshing gears, 0.5 of the value represents the wear per gear.

The arrangement shown in Fig 3.16(b) shows a relationship established between gear tooth surface wear and a resultant rotational movement of the loaded arm about the pivot. Mao et al [123] goes into detail as to how the pivotal rotational movement can be used to calculate tooth surface wear by considering the work-energy balance in the system. This is summarised by equation (4) below:

$$T_w = y\, d_p\, (\cos \alpha) \times \theta \qquad\qquad (3.15)$$

Where y represents the pivot block rotation, d_p is the pitch circle diameter of the test gears, and α is the pressure angle.

In practice, θ is very small (generally below 3°), and so is difficult to measure without expensive high precision transducers. For small rotation movements such as these, sufficient accuracy can be obtained by taking a linear measurement, d, along a line at a perpendicular distance, L_1, from the pivot can be taken. In this case,

$$y = d/L_1 \qquad\qquad (3.16)$$

Substituting equation (3.16) into (3.15)

$$T_w = (d/L_1)d_p\cos\alpha \qquad\qquad (3.17)$$

In order to obtain wear per gear, the value obtained in equation (3.16) is divided by 2.

Rearranging (3.17)

$$d = (T_w/d_p\cos\alpha) \times L_1 \qquad\qquad (3.18)$$

3.15 Linear Vertical Displacement Transformer

The linear displacement, d, in equation (3.18) is measured by a 20mm range inductive LVDT sensor [M14], placed at a distance of $L1$ from the pivot. It has a resolution of ±0.25%, and an accuracy of 0.1µm. Sensitivity to arm movement as wear occurs is improved by increasing L1, but this also makes measurements suspectable to errors caused by vibrations, thermal deformation, or tooth flexural distortions. The ideal distance was found to be 120mm from the pivot.

3.16 Wear rate analysis

According to VDI 2736, linear wear characterisation of gear teeth can be expressed as in equation 3.19:

$$W_m = \frac{T.2.\pi.N_L.H_V.K}{b.z.F} \qquad (3.19)$$

where:

T is the applied torque, N_L is the gear working cycle, H_V is degree of tooth loss, K is the wear coefficient of a polymer/steel gear pairing, b is gear tooth width, z is the number of gear teeth, and F is the meshing length.

The use of the wear coefficient, K, in equation 3.19 makes its use in this current study inappropriate due to two reasons:

1. It is based on a polymer/steel gear pairing. This is not the case in this study. The work done by Mao et al [82], and Wood [97], established that gear pairing has a significant bearing on the wear rate.

2. The wear rates of metallic gears have been shown to greatly vary according to the cooling rates employed during the production process. It would therefore be more appropriate to use another novel way of calculating both the wear rate and wear coefficient directly from experimental data without employing equation 3.18.

Considering these points, VDI 2736 was therefore not used.

There are two appropriate alternative methods for calculating the wear rates. The first method used is that proposed by Friedrich et al [96], and is expressed by equation 2.10. It is based on the fact that the loss of material per minute represents the rate of wear. Referring to equation 2.11:

$$k = \frac{V}{F.S}$$

where k is the specific wear rate (m^3/Nm), V is wear volume (m^3), F is the normal force (N), and S is the sliding distance (m).

If equation 2.10 is rearranged for tooth profiles, the specific wear rate for HDPE gears produced at a particular temperature, can be expressed as:

Qbd = k T/r d x n (3.20)

Rearranging equation:

$$k = \frac{Qbr}{Tn}$$ (3.21)

where Q represents wear depth, b represents tooth face width, d is tooth depth, r is gear pitch circle radius, T is time, and n is the number of cycles corresponding to the wear depth.

The second method used is simpler, and yet just as accurate and involves the calculation of the gradient of each wear curve. This enables the wear rates to be expressed in two main ways: as a function of time (mm/min); or as a function of cycles (mm/cycle).

$$\text{Wear rate (mm/min)} = \frac{Change\ in\ height\ (wear)}{Time\ taken\ (\text{min})}$$ (3.22)

$$\text{Wear rate (mm/cycle)} = \frac{Change\ in\ height\ (wear)}{Number\ of\ cycles\ (\text{cycles})}$$ (3.23)

Since this is different on each part of the curve, the average wear rate for the entire curve is taken.

3.17 Data logging system

Wear measurements are captured through a data logging system, as shown in Fig 3.22. This system consists of a 4-block gear test rig, an LVDT sensor, and LabView software.

```
                    ┌──────────┐
                    │ Voltage  │
                    │ 6v       │
                    └────┬─────┘
                         │
                         ▼
┌──────────┐        ┌──────────┐        ┌──────────┐
│ Gear test│────────│ LVDT     │────────│ LabView  │
│ rig      │        │          │        │          │
└──────────┘        └──────────┘        └────┬─────┘
                                             │
                             ┌───────────────┴──────────────┐
                        ┌──────────┐                    ┌──────────┐
                        │ Waveform │                    │ Write to │
                        │ Graph    │                    │ Excel file│
                        └──────────┘                    └──────────┘
```
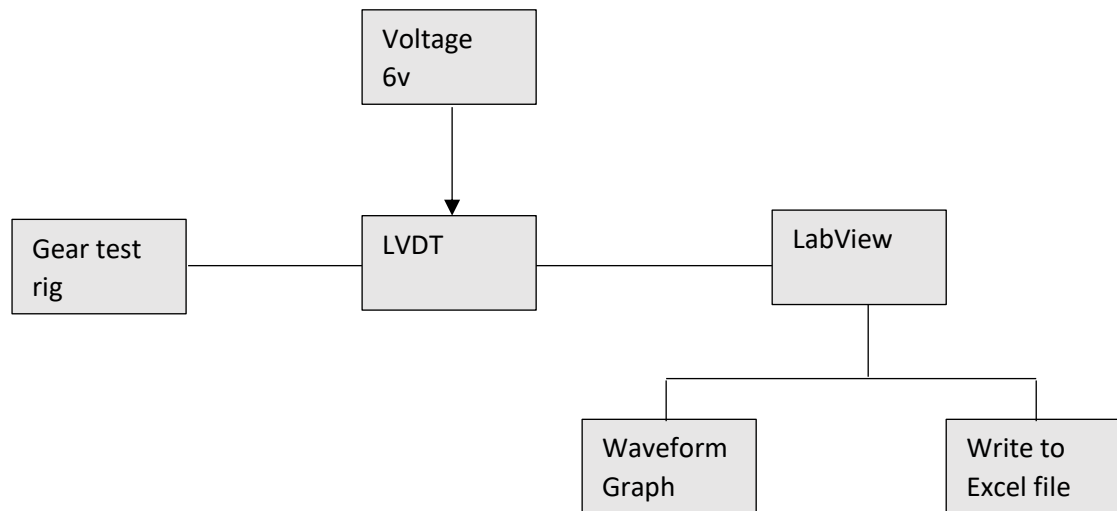
Fig 3.22 Schematic representation of data logging system.

LabView 2014 is the software used to collect the linear displacement data of the LVDT and record it as a function of time. It displays a real-time graphical representation of the LVDT position, and at the same time save data to an .xml file. The software relies on a 2-window construction: the front panel, and the block diagram. The front panel is the graphical user interface (GUI), and the block diagram is the program interacting with external instruments.

To get the gear cycles, the set RPMs are multiplied by time:

Gear cycles = RPM x time   (3.24)

3.18 Scanning Electron Microscopy (SEM) analysis

SEM was used to examine gear teeth surfaces in order analyse the mechanism of wear for gears produced at different mould temperatures and subjected to different test conditions. It works by focusing and scanning a beam of electrons over a surface and producing an image as shown by the schematic diagram in Fig 3.23(a) and Fig 3.23(b)

A Philips XL30 ESEM scanner was used to perform worn gear analysis. It uses a point-source tungsten cathode gun with a surface layer of zirconium oxide (ZrO), and is based on a Schottky design. Fig 3.23(b). The Schottky-emission effect is a phenomenon in which thermo-electrons are easily emitted from a heated metal surface when a strong electric field is applied, due to the lowering of the potential

barrier. Coating of ZrO greatly reduces the work function enabling a large emission current to be obtained at a relatively low cathode temperature of about 1800K.

(a)   (b)
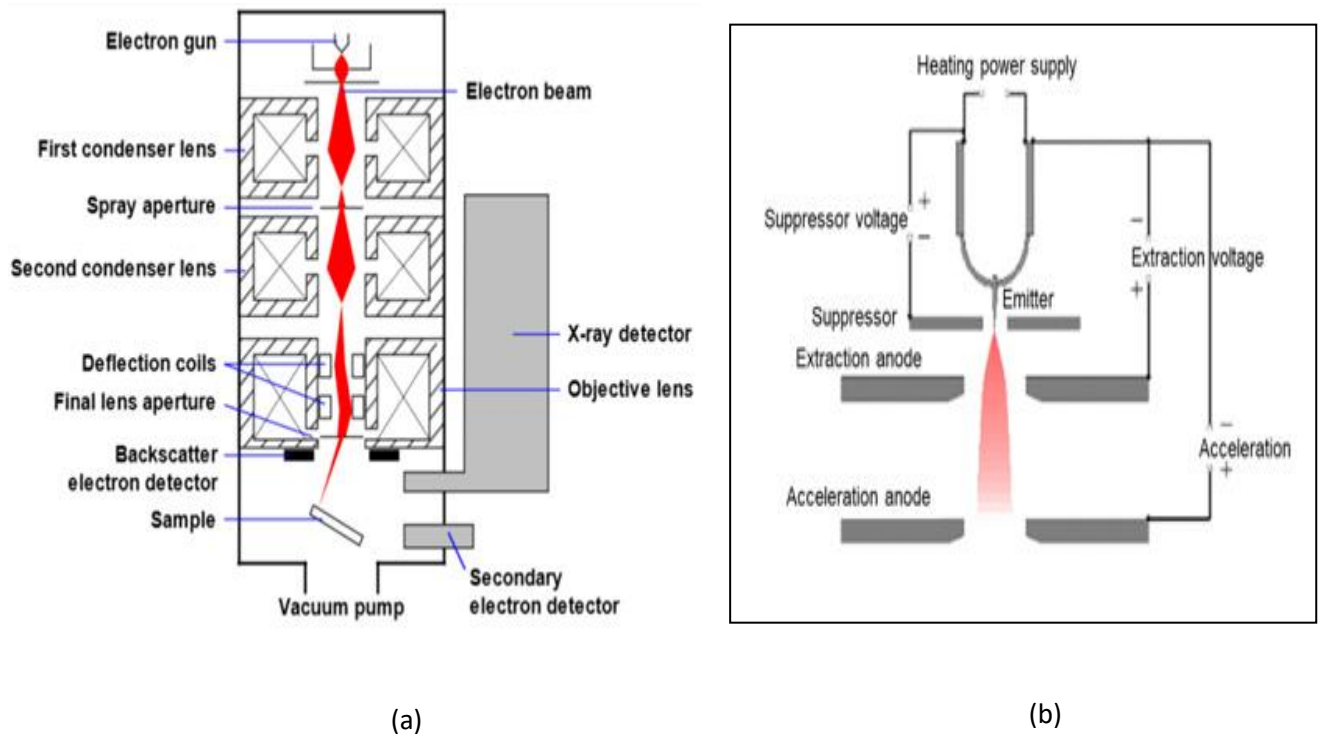
Fig 3.23 (a) Schematic of a scanning electron microscope (b) Basic structure of a Schottky-emission electron

Fig 3.24 Philips XL30 ESEM scanning machine.

3.18.1 Sample preparation and analysis procedure

Samples not bigger than 5mm in length, width or depth are attached onto a holding flat-surfaced pan and placed into a Bio-Rad SEM (Philips) coating system, where they are gold coated in a vacuous environment, before being placed into an analysing chamber. The gold coating creates a conductive layer on the sample surface which promotes the emission of secondary electrons, thereby improving the topographic imaging of the sample. The chamber is then vented to a pressure of between 3 – 2.5 x 10^{-7} Pa. Once this is reached, the distance between the sample and lens, together with the brightness and contrast, is adjusted so that the illuminated area of the sample starts to show some detail.

An accelerating voltage of 10kV was used as it enabled good penetration depth of the incident electrons, resulting in good image resolution.

The magnification factor was varied from 20 times (20x) to 500 times (50x). A lower magnification enabled a broad section of the sample to be viewed, giving a 'fisheye' view, while a higher magnification enabled the focusing of a specific spot of the surface.

3.19 Summary

It has been shown that each stage of this experimental research requires a unique methodological approach to achieve the expected objective. The methodologies employed, and equipment used at different experimental stages of this research project have been discussed in detail.

During the injection moulding stage, the Taguchi DoE was shown to produce a robust production process.

The measured parameters during gear manufacture, gear testing, and DSC analysis have been identified and controlled to give a comprehensive thorough manufacturing process.

CHAPTER 4

PRODUCTION OF HDPE GEARS USING INJECTION MOULDING

_____

4.1 INTRODUCTION

This chapter outlines an in-depth analysis of injection moulding as the process used to produce HDPE gears. The Taguchi design of experiments described in chapter 3 is applied in order to produce high quality gears by first obtaining optimised input parameters and holding these constant while varying the mould temperatures.

4.2 Material preparation

As outlined in Table 4.1, the HDPE grade used is Holstalen GC 7260, with a low water absorption of less than 0.05 at 23°C. Although this is very low, the material was dried at 30°C for 30mins using an Engel air dryer before each experimental run.

4.3 Engel Victory 60T injection moulding machine

The graphical user interface (GUI) panel enables the user to input desired parameters.
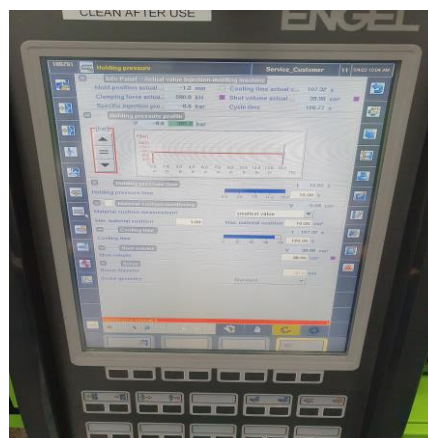
Fig 4.1 Engel Victory 60T GUI

Once the machine is switched on, and the boot process completes, all input parameters are entered. The desired mould temperature is set into the external chillers, which pump coolant at the set temperature via connecting hoses.

4.4 Processing parameters chosen for optimization

To isolate mould temperature as the single processing parameter to be varied, all other input parameters need to be optimised so that they do not become 'noise'. Four parameters were chosen for optimisation: melt temperature, injection volume, hold pressure, and hold time. As discussed in Chapter 3, these parameters were chosen because they represent each of the four main categories outlined by the Ishikawa diagram (Fig 2.7). The median value of the range supplied by the manufacturer were used for all other input parameters. The optimised and median values are then held constant.

4.5 Parameter Optimisation

The input optimisation parameter levels are high, medium, and low. This makes the experiment a 3-level, 4-factor experiment.

The input values for the four factors are listed in Table 4.1.

Table 4.1 Variable factor level

Factors	Level 1	Level 2	Level 3
Melt temperature, A (°C)	180	200	225
Injection volume, B (cm^3)	38	40	42
Hold pressure, C (MPa)	70	80	90
Hold time, D (s)	15	30	45

Using the Taguchi design of experiment notation:

$$\text{Number of Experiments} = L_i^{(F-1)} \qquad (4.1)$$

Where L_i is the number of levels, F is the number of factors.

Substituting 3-levels, 4-factors into equation 4.1:

Number of Experiments = $L_i^{(F-1)} = 3^{(4-1)} = 27$

An L_{27} orthogonal array is therefore chosen, Table 4.2

Table 4.2 L27 Orthogonal Array

L_{27} **Orthogonal Array**							
Independent Variables					Gear features		
Experiment #	Melt temperature (A)	Injection volume (B)	Hold Pressure (C)	Hold time (D)	Gear Diameter	Gear Mass	S/N
1	1	1	1	1	D_1	M_1	
2	1	2	2	2	D_2	M_2	
3	1	3	3	3	D_3	M_3	
4	1	1	1	2	D_4	M_4	
5	1	2	2	3	D_5	M_5	
6	1	3	3	1	D_6	M_6	
7	1	1	1	3	D_7	M_7	
8	1	2	2	1	D_8	M_8	
9	1	3	3	2	D_9	M_9	
10	2	2	3	1	D_{10}	M_{10}	
11	2	3	1	2	D_{11}	M_{11}	
12	2	1	2	3	D_{12}	M_{12}	
13	2	2	3	2	D_{13}	M_{13}	
14	2	3	1	3	D_{14}	M_{14}	
15	2	1	2	1	D_{15}	M_{15}	
16	2	2	3	3	D_{16}	M_{16}	
17	2	3	1	1	D_{17}	M_{17}	
18	2	1	2	2	D_{18}	M_{18}	
19	3	3	2	1	D_{19}	M_{19}	
20	3	1	3	2	D_{20}	M_{20}	
21	3	2	1	3	D_{21}	M_{21}	
22	3	3	2	2	D_{22}	M_{22}	
23	3	1	3	3	D_{23}	M_{23}	
24	3	2	1	1	D_{24}	M_{24}	
25	3	3	2	3	D_{25}	M_{25}	
26	3	1	3	1	D_{26}	M_{26}	
27	3	2	1	2	D_{27}	M_{27}	

4.5.1 Melt temperature

The reviewed literature has shown that melt temperature is one of the most fundamental variables in the injection moulding process [118 - 121]. For the purposes of this study, it is defined as the temperature of the molten HDPE material as it exits the nozzle and enters the mould cavity. Before

commencement of production, the melt temperature is measured by pouring the melt into a Teflon cup and inserting a thermo-probe into the melt.

The temperatures of the four heating zones of the barrel are set to aid in the plasticization of the material as it moves along the barrel. Table 4.3 shows the different temperature settings for each level.

Table 4.3 Barrel heating settings

Level Setting	Temperature setting ($^\circ$C)			
	Zone 0	Zone 1	Zone 2	Zone 3
1	180	170	160	150
2	200	190	180	170
3	225	215	205	195

4.5.1.1 Level 1 temperature setting

Using the L27 orthogonal array shown in Table 4.2, level 1 temperature settings are held constant between experiment number 1 and number 9, while the injection volume, hold pressure and hold time parameters are changed according to the outlined combinations.

The deviation of gear diameter from that of the mould is expressed a percentage using equation 3.4.

Table 4.4 shows the results of level 1 melt temperature settings. The least amount of gear diameter shrinkage for a melt temperature of 180°C is obtained when all other input factors are at maximum value. This is consistent with the findings of Bain et al [128] and Han et al [129] who reported that a low melt temperature and high hold pressure resulted in less shrinkage.

Table 4.4 Level 1 melt temperature

Experiment #	Melt temperature (A)	Injection volume (B)	Hold Pressure (C)	Hold time (D)	Change in Diameter (% Shrinkage)	S/N Ratio (dB)
1	180	38	70	15	2.812	-8.980
2	180	40	80	30	1.995	-5.999
3	180	42	90	45	1.715	-4.685
4	180	38	70	30	2.574	-8.212
5	180	40	80	45	2.383	-7.542
6	180	42	90	15	2.193	-6.821
7	180	38	70	45	2.574	-8.212
8	180	40	80	15	2.24	-7.005
9	180	42	90	30	1.906	-5.602

4.5.1.2 Level 2 temperature setting

The nozzle exit melt temperature for level 2 is 200°C. Table 4.5 represents the input factor combinations, and the resultant change in diameter.

Table 4.5 Level 2 melt temperature

Experiment #	Melt temperature (A)	Injection volume (B)	Hold Pressure (C)	Hold time (D)	Change in Diameter (%)	S/N Ratio (dB)
10	200	40	90	15	2.05	-6.235
11	200	42	70	30	2.478	-7.882
12	200	38	80	45	2.097	-6.432
13	200	40	90	30	1.668	-4.444
14	200	42	70	45	2.002	-6.029
15	200	38	80	15	2.144	-6.624
16	200	40	90	45	1.621	-4.196
17	200	42	70	15	2.765	-8.834
18	200	38	80	30	2.478	-7.882

Experiment number (#) 16 shows the least amount of shrinkage. This represents an injection volume of 40cm^3, a hold pressure of 90MPa, and a hold time of 45 secs. Although the hold pressure and hold time are at maximum values, the injection volume has decreased to level 2. This suggests that the density of HDPE has increased as the melt temperature rises. An increase in density is indicative of an increase in molecular weight, as shown by equation 3.2.

4.5.1.3 Level 3 temperature setting

The nozzle exit melt temperature for level 3 is 225°C.

Table 4.6 Level 3 melt temperature

Experiment #	Melt temperature (A)	Injection volume (B)	Hold Pressure (C)	Hold time (D)	Change in Diameter (%)	S/N Ratio (dB)
19	225	42	80	15	1.906	-5.602
20	225	38	90	30	2.002	-6.029
21	225	40	70	45	1.859	-5.386
22	225	42	80	30	1.906	-5.602
23	225	38	90	45	1.525	-3.665
24	225	40	70	15	2.383	-7.542
25	225	42	80	45	1.763	-4.925
26	225	38	90	15	2.002	-6.029
27	225	40	70	30	2.29	-7.197

Experiment # 23 shows the parameter combination which produces the least amount of shrinkage. As the temperature increases to level 3, the least amount of shrinkage is obtained by employing the maximum holding pressure and maximum holding time, but the injection volume needed has reduced to minimum. This finding is consistent with the work conducted by previous authors [120, 128, 129]. This is most likely due to three main reasons:

➢ An increase in density

➢ An increase in material viscosity

➢ A shorter cavity fill time.

Table 4.7 Variation of injection volume with temperature

Melt temperature (°C)	Injection Volume (m^3)
180	42
200	40
225	38
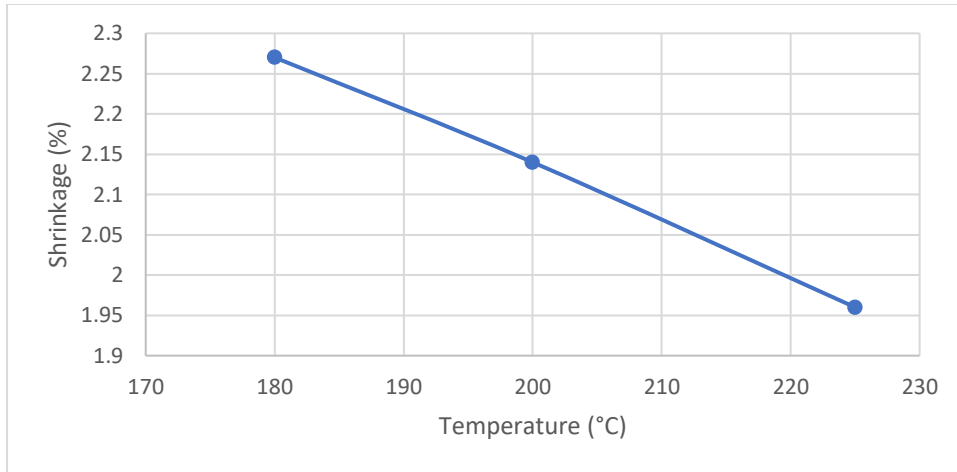
Fig 4.2 Changes in shrinkage with increase in melt temperature

Combining Tables 4.4, 4.5 and 4.6 gives a complete L27 orthogonal array, as shown in Table 4.8.

Table 4.8 L27 orthogonal array

Experiment #	Melt temperature (A)	Injection volume (B)	Hold Pressure (C)	Hold time (D)	Change in Diameter (%)	S/N Ratio (dB)
1	180	38	70	15	2.812	-8.980
2	180	40	80	30	1.995	-5.999
3	180	42	90	45	1.715	-4.685
4	180	38	70	30	2.574	-8.212
5	180	40	80	45	2.383	-7.542
6	180	42	90	15	2.193	-6.821
7	180	38	70	45	2.574	-8.212
8	180	40	80	15	2.24	-7.005
9	180	42	90	30	1.906	-5.602
10	200	40	90	15	2.05	-6.235
11	200	42	70	30	2.478	-7.882
12	200	38	80	45	2.097	-6.432
13	200	40	90	30	1.668	-4.444
14	200	42	70	45	2.002	-6.029
15	200	38	80	15	2.144	-6.624
16	200	40	90	45	1.621	-4.196
17	200	42	70	15	2.765	-8.834
18	200	38	80	30	2.478	-7.882
19	225	42	80	15	1.906	-5.602
20	225	38	90	30	2.002	-6.029
21	225	40	70	45	1.859	-5.386
22	225	42	80	30	1.906	-5.602
23	225	38	90	45	1.525	-3.665
24	225	40	70	15	2.383	-7.542
25	225	42	80	45	1.763	-4.925
26	225	38	90	15	2.002	-6.029
27	222	40	70	30	2.29	-7.197

4.5.1.4 Identification of optimum melt temperature

To identify the optimum melt temperature, an average value of the S/N ratio for each temperature level setting is taken. The setting with the highest S/N ratio is the optimum temperature setting, in this case, 225°C. Table 4.9.

Table 4.9 Melt temperature S/N Ratio

	S/N Ratio
Level 1	-7.006
Level 2	-6.506
Level 3	-5.775
Difference	-1.231

4.5.1.5 Visual observations for different melt temperatures

It was observed that HDPE gears produced at 180°C showed a dull white natural colour compared to those which were produced at 225°C. For a melt temperature of 235°C, the following observations were made:

i.   White gases with a pungent smell begun to come out of the nozzle.

ii.   The colour of the gears transitioned from an opaque white colour to a slightly translucent white. This was indictive of material degradation due to high melt temperatures.

For temperatures just below 180°C, gears with an uneven texture were produced. This was because of un-melted HDPE pellets being injected into the mould.

4.5.2 Injection volume

The injection volume (shot volume) is varied from 38cm^3, to 40cm^3 and 42cm^3.

4.5.2.1 Level 1 injection volume

Taking the injection volume values of Level 1 from Table 4.8 produces Table 4.10.

Table 4.10 Level 1 injection volume

Experiment #	Injection Vol	Melt Temperature	Hold Pressure	Hold Time	Change in Diameter (%)	S/N Ratio
1	38	180	70	15	2.812	-8.980
2	38	180	70	30	2.574	-8.212
3	38	180	70	45	2.574	-8.212
4	38	200	80	45	2.097	-6.432
5	38	200	80	15	2.144	-6.624
6	38	200	80	30	2.478	-7.882
7	38	225	90	30	2.002	-6.029
8	38	225	90	45	1.525	-3.665
9	38	225	90	15	2.002	-6.029

4.5.2.2 Level 2 injection volume

Level 2 injection volume is 40cm^3.

Table 4.11 Level 2 injection volume

Experiment #	Injection Vol	Melt Temperature	Hold Pressure	Hold Time	Change in Diameter (%)	S/N Ratio
10	40	180	80	30	1.995	-5.999
11	40	180	80	45	2.383	-7.542
12	40	180	80	15	2.24	-7.005
13	40	200	90	15	2.05	-6.235
14	40	200	90	30	1.668	-4.444
15	40	200	90	45	1.621	-4.196
16	40	225	70	45	1.859	-5.386
17	40	225	70	15	2.383	-7.542
18	40	225	70	30	2.29	-7.197

4.5.2.3 Level 3 injection volume

Level 3 injection volume is 42cm^3

Table 4.12 Level 3 injection volume

Experiment #	Injection Vol	Melt Temperature	Hold Pressure	Hold Time	Change in Diameter (%)	S/N Ratio
19	42	180	90	45	1.715	-4.685
20	42	180	90	15	2.193	-6.821
21	42	180	90	30	1.906	-5.602
22	42	200	70	30	2.478	-7.882
23	42	200	70	45	2.002	-6.029
24	42	200	70	15	2.765	-8.834
25	42	225	80	15	1.906	-5.602
26	42	225	80	30	1.906	-5.602
27	42	225	80	45	1.763	-4.925
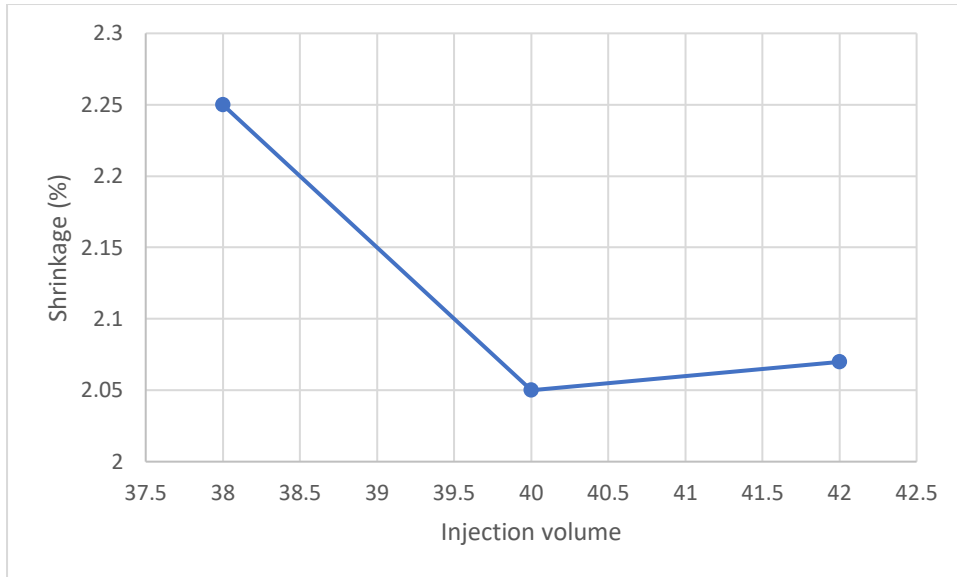
Fig 4.4 Effects of injection volume on shrinkage

4.5.2.4 Identification of optimum injection volume

Fig 4.4 shows that minimum shrinkage is attained at $40cm^3$.

The average S/N values are shown in Table 4.13.

Table 4.13 Injection volume S/N Ratio

Level setting	S/N Ratio
Level 1	-6.896
Level 2	-6.172
Level 3	-6.220
Difference	-0.724

The highest S/N ratio is for level 2. The optimum injection volume is therefore $40cm^3$.

A difference of -0.724 in the S/N ratio shows that there is little variation in shrinkage as the injection volume is varied.

4.5.2.5 Visual observations for different injection volumes

The variation of injection volume between level 1 and 3 did not produce any obvious visual differences. Interesting observations were, however, noticed at injection volumes which were slightly outside these levels.

An injection volume of 36cm^3 produced HDPE gears which had regions of unequal shrinkage (warpage) and were deformed. This was an indication of insufficient material being injected into the mould, as shown in Fig 4.5(a).

(a)	(b)
Fig 4.5 Insufficient injected material (36cm3)	Too much material injected (44cm3)

Gears produced at 44cm^3 showed signs of material 'flash', Fig 4.5(b), indicating too much material being injected into the mould.

4.5.3 Hold pressure

The hold pressure was varied between 70MPa and 90MPa, as shown in Table 4.14.

4.5.3.1 Level 1 hold pressure

Table 4.14 Hold pressure level 1

Experiment #	Hold pressure	Melt Temperature	Injection Vol	Hold Time	Change in Diameter (%)	S/N Ratio
1	70	180	38	15	2.812	-8.980
2	70	180	38	30	2.574	-8.212
3	70	180	38	45	2.574	-8.212
4	70	200	42	30	2.478	-7.882
5	70	200	42	45	2.002	-6.029
6	70	200	42	15	2.765	-8.834
7	70	225	40	45	1.859	-5.386
8	70	225	40	15	2.383	-7.542
9	70	225	40	30	2.29	-7.197

4.5.3.2 Level 2 hold pressure

Table 4.15 Hold pressure level 2

Experiment #	Hold pressure	Melt Temperature	Injection Vol	Hold Time	Change in Diameter (%)	S/N Ratio
10	80	180	40	30	1.995	-5.999
11	80	180	40	45	2.383	-7.542
12	80	180	40	15	2.24	-7.005
13	80	200	38	45	2.097	-6.432
14	80	200	38	15	2.144	-6.624
15	80	200	38	30	2.478	-7.882
16	80	225	42	15	1.906	-5.602
17	80	225	42	30	1.906	-5.602
18	80	225	42	45	1.763	-4.925

4.5.3.3 Level 3 hold pressure

Table 4.16 Hold pressure Level 3

Experiment #	Hold pressure	Melt Temperature	Injection Vol	Hold Time	Change in Diameter (%)	S/N Ratio
19	90	180	42	45	1.715	-4.685
20	90	180	42	15	2.193	-6.821
21	90	180	42	30	1.906	-5.602
22	90	200	40	15	2.05	-6.235
23	90	200	40	30	1.668	-4.444
24	90	200	40	45	1.621	-4.196
25	90	225	38	30	2.002	-6.029
26	90	225	38	45	1.525	-3.665
27	0	225	38	15	2.002	-6.029
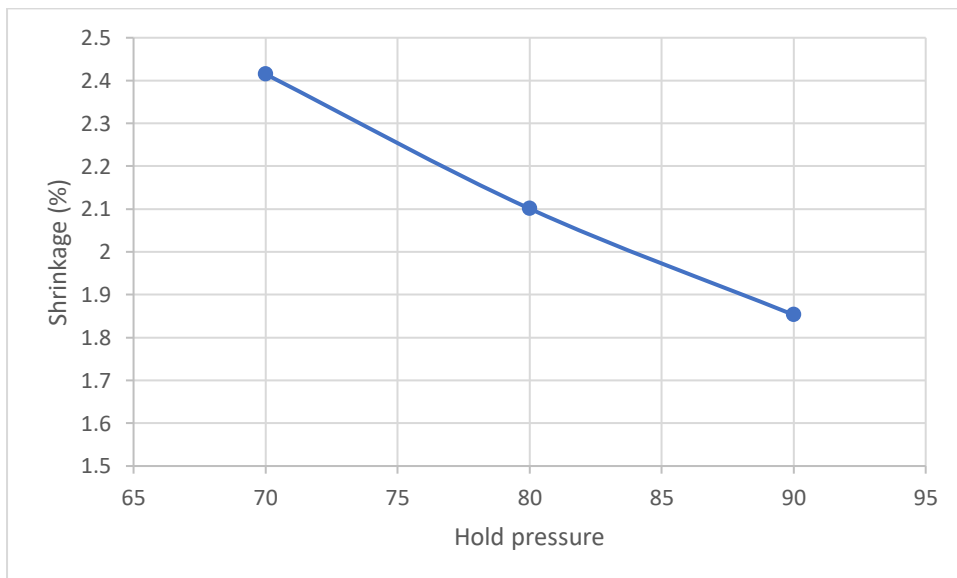
Fig 4.6 Change in shrinkage with hold pressure

4.5.3.4 Identification of optimum Hold Pressure

Table 4.17 Hold pressure S/N ratio

	S/N Ratio
Level 1	-7.586
Level 2	-6.401
Level 3	-5.301
Difference	-2.285

Using the results of Table 4.17, the optimum hold pressure value is 90MPa.

4.5.4 Hold Time

The hold time was varied between 15 and 45 seconds.

4.5.4.1 Level 1 hold time

Table 4.18 Hold time level 1

Experiment #	Hold Time	Hold Pressure	Melt Temperature	Injection vol	Change in Diameter (%)	S/N Ratio
1	15	70	180	38	2.812	-8.98
2	15	90	180	42	2.193	-6.821
3	15	80	180	40	2.24	-7.005
4	15	90	200	40	2.05	-6.235
5	15	80	200	38	2.144	-6.624
6	15	70	200	42	2.765	-8.834
7	15	80	220	42	1.906	-5.602
8	15	70	220	40	2.33	-7.542
9	15	90	220	38	2.002	-6.029

4.5.4.2 Level 2 Hold Time

Table 4.19 Hold time level 2

Experiment #	Hold Time	Hold Pressure	Melt Temperature	Injection vol	Change in Diameter (%)	S/N Ratio
10	30	80	180	40	1.995	-5.999
11	30	70	180	38	2.574	-8.212
12	30	90	180	42	1.906	-5.602
13	30	70	200	42	2.478	-7.882
14	30	90	200	40	1.668	-4.444
15	30	80	200	38	2.478	-7.882
16	30	90	225	38	2.002	-6.029
17	30	80	225	42	1.906	-5.602
18	30	70	225	40	2.29	-7.197

4.5.4.3 Level 3 Hold Time

Table 4.20 Hold time level 3

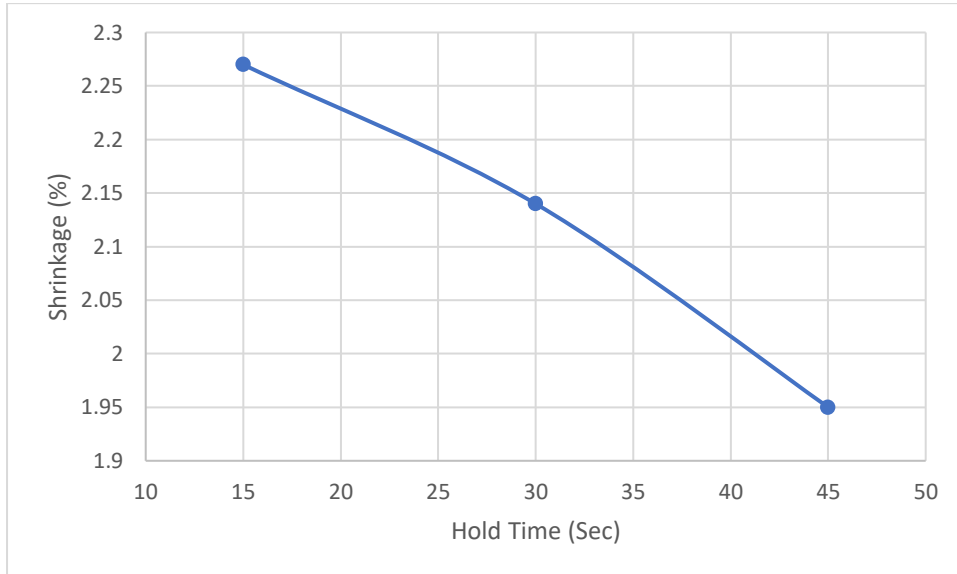| Experiment #	Hold Time	Hold Pressure	Melt Temperature	Injection vol	Change in Diameter (%)	S/N Ratio
19	45	90	180	42	1.715	-4.685
20	45	80	180	40	2.383	-7.542
21	45	70	180	38	2.574	-8.212
22	45	80	200	38	2.097	-6.432
23	45	70	200	42	2.002	-6.029
24	45	90	200	40	1.621	-4.196
25	45	70	225	40	1.859	-5.386
26	45	90	225	38	1.525	-3.665
27	45	80	225	42	1.763	-4.925

Fig 4.7 Variation of shrinkage with hold time

4.5.4.4 Identification of optimum Hold Time

Table 4.21 Optimum hold time S/N ratio

Level setting	S/N Ratio
Level 1	-7.075
Level 2	-6.539
Level 3	-5.675
Difference	-1.400

The optimum hold time is level 3, 45 seconds.

4.6 Optimum parameter results

The overall response S/N ratios are presented in Table 4.22, and the optimum values for the melt temperature, injection volume, hold pressure and hold time are presented in Table 4.23.

Table 4.22 Response table of S/N ratios for HDPE

	Melt temperature	Injection volume	Hold pressure	Hold time
Level 1	-7.006	-6.896	-7.586	-6.821
Level 2	-6.506	-6.172	-6.401	-7.075
Level 3	-5.775	-6.220	-5.301	-6.539
Difference	-1.231	-0.724	-2.285	-0.536

Table 4.23 Optimum input factors

Input parameter	Optimum value
Melt temperature	225°C
Injection volume	40cm^3
Hold pressure	90MPa
Hold time	45 Secs

The experimental data results presented above show that varying input parameters produces different shrinkage rates.

Fig 4.8 shows the effects of input parameters on shrinkage using the data provided in Table 4.22.
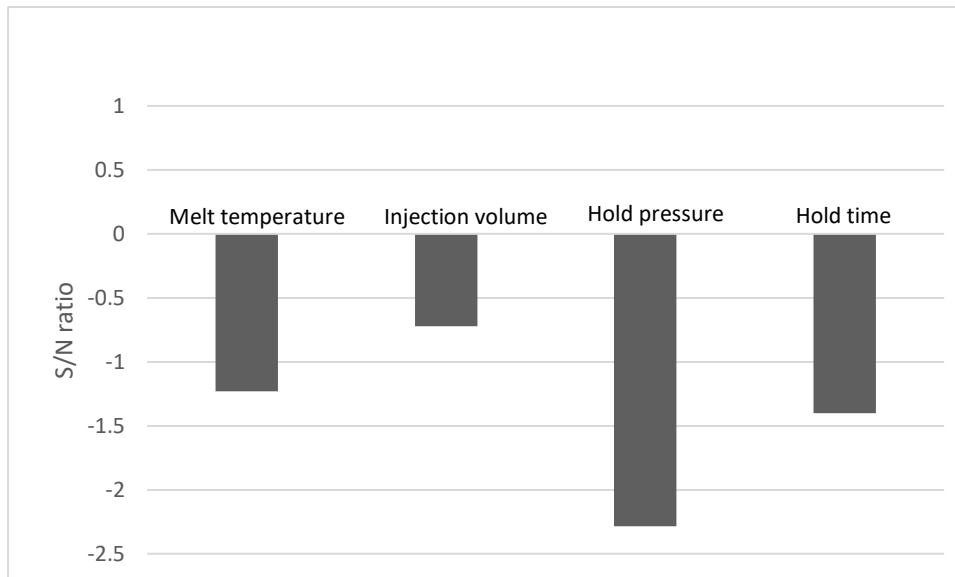
Fig 4.8 Effects of input parameters on shrinkage for HDPE

The highest S/N variation of any parameter between its level settings is shown by the holding pressure. This means that the hold pressure is the single most important variable affecting as-mould shrinkage in HDPE gears. The data also reveals that hold time and melt temperature, have very close effectual values in HDPE shrinkage.

The hold time determines how long the hold pressure is applied for, and if this is less than the gate freeze time, then an increase in shrinkage will occur.

An increase in melt temperature resulted in less shrinkage. This seems to be due to the change in viscosity and density of the material. A change in density does not seem to affect shrinkage during the filling stage, but seems to be playing an important role during the solidification phase. As the melt begins to solidify in the mould, shrinkage starts to occur, and if the hold pressure is continuously applied, more material is packed into the void left by the shrinking part, until the either the hold time limit is reached, or solidification and gate freeze occurs. The rate at which the molten material continues to flow (mass flow rate) as it solidifies is represented in Fig 4.9.
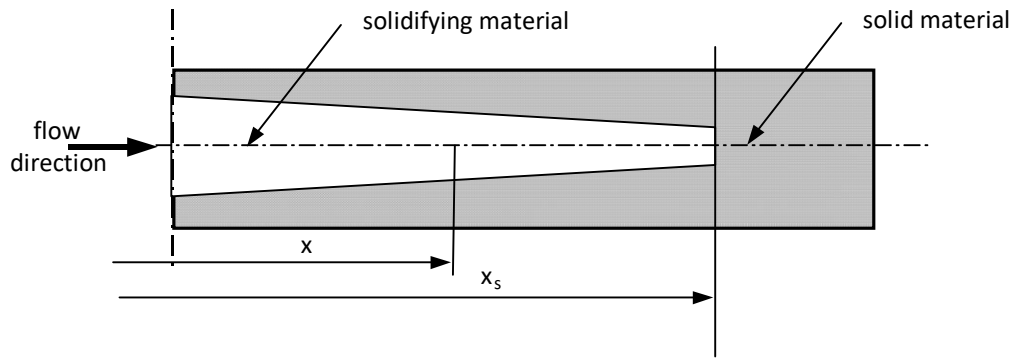
Fig 4.9 Schematic view of the solidification process

Fig 4.9 shows a schematic view of the solidification process taken at a cross-section perpendicular to the main flow direction. Point x_s represents the distance from the injection nozzle to section at which the material has completely solidified. The material viscosity is determined by variations in temperature, pressure, and the solidification (crystallisation) process. As x_s reduces towards x, both the viscosity and density of the material reduce. Complete solidification occurs when x_s = x.

4.6.1 Shrinkage after 24 hours

The gears were left at room temperature for 24 hours after production, and shrinkage measurements were taken again taken. It can be seen in Fig 4.10 that the shrinkage caused by melt temperatures has increased the most, from 1.96% to 2.05%.
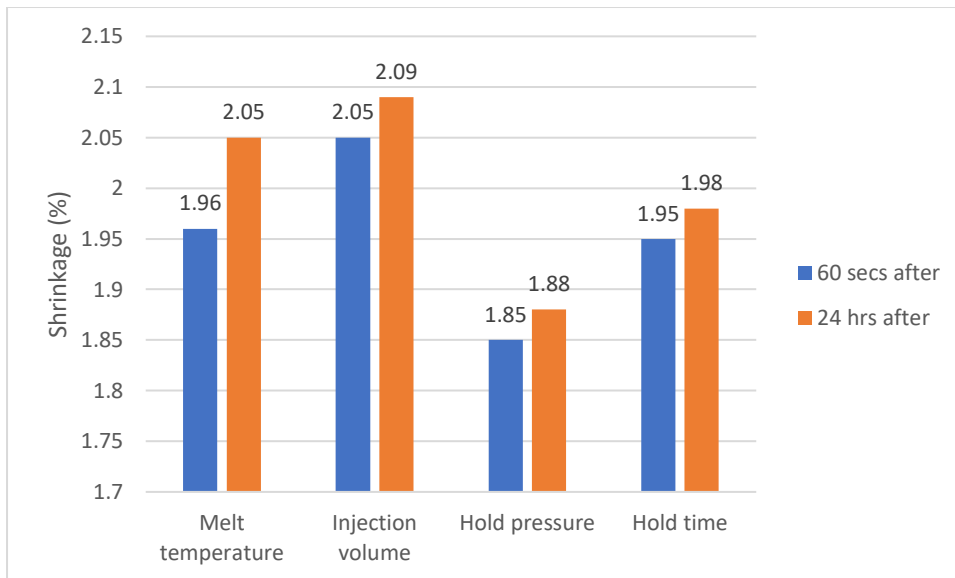
Fig 4.10 Comparison of shrinkage after 60 secs and 24 hours after production

4.7 HDPE gear production using optimised parameter values

4.7.1 Mould temperature

The mould temperature determines the actual temperature at which the injected melt is cooled. This can also be referred to as the cooling rate, or cooling time. The aim is to employ the optimised input values obtained and keep them constant, while using different mould temperature settings. Analysis will then be carried out to ascertain what effects this has on crystallinity, physical appearance, performance, and on wear rates.

4.7.2 Experimental procedure

The mould temperature settings used were 22°C, 34°C, 50°C, and 65°C.

An average of ten gears are produced for each temperature setting and the average diameter and mass are recorded, as shown in Table 4.23.

Early experimental runs noted that the set mould cavity temperature tended to creep upwards by 3 to 4°C soon after opening and ejecting a moulded gear. This meant that the cycle time between successive runs was set to 2 minutes to enable uniformity of cavity temperature to the set value to be

reattained. It was therefore important to ensure that thermal degradation did not occur by exceeding the recommended MRT of 3 to 5 minutes. Using equation 3.3:

$$\text{MRT} = \frac{\pi D^3}{v} \ x \ \frac{t}{60}$$

where MRT = 3 mins, D = 30cm, v = 40cm^3

$$t = \frac{60 \ x \ v \ x \ MRT}{\pi D^3} = \frac{60 \ x \ 0.04 \ x \ 3}{\pi (0.3)^3} = 84.9 \text{ secs}$$

The maximum amount of time which the melt could therefore be kept in the barrel was 85 seconds. Since the injected melt cooling time was 60 seconds, and the mould temperature recovery time was set to 2 minutes, the maximum MRT of 85 seconds was exceed. The melt in the barrel therefore needed to be emptied and refilled with fresh melt between each cycle run.

Table 4.24 Mould temperature influences

Mould Temperature (°C)	Diameter (mm)	Mass (g)	Shrinkage (%)
22	62.4	28.4	2.5
34	62.8	28.9	1.9
50	63.0	29.6	1.6
65	63.5	30.3	0.78

4.8 DSC analysis

Samples of between 4 and 6 grams from each mould temperature group were taken at identical points on each gear as identified in Fig 3.11. Each sample was subjected to thermo-analysis as described in section 3.8.6. The peak melting temperature from each thermogram reflects the amount of crystallinity.
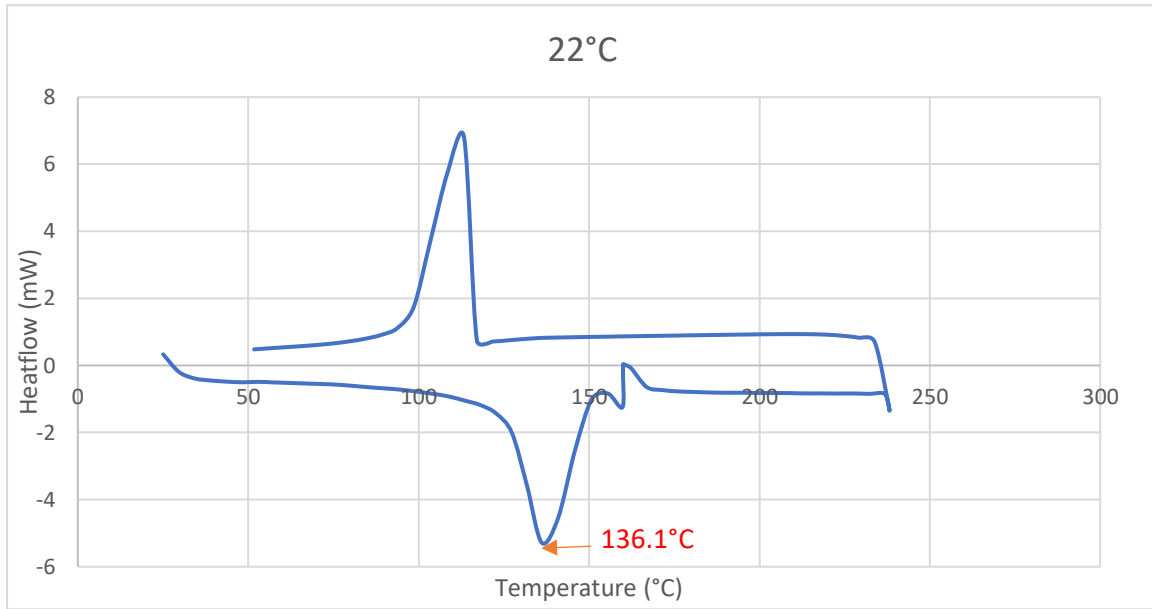
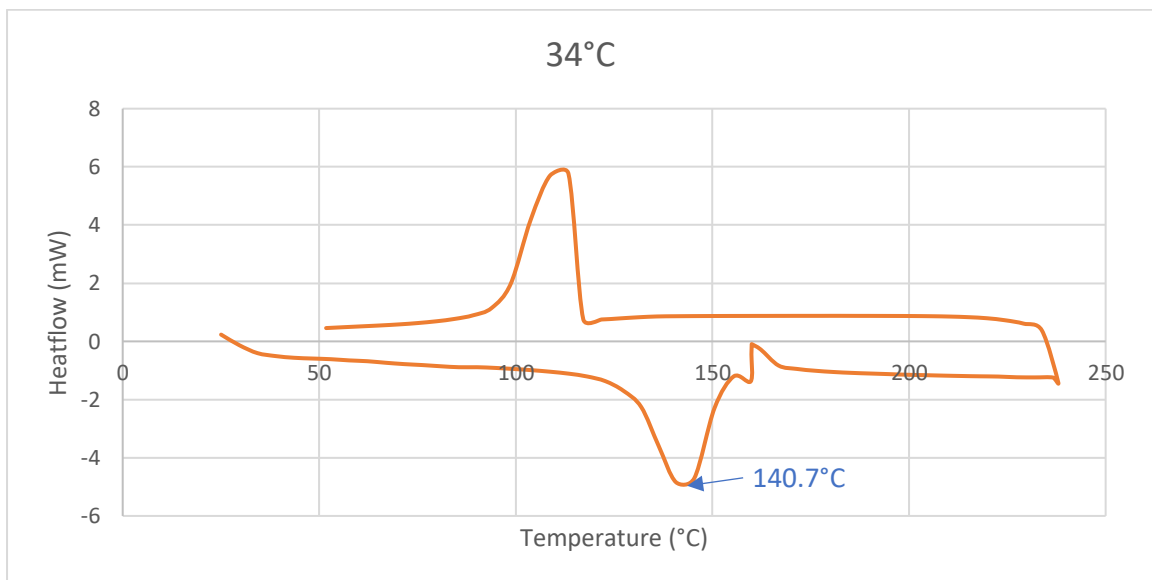Fig 4.11 22°C thermogram showing a peak melting temperature of 136.1°C

Fig 4.12 34°C thermogram showing a peak melting temperature of 140.7°C
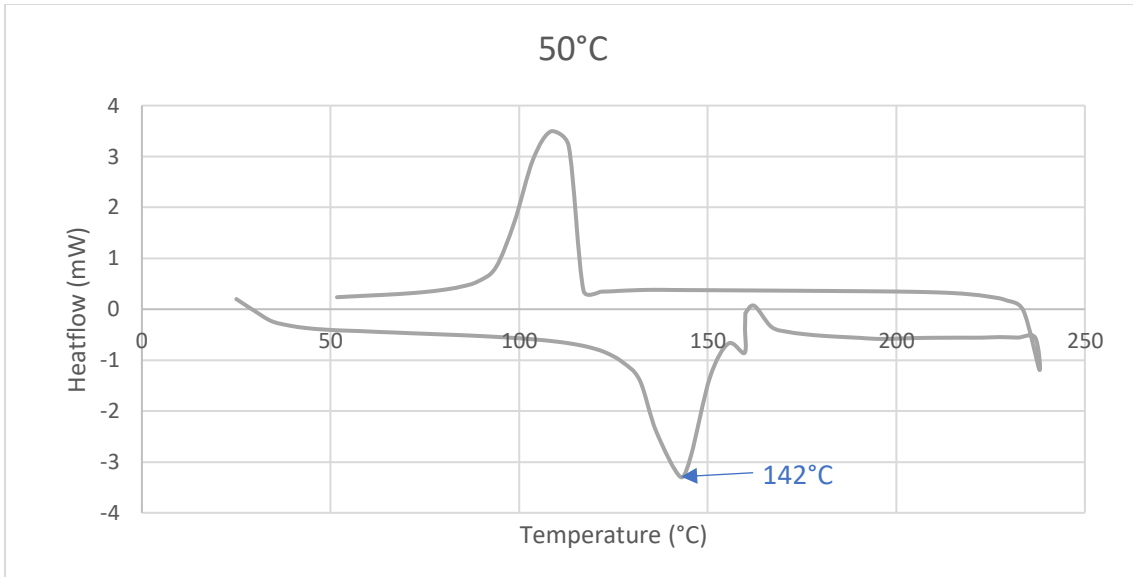
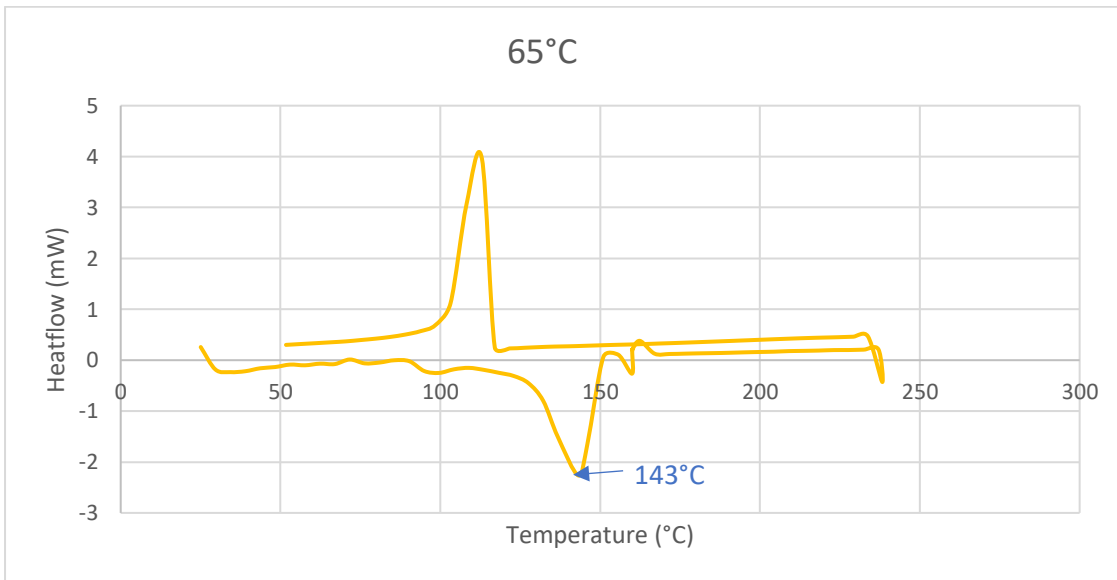Fig 4.13 50°C thermogram showing a peak melting temperature of 142°C

Fig 4.14 65°C thermogram showing a peak melting temperature of 143°C

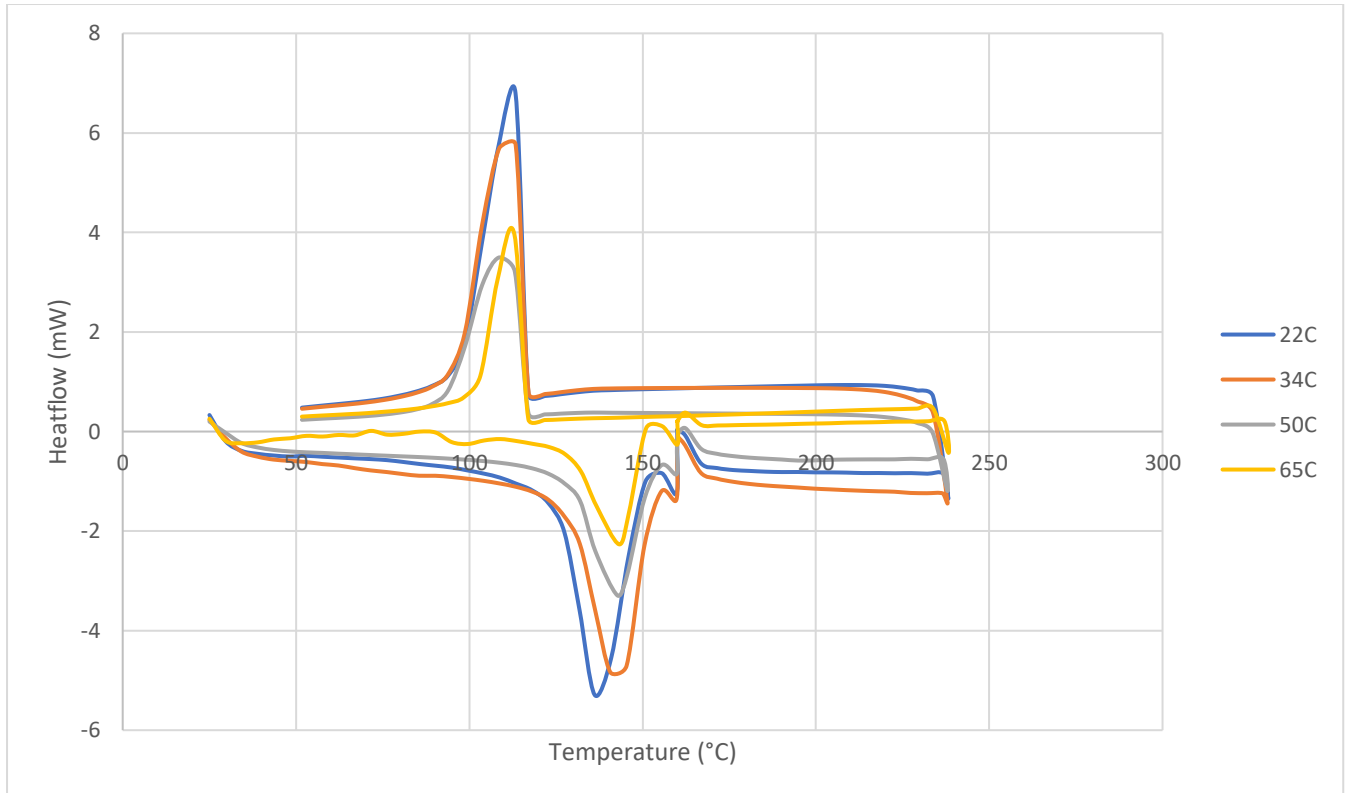A comparison of all temperature group thermograms are shown in Fig 4.15

Fig 4.15 DSC thermograms for different mould temperatures

It can be seen from the thermograms that the 22°C mould produced gears have the lowest peak melting temperature of 136.1°C, while the 65°C gears have the highest of 143°C.

4.9 Discussion of the injection moulding process

The production of HDPE gears using the injection moulding process described in this chapter, has shown that employing the Taguchi method of experimental design can lead to a robust methodology which ensures that the gears produced have minimum deviation from target specifications.

Shrinkage (%) and changes in mass are widely used in industry as quality control measurements. These have been effectively used in the injection moulding process conducted in this experiment. Through their measurement, melt temperature, injection volume, hold pressure, and hold time, have been proved to have definitive effects on the moulded gears.

The S/N ratios show that injection volume had the least effects on HDPE gear quality when its value was changed within the selected range. Using values which were slightly below range, however, produced gears which showed significant physical deformities. The gears appeared withered, with ill-

defined tooth profiles, indicating material deficiency. On the other hand, when values which were slightly above the range were used, flash occurred.

Hold pressure was the parameter which had the greatest effect on shrinkage, showing a shrinkage of 2.41% at the lowest setting of 70MPa, and 1.85% at the highest setting of 90MPa. Further increase of hold pressure beyond the selected range did not result in further improvements. From this, it can be concluded that a higher hold pressure within a given range, produces HDPE gears of a higher quality.

The hold time is important in determining the effectiveness of the chosen hold pressure. A hold time which is shorter than the gate freeze time, limits the length of time which the hold pressure is maintained, whereas a hold time which is longer than gate freeze unnecessarily increases the cycle time, since the hold pressure will no longer have any effect on the mould. The importance of hold time is shown in Fig 4.8.

Melt temperature variations produced shrinkage rates which were very similar to those of the hold time soon after production. At the highest-level setting of 225°C, the shrinkage was 1.96%, while at the lowest setting, it was 2.27%. What was of interest, however, was the fact that measurements taken 24 hours after the initial ones showed a shrinkage of 2.05%, which was the highest increase in any of the chosen parameters. This raises a complex question of when the ideal time after production would be to conduct quality measurements. This has been highlighted by the work of previous researchers [128, 129, 130]. Accurate gear measurements are important in meshed arrangements as changes introduce dimensional instabilities which require continual backlash adjustments. The practical approach taken in this research was to take and record measurements 60 seconds after gear ejection. These were the measurements used for all calculations. Backlash adjustments were then made according to individual gear testing.

Gear mass measurements show a 6.7% increase in mass between gears produced at 22°C and those produced at 65°C, Table 4.23.

To simplify crystallinity calculations, the DSC analysis of gear samples produced at different mould temperatures focused on the shift in the peak melting points. This was based on the fact that a higher crystalline formation of the same amorphous or semi-crystalline material results in a higher melting temperature, as shown by the work done by Ronkay et al [131]. The exact crystallisation percentages were therefore not calculated, but a higher temperature was taken as an indication of higher crystallinity. From the results presented, it can be seen that the 22°C mould temperature produced gears which had a melting peak of 136.1°C. This melting temperature increased to 140.7°C for 34°C produced gears, 142°C for the 50°C group, and 143°C for the 65°C gears. The increase in melting points

indicate increases in crystallinity as the mould temperatures increased. It was noted, however, that the melting points revealed by DSC thermograms were much lower than the melting point of 180°C stated by the manufacturer. This shows that there can be variations between manufacturer stated values and actual values exhibited by the material.

The importance of stating mould temperatures used by manufacturers has been highlighted by the work presented in chapter 4. Gear ratings based on input parameters used during manufacturing process are non-existent in standardised form. This information is important in arrangements where tight tolerances are critical for reliable gear operation.

4.9 Summary

In this chapter, a design of experiments based on the Taguchi method was used to obtain optimum values which were used to produce HDPE gears using injection moulding. The gears produced showed good dimensional stability as the shrinkage rates of between 1.5% and 2.5% compare well with those of between 1% and 4% stated by the manufacturer.

DSC analysis was used to analyse how the melting point of the different mould temperature gear groups were affected. A shift in the peak melting point was used as an indication of crystallinity change of the gears. It was determined the lower mould temperatures produced less crystalline gears.

CHAPTER 5

WEAR ANALYSIS OF HDPE GEARS PRODUCED AT DIFFERENT MOULD TEMPERATURES

_____

5.1 Introduction

As discussed in Chapter 2, the wear behaviour and performance of polymetric gears has been studied by several authors [11, 15, 21, 34, 64, 88], but to date there has been little focus on understanding the link between the input parameters used during the manufacturing process, and their corresponding physical and performance characteristics. Most of the emphasis on polymetric gear performance is solely based on the polymer or polymer composite type and composition. This approach seems peculiar to polymer gears, as metal gears tend to be tested and graded not only by their material type, but also according to their mode of manufacture.

An important processing input parameter in injection moulding is the mould temperature, or cooling rate. The previous Chapter has outlined how HDPE gears were produced by obtaining optimum input parameters first and holding them constant while varying the mould temperature.

This Chapter investigates the links between mould temperatures and performance by conducting wear tests on nominally aligned gears using a non-metallic gear test rig, as described in Chapter 3. The study will focus on the following main issues:

- The nature of wear exhibited by gears produced at different mould temperatures. This will involve analysing wear curves and observing how the different phases of wear are affected.
- The relationship between mould temperatures and the load carrying capabilities of different temperature groups
- The mode of failure for different mould temperatures
- The effects which mould temperature has on the coefficient of friction
- The nature of debris produced as the gears wear

Through analysis of the first three points, it should be possible to ascertain whether there is a direct correlation between mould temperature, gear performance and mode of failure.

The last two points will give an indication of changes at the microstructural level in response to varying mould temperatures. An in-depth microstructural analysis using SEM will then be carried out.

5.2 Gear mesh groupings

During the injection moulding process, the produced HDPE gears were grouped according to the mould temperature they were produced at. As discussed in Chapter 4, these temperatures were 22°C, 34°C, 50°C, and 65°C.

The variation of mould temperatures during the injection moulding process resulted in differences in the dimensional stability of the gears. This meant that each mould temperature group had to be measured and the centre distances adjusted to obtain a specific backlash which was consistent across the groups. The average pitch circle diameter for the group is shown in Table 5.1.

Table 5.1 Gear diameters according to mould temperature.

Mould temperature group	Gear diameter (mm)
22°C	61.48
34°C	61.62
50°C	61.81
65°C	62.0

The work done by Mao [82] and Wood [97], revealed that the wear rate for polymetric gears is dependent on whether gears of the same polymer type are paired. Accordingly, only gears produced at the same mould temperature were paired.

5.3 Load test method

Meshed gear pairs were subjected to lifetime tests. These tests involve the application of a constant load, at a constant speed, under dry conditions until the gears fail. Torque loadings of 0.5 Nm, 1 Nm, 2 Nm, 3 Nm, and 4 Nm were applied at 1000 rpm. Torque loadings of 0.5 Nm and 4 Nm were also tested at 500 rpm. The rationale for this approach was that these settings would show the greatest differences in values between the wear performance responses between the different mould temperature settings at the lowest and highest loadings as a result of doubling the speed of rotation.

Lifetime tests, as opposed to step-load tests, were used as these provide more accurate data. Once the load and speed are set, there is no external interference with the test. This allows the tested gears to follow a natural wear path for the set load. The main disadvantage is that lifetime tests take a long time to complete and consume a large number of gears. As a result, many gears had to be constantly manufactured as the tests were conducted. This type of testing would not have been economically possible were it not for the fact that gear production was conducted in-house.

Table 5.2 Gear groupings.

Production Temperature grouping	Revolutions Per Second (rpm)	Torque (Nm)
22°C, 34°C, 50°C, 65°C	500	0.5, 4
	1000	0.5, 1, 2, 3, 4

5.4 Wear curves/Wear rate

As meshed gears wear, the signal from the LDVT sensor is used to plot a wear curve against the number of cycles. Each curve is unique and is dependent on torque applied, rotational speed (rpm), and on the mould temperature employed during the injection moulding stage. As discussed in section 3.16, the wear rate is defined as a change in gear teeth depth per cycle. This can be expressed as a measure of wear curve gradients, as expressed in equation 3.22.

The different phases of running-in, linear or steady, and final rapid wear, identified by previous researchers [21, 93] are clearly visible on most curves. Some wear curves also display a transition wear phase.

5.5 HDPE gear tribology

As discussed in section 2.3.2, meshing gear teeth are subjected to both contact and bending stresses, which are dependent on factors such as load and rotational speed (rpm). The bending stress can be calculated using the Lewis bending equation as given in equation 2.3, while the contact stress is calculated using the Hertzian equation given by equation 2.5. Due to limitations of time, the exact bending and contact stress values for different mould temperature settings are not directly calculated

here, but have been shown by other studies to increase as both the load and cycles per given time are increased [11, 21, 32, 51]. This is the assumption assumed here.

5.6 Wear performance Test results

5.6.1 0.5 Nm torque at 500 rpm

5.6.1.1 Wear curves

Fig 5.1 shows the wear test results for the different temperature-produced gears subjected to a torque loading of 0.5 Nm, at 500 rpm. The three different phases of running-in, linear or steady wear, and final rapid wear, are visible on the 34°C, 50°C, and 65°C temperature settings. The wear curve for the lowest temperature group (22°C) shows an additional phase. This phase is between the initial running in phase, and the steady wear phase. This is a transition phase in which the curve gradient is slightly lower than the running-in phase, but higher than the steady wear phase. This happens between 1×10^5 and 6×10^5 cycles.

The increase in curve gradient during the steady or linear wear phase is similar for all mould temperatures.

The final wear phases show interesting differences. The 22°C and 34°C produced gears show a sudden and steep increase in the curve gradient just before failure, whereas the 65°C and 50°C curves show a steep, but gradual increase.
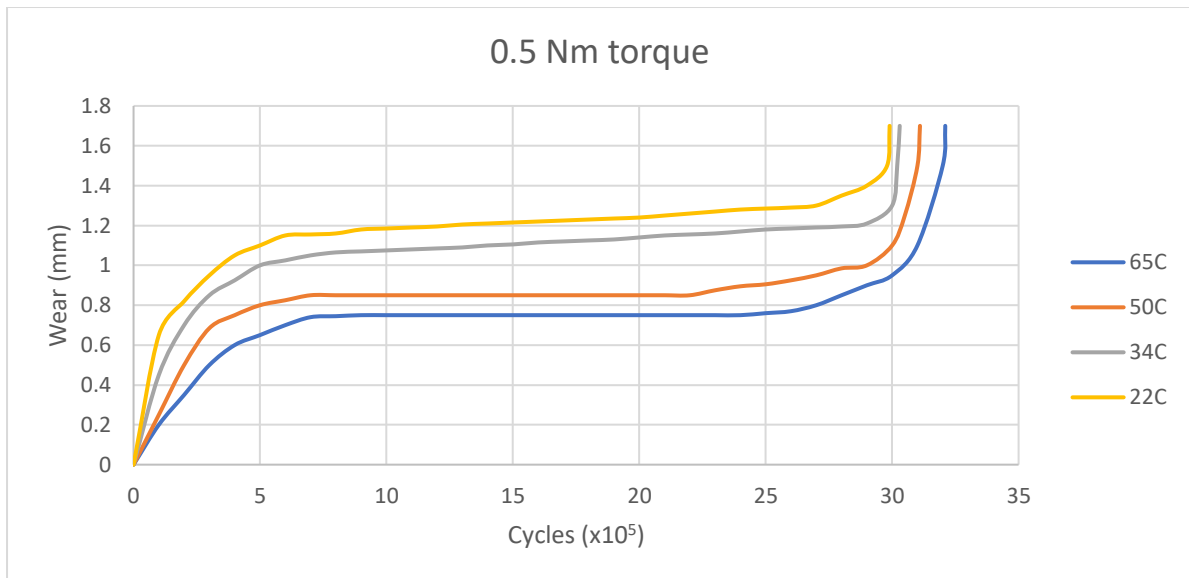
Fig 5.1 0.5 Nm wear curve comparisons for different mould temperatures at 500 rpm.

Using equation 3.22, the wear rate as a function of cycles to failure for the different mould temperatures are shown in Fig 5.2. At 0.5 Nm loading, lower mould temperatures produce higher wear rates. As the mould temperature increases, the wear rates decrease. These findings are consistent with those of Russel et al [L3], who carried out conformal tests on PA66 injection moulded discs, and observed that increases in mould temperature increased yield strength due to an increase in crystallinity.
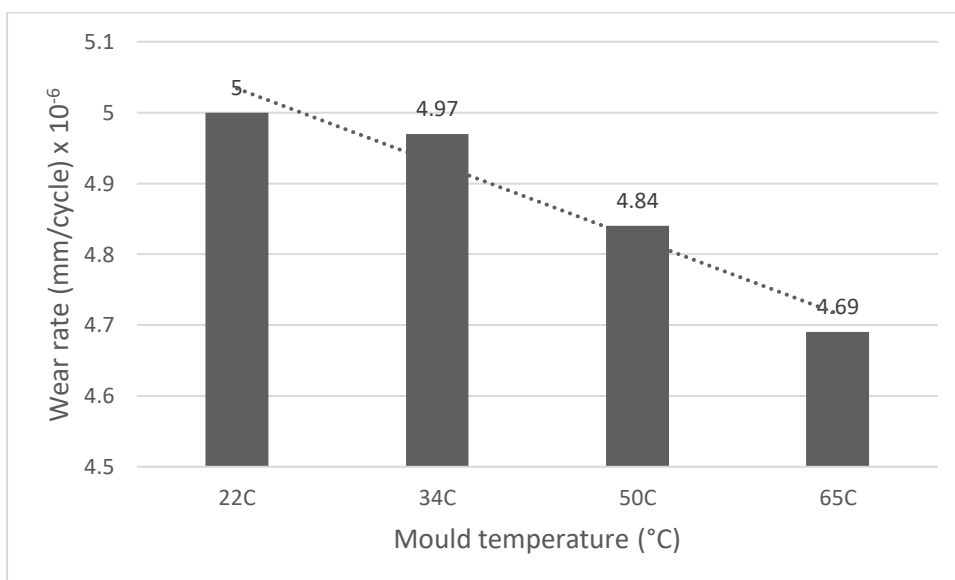

Fig 5.2 Wear rate dependency of HDPE gears on mould temperature at 0.5 Nm, 500 rpm.

5.6.1.2 SEM analysis

SEM analysis shows that there are differences between the wear mechanism for the different mould temperature groups.

For 65°C, the images show that wear is concentrated at the pitch line, and is caused by the detachment of material, as shown in Fig 5.3 and Fig 5.4. There does not appear to be any peeling of material, showing that there was good bonding within the molecular structure of the material.
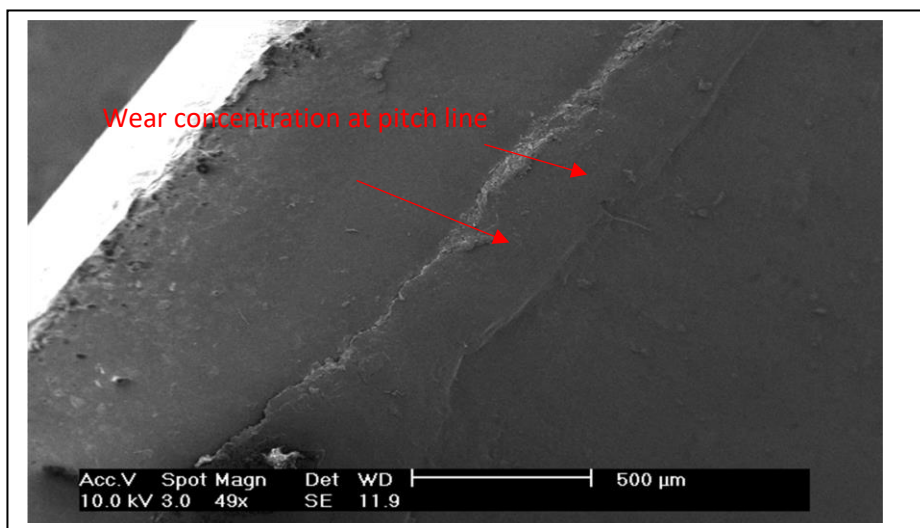

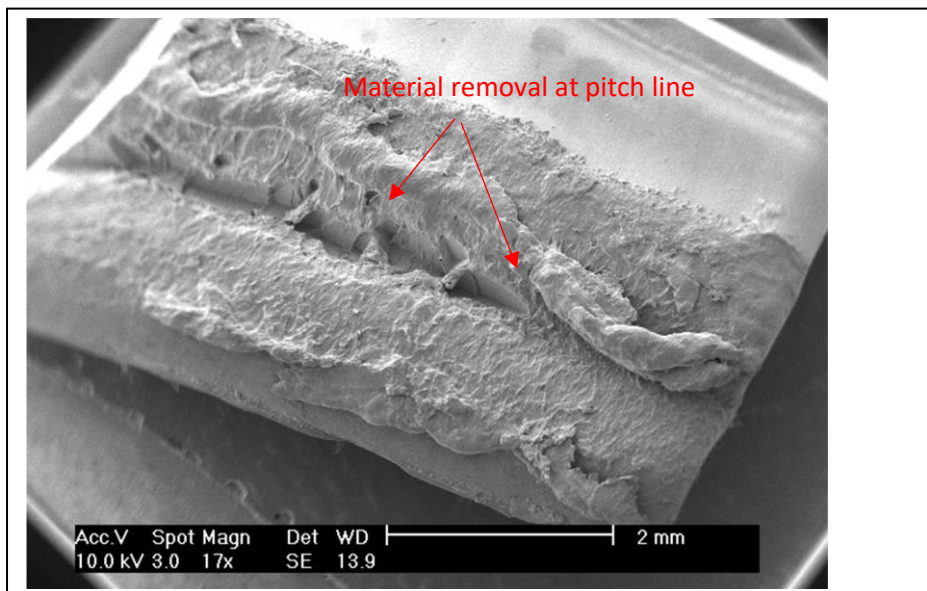Fig 5.3 Material removal starting at the pitch line.

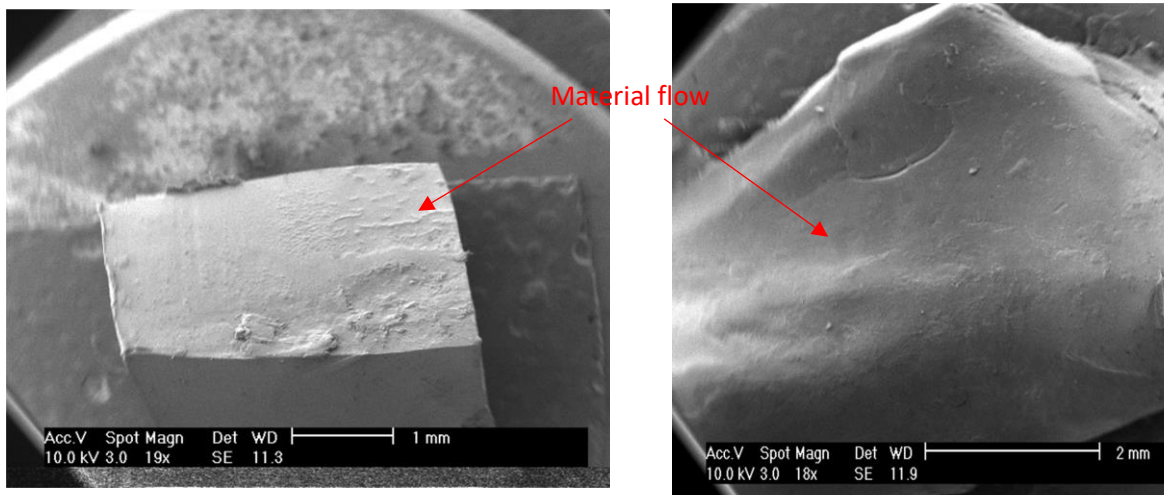Fig 5.4 Material removal along pitch line

Fig 5.5 Wear caused by material flow for 22°C produced gears

SEM images for the 22°C produced gears show wear as resulting from the gradual flow of material starting at the pitch line, Fig 5.5.

5.6.1.3 Debris formation

It was observed that the rate at which debris accumulated at the base of the meshed gears was dependent on the wear phase in which the gears were going through. More debris was produced during the running-in and rapid wear phases, than the linear or transition phases.

22°C gears produced little debris compared to those of 65°C. There were also differences in texture, colour, and size. 65°C gears produced very fine debris which were shiny in appearance, while those of 22°C were dull. These differences can be put down to the differences in crystallinity caused by the different cooling rates. This is consistent with the findings of Zhuang et al [67], who observed that, in general, colder moulds produce glossy parts, and hotter moulds, crystalline parts.
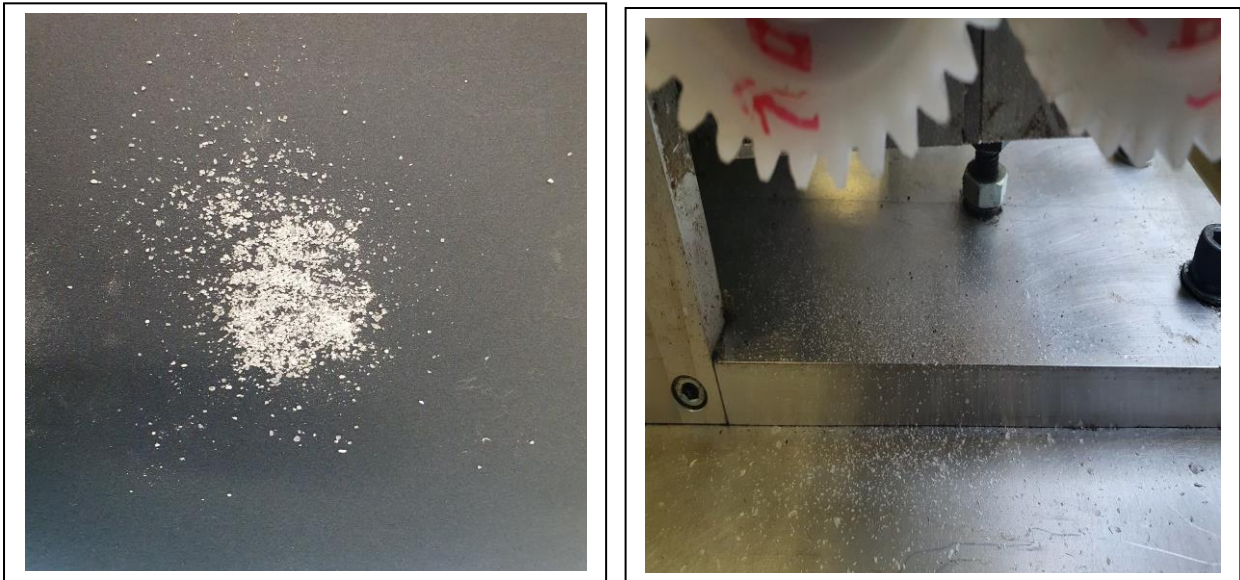
(a)

(b)
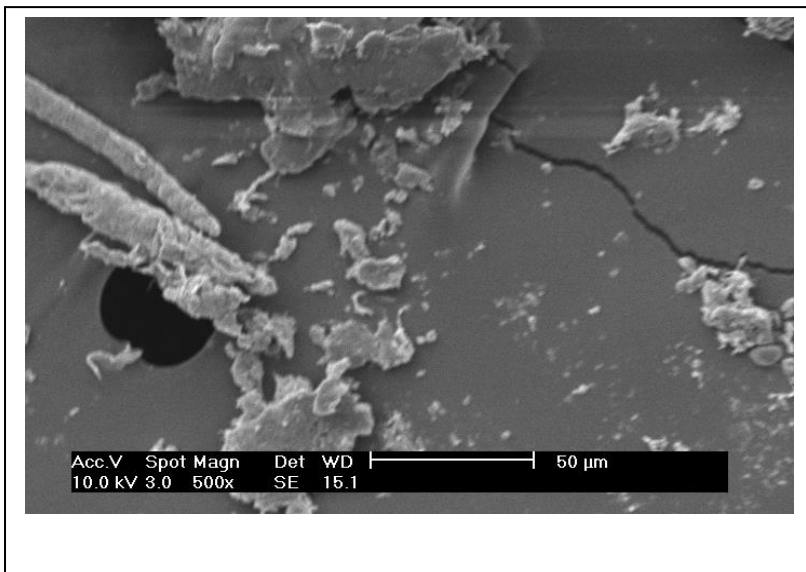
(c)

Fig 5.6   (a) Fine debris produced by 65°C mould temperature gears just before failure
(b) Debris produced by 22°C mould temperature gears at failure
(c) SEM debris for 22°C mould temperature gears at failure

5.6.1.4 Visual appearance

Visual examination of the gears showed obvious differences in appearance between the different

mould settings and between the driving and driven gears. The driving gear for the 65°C mould setting

has two different types of tooth wear, depending on whether it is the leading face (direction of rotation forward-facing teeth), or it is the rear-facing tooth surface. The leading tooth face has wear from the pitch line which increases towards the tip. The tooth tip is rounded, and points in the opposite direction of rotation. The rear face of the tooth flank shows deep wear at the pitch line, which reduces towards the tip. The root does not show much wear, as depicted in Fig 5.7(a).

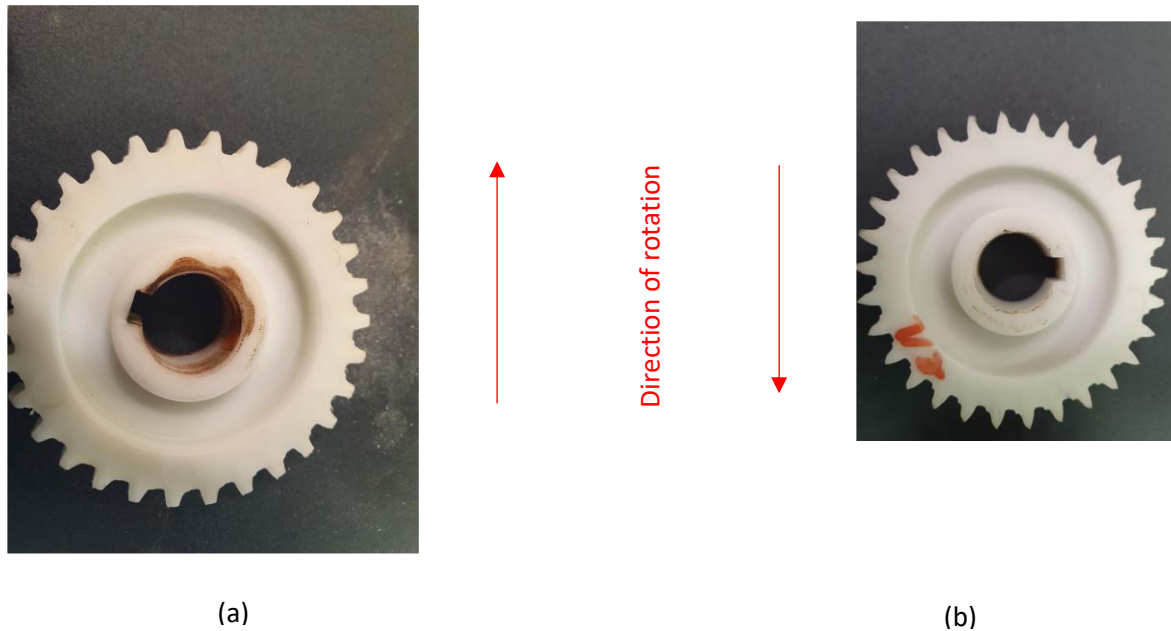(a)   (b)

Fig 5.7. (a) 65°C driving gear wear.
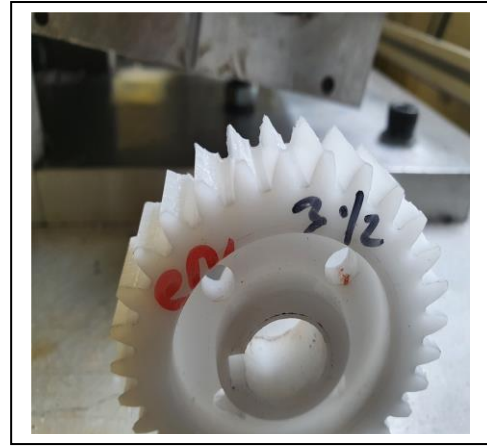(b) 65°C driven gear wear

The forward-facing teeth for the driven gear have wear which starts at the root and evenly increases towards the pitch line and addendum. The tips are more pointed compared to those of the driving gear. The rear-facing teeth (opposite direction of rotation) are worn at the pitch line, Fig 5.7(b).

Both gears were covered with white powdery dust which easily transferred to any surface coming into contact with them.

On the other hand, the driving gear teeth for 22°C have gloss looking worn teeth with a slight angle of inclination towards the opposite direction of rotation. The driven gear teeth show an inclination towards the direction of rotation. Fig 5.8(b). The powdery deposits seen on the 65°C gears were not present on the 22°C gears.

(a)

(b)

Fig 5.8   (a) 22°C driving gear wear at 500 rpm
          (b) 22°C driven gear wear at 500 rpm

5.6.2 0.5 Nm torque at 1000 revs/min

5.6.2.1 Wear curves

An increase in rotational speed to 1000 rpm causes a change in the wear curves for all mould temperature settings for the same torque loadings, as shown in Fig 5.9.
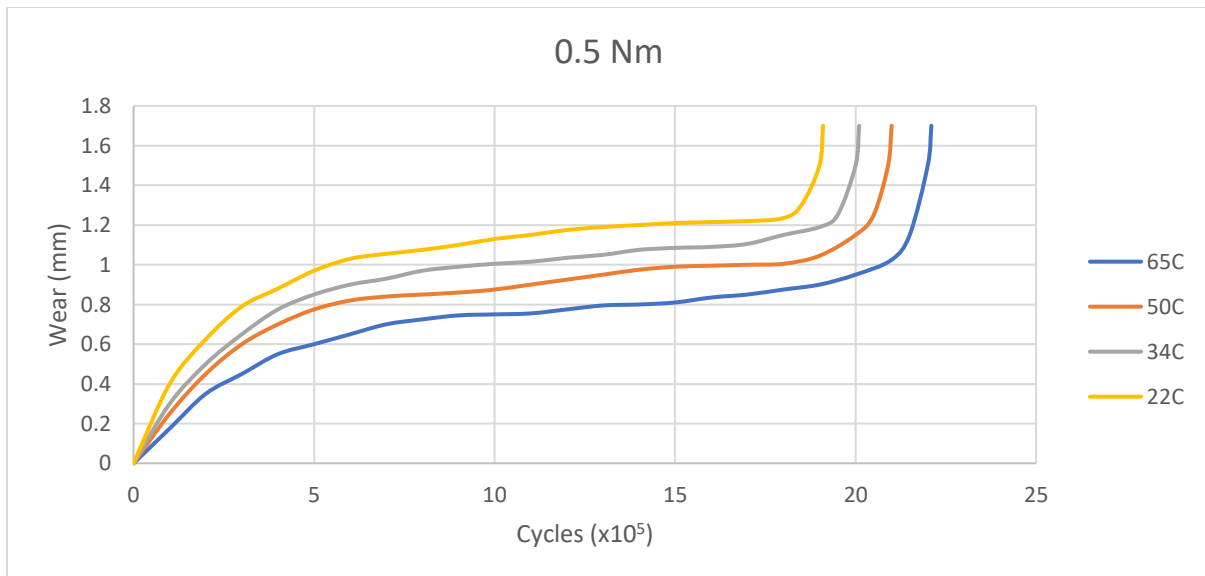
0.5 Nm

Fig 5.9 0.5 Nm wear curve comparisons for different mould temperatures at 1000 rpm

It is apparent that there are three wear phases on all curves. The running-in phase for all curves shows the characteristically high gradient, indicating a high wear rate. The lowest wear is experienced by the highest mould temperature group, and this increases with mould temperature.

The linear or steady wear phase is no longer as apparent as it was at 500 rpm, but instead, there is now a transition phase in which wear increases at a faster rate with cycles. This leads to shorter cycles to failure for all groups, with gears produced at 65°C failing at 2.2×10^6 cycles, while those produced at 50°C fail at 2.15×10^6 cycles, those produced at 34°C at 2.1×10^6, and those produced at 22°C fail at 2×10^6. These cycles to failure represent a 30% reduction for the 65°C, 50°C, and 34°C groups, while the 22°C reduces by 33%. Fig 5.10.

The rapid wear phases are all similar to those displayed at 500 rpm.
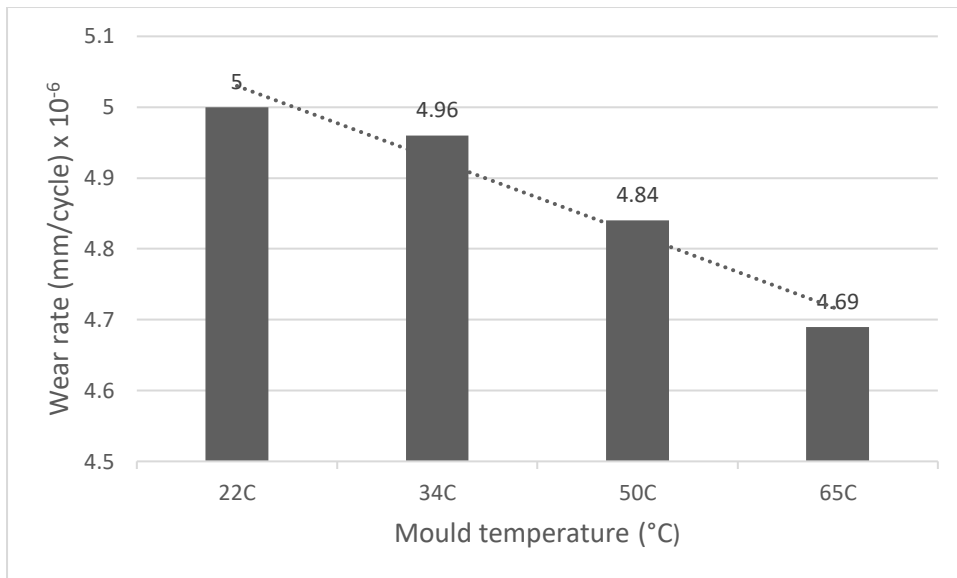
Fig 5.10 Wear rate dependency of HDPE gears on mould temperature at 0.5 Nm, 1000 rpm

5.6.2.2 SEM analysis for 0.5 Nm loaded gears tested at 1000 rpm

SEM analysis for gears tested at 1000 rpm show similarities in the wear mechanism with those tested at 500 rpm. There are, however, interesting differences. At the point of failure, the images for 65°C gear surfaces show an otherwise smooth surface, but there are now pits caused by material detaching as the gears wear. The pitting is more pronounced at the dedendum.
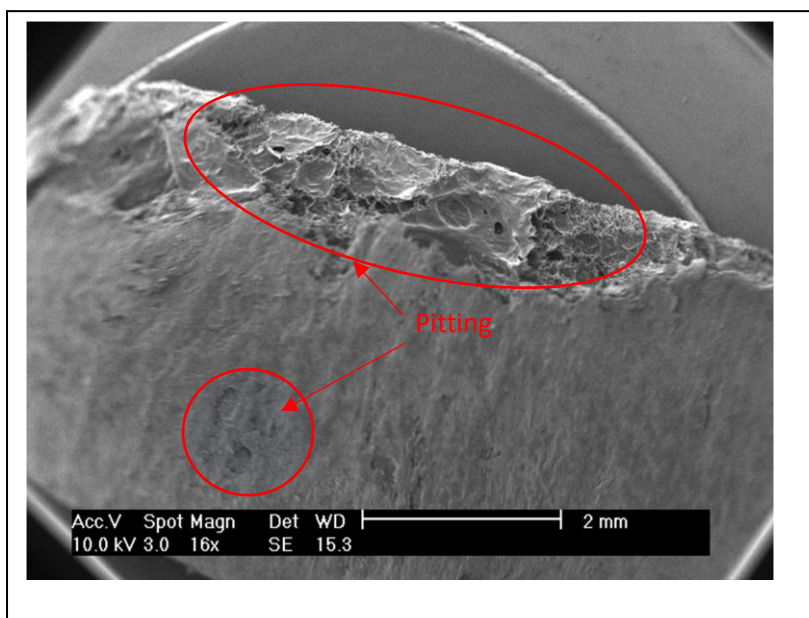
Fig 5.11 Surface pitting caused by material removal.

22°C produced gears showed an increase in material flow from one area of a tooth flank to another, indicating weak molecular bonding. Fig 5.12.

 Fig 5.12 Material flow at 0.5 Nm, 1000 rpm for 22°C produced gear tooth.

5.6.2.3 Debris formation for 0.5 Nm loading at 1000 rpm

At 1000 rpm, 22°C gears produced slightly bigger debris than they did at 500 rpm. The differences in texture and colour exhibited at 500 rpm were also evident.

65°C gears produced more debris than at 500 rpm, but with similar texture and colour.

(a)

(b)

Fig 5.12 (a) Debris formation for 65°C gears at 1000 rpm
        (b) Debris formation for 22°C gears at 1000 rpm

5.6.2.3 Visual appearance

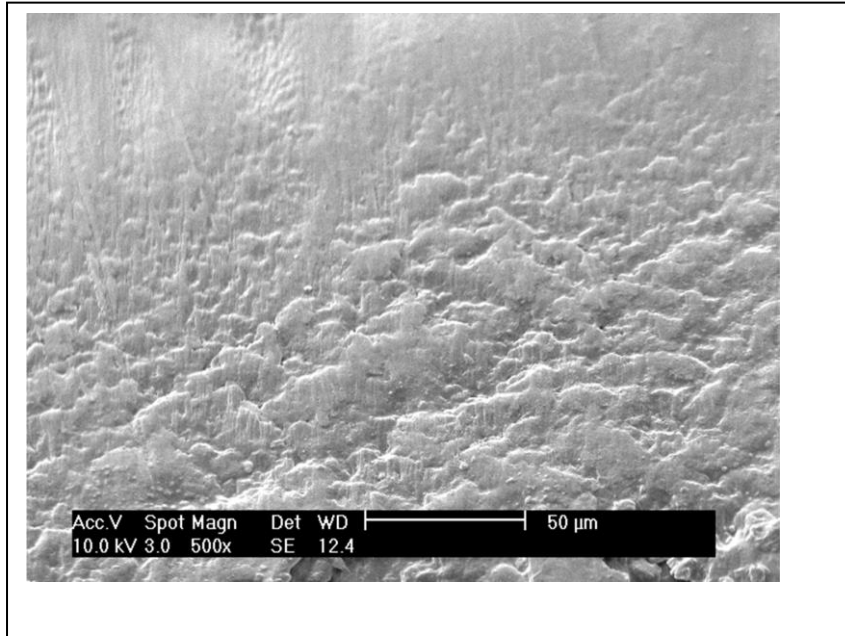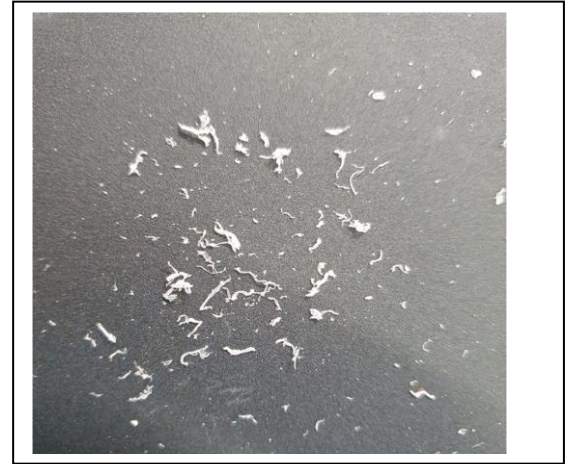There was a clear difference in appearance between the worn gears tested at 500 rpm and 1000 rpm for the same torque of 0.5 Nm. The teeth inclinations described in section 5.6.1.4 for 1000 rpm were no longer as pronounced at as they were. The 22°C mould temperature gears teeth showed deep and even wear, which originated from the pitch line and progressed into the addendum. The 65°C driving teeth were less round at the tips and the addendum was slightly longer at failure than those seen at 500 rpm.

The higher mould temperature worn gear teeth appeared shiny in colour, while those for the lower temperature appeared dull.
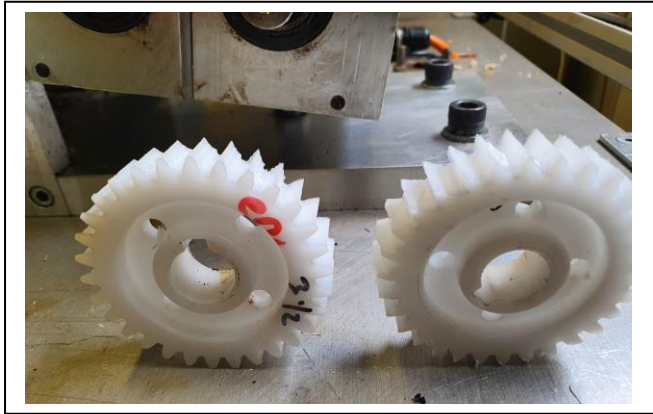
(a)

(b)

Fig 5.13 (a) Visual appearance for 65°C and 22°C produced gears.
(b) Close-up view of a worn 22°C produced gear.

5.6.3 1 Nm torque loading at 1000 rpm

5.6.3.1 Wear curves

An increase in torque to 1 Nm produced distinct changes in the wear curves of all mould temperature settings compared to those of 0.5 Nm, as can be seen in Fig 5.14.

The cycles to failure for the 65°C temperature setting reduces from 2.2 x 10^6 to 2 x 10^6, while those for 50°C decrease from 2.15 to 1.98 x 10^6 cycles. The 34°C gears show a decrease from 2.1 x 10^6 to 1.95 x 10^6 cycles, while those of 22°C decrease from 2 x 10^6 to 1.92 x 10^6 cycles.

At this torque setting, there is very little difference in cycles to failure between the different mould temperature settings.

All three wear phases for the 22°C and 34°C gears show a similar trajectory. The 50°C wear curve shares similarities with that of the 65°C: they both have a transition phase before moving into a steady wear phase.
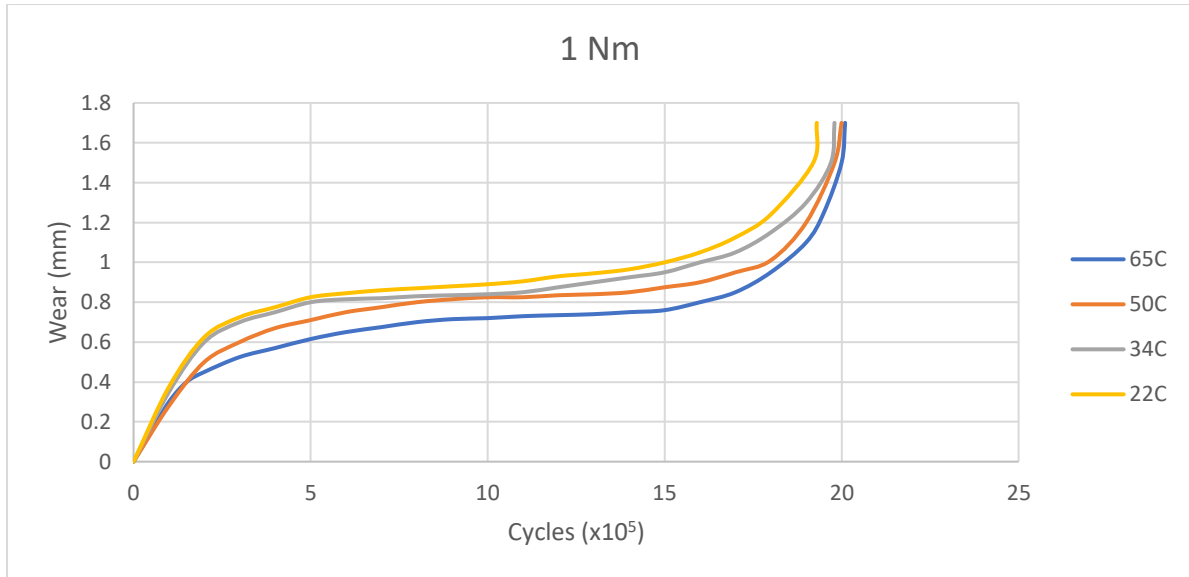
Fig 5.14 1Nm wear curve comparisons for different mould temperatures

The sudden gear failure which was experienced by 22°C and 34°C gears at 0.5 Nm, no longer happens as the gears show accelerated, but even wear.

The wear rates for 1 Nm are shown in Fig 5.15.
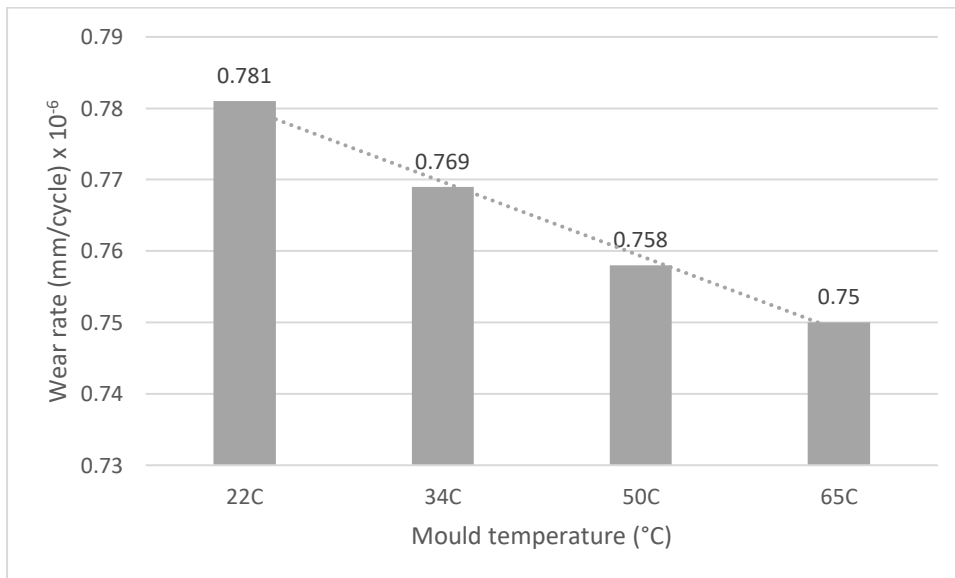
Fig 5.15 Wear rate dependency on mould temperature at 1 Nm, 1000 rpm

5.6.3.2 SEM analysis for 1 Nm gears

SEM analysis shows a slight increase in material flow in the direction of rotation for the driven gear, and the opposite direction of rotation for the driving gear, for the 22°C mould setting. The 34°C, 50°C, and 65°C gears do not show any significant changes in the wear mechanism in comparison to those of 0.5 Nm.
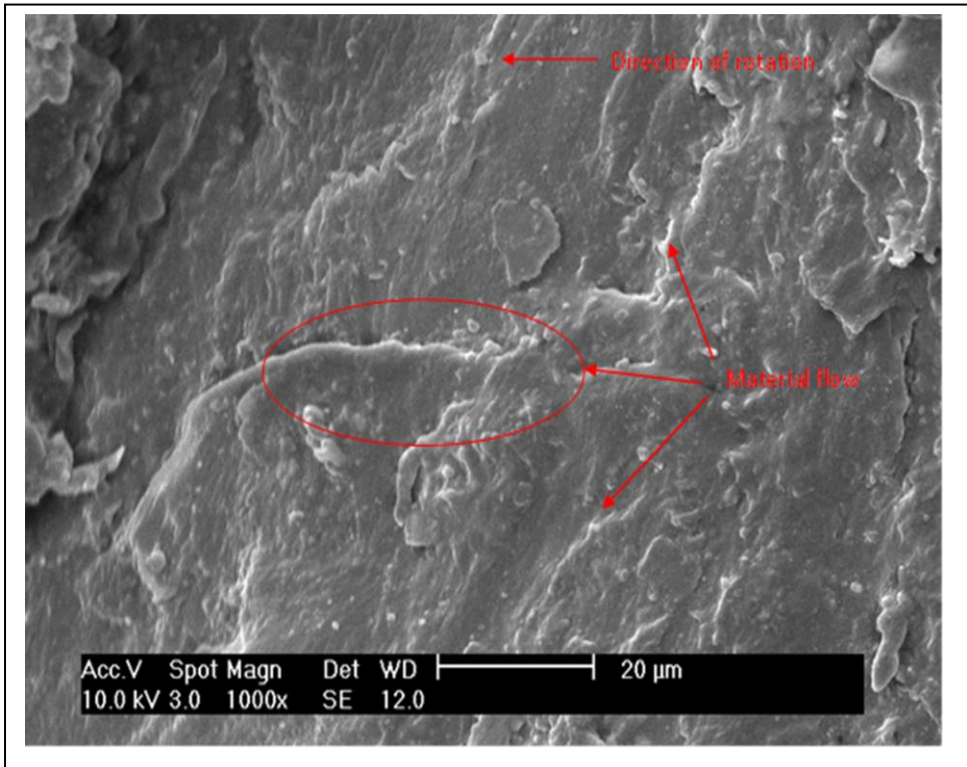
Fig 5.16 Slight increase in material flow for 22°C gears.

5.6.3.3 Visual appearance

The worn teeth appearance for all mould temperature gears at 1 Nm were very similar to those of 0.5 Nm.
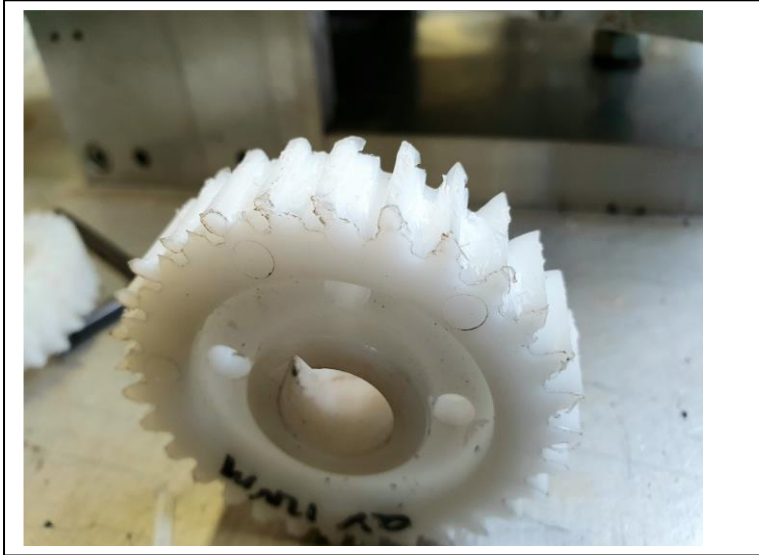
Fig 5.17 Visual appearance of a worn 22°C produced gears.

5.6.4 2 Nm torque loading at 1000 rpm

5.6.4.1 Wear curves

An increase from 1 Nm to 2 Nm represents the most significant changes in the wear curves for all mould temperature settings. Fig 5.18. The biggest variations are shown by the 22°C and 65°C curves. The cycles to failure for 65°C decreases from 2×10^6 cycles to 1.7×10^6 cycles, signifying a 15% decrease, while those of 22°C gears decrease from 1.92×10^6 to 1.82×10^6, signifying a 10% decrease. The 34°C temperature setting gears decrease from 1.95 to 1.8×10^6 while those of 50°C decrease from $1.98 \times 10^{\wedge}6$ to 1.75×10^6, representing a decrease of 7.7% and 11.6% respectively.

2 Nm torque
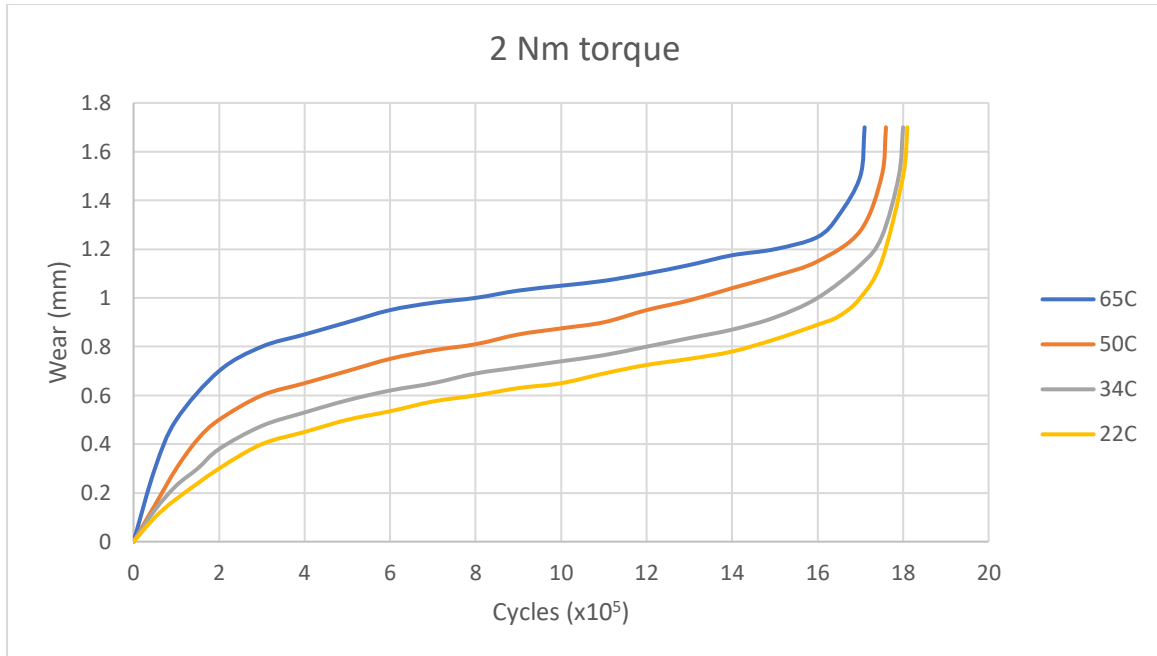
Fig 5.18 2 Nm wear curve comparisons for different mould temperatures

As the wear curve gradient is a measure of the average wear rate, the main changes in wear rates at 2 Nm are for those of 65°C and 22°C. The wear rate for 22°C decreases, while those for 65°C increase. This is an indication that the wear rate of HDPE gears is not only dependent on the level of crystallinity, but also on the torque loading imposed on the gears.
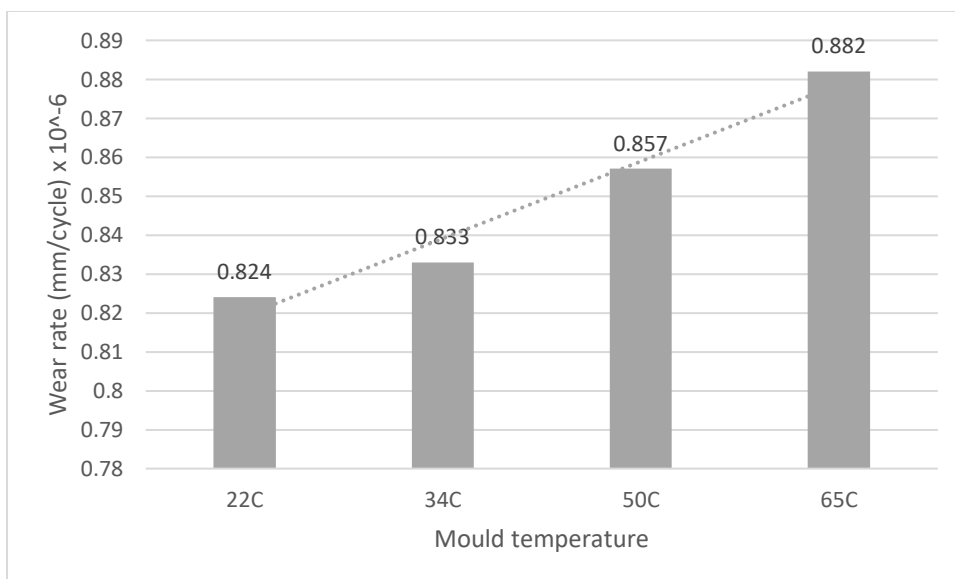
Fig 5.19 Wear rate dependency on mould temperature at 2 Nm, 1000 rpm.

It can be seen from these wear curves that there is a torque setting between 1 Nm and 2 Nm at which mould temperatures have no bearing on the wear performance of HDPE gears. At this torque, the morphological formations imposed on HDPE gears by mould temperature, become insignificant to gear performance.

5.6.4.2 Visual appearance

Examination of the worn gears reveals that the 65°C mould temperature gears fail as result of cracked teeth along the pitch line. Of particular interest, however, is the fact that although the teeth are fractured, most of them remain attached by a thin layer of material at the rear facing tooth. Fig 5.20.

Fig 5.20 Cracked driving teeth still attached to gear at failure.

The 22°C produced gears show gear failure due to material flow. As the material flows, it begins to detach from the gear tooth surface as flakes. Fig 5.21.

The main difference in failure between the 65°C gears and the 22°C produced gears at this torque setting is the absence of broken teeth for the 22°C gears. The driving gear had flakes of material which appear to have been removed from the addendum as thin layers of material and attached around the teeth surfaces and at an angle behind the direction of rotation.
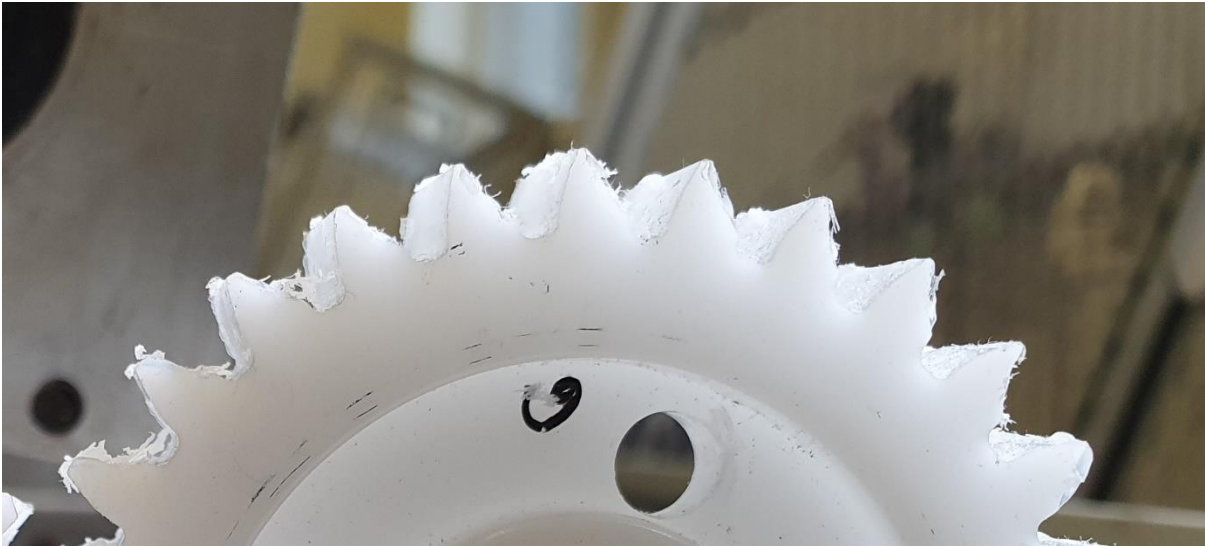
Fig 5.21 Failure of 22°C produced gear as result of material flow.

5.6.4.3 SEM analysis for 2 Nm gears

Fig 5.21 shows material flow and detachment as wear occurs for a 22°C produced gear tooth surface.
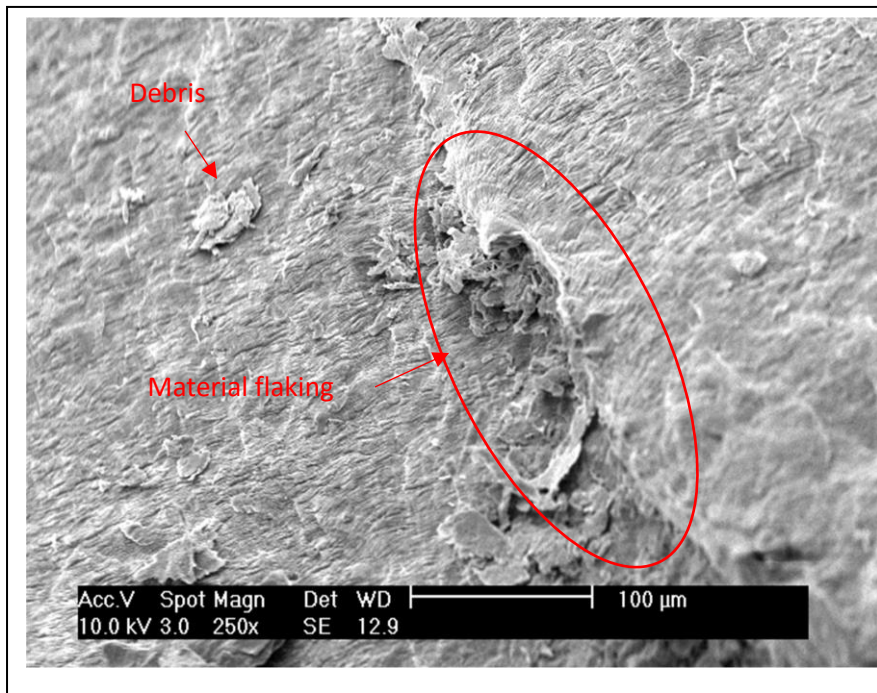
Fig 5.21 Material flow for a 22°C produced gear tooth.
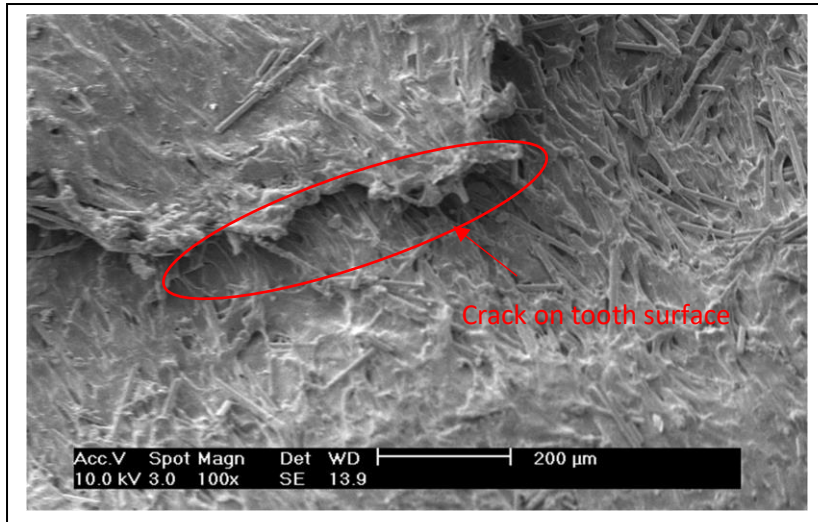
Fig 5.22 Area of tooth crack for 65°C gear tooth.

5.6.4.4 Debris formation at 2Nm

At 2 Nm, there was an increase in the amount of debris produced by 22°C gears, although the size and texture remained the same as those produced at 1 Nm.

(a)
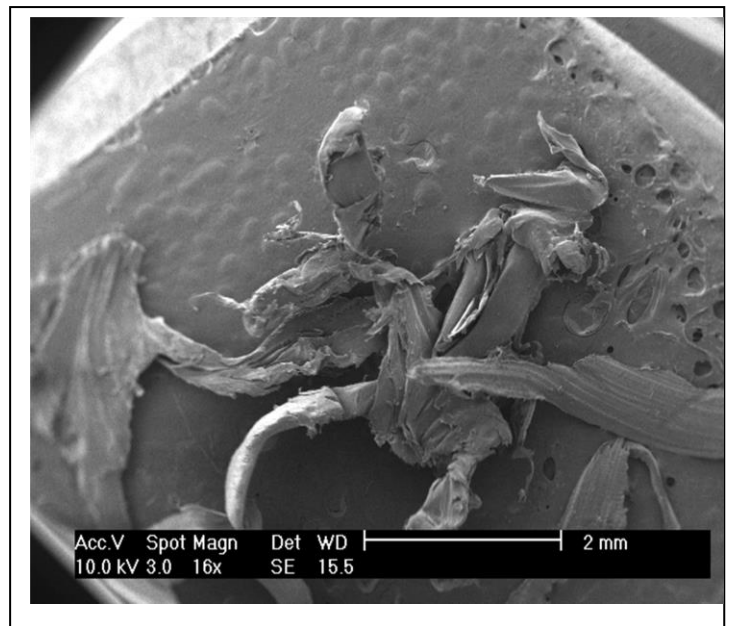
(b)

Fig 5.23 (a) Debris at failure for 22°C mould temperature.
(b) SEM image of debris.

The 65°C mould temperature gears had a mixture of both fine and course debris. There were also broken teeth present. Fig 5.24.

Fig 5.24 Debris at failure for 65°C mould temperature

5.6.5 3 Nm torque at 1000 rpm

5.6.5.1 Wear curves

The wear curves for all mould temperature settings continue to display a similar three wear phase pattern, with similar gradients during the running-in and transition stages, Fig 5.25. While the 22°C, 34°C, and 50°C curves continue to display rapid, but gradual gradients, that of the 65°C is now displaying a much steeper and shorter duration, indicating a more accelerated wear rate than previously experienced in the lower torque loadings.

Of particular interest at this loading is the distinct separation of cycles to failure between the different mould settings. Gears produced at 65°C failed at 1.4×10^6 cycles, while those produced at 22°C failed at 1.7×10^6, which represents a 21% improvement on performance through the reduction of mould temperature from 65°C to 22°C.
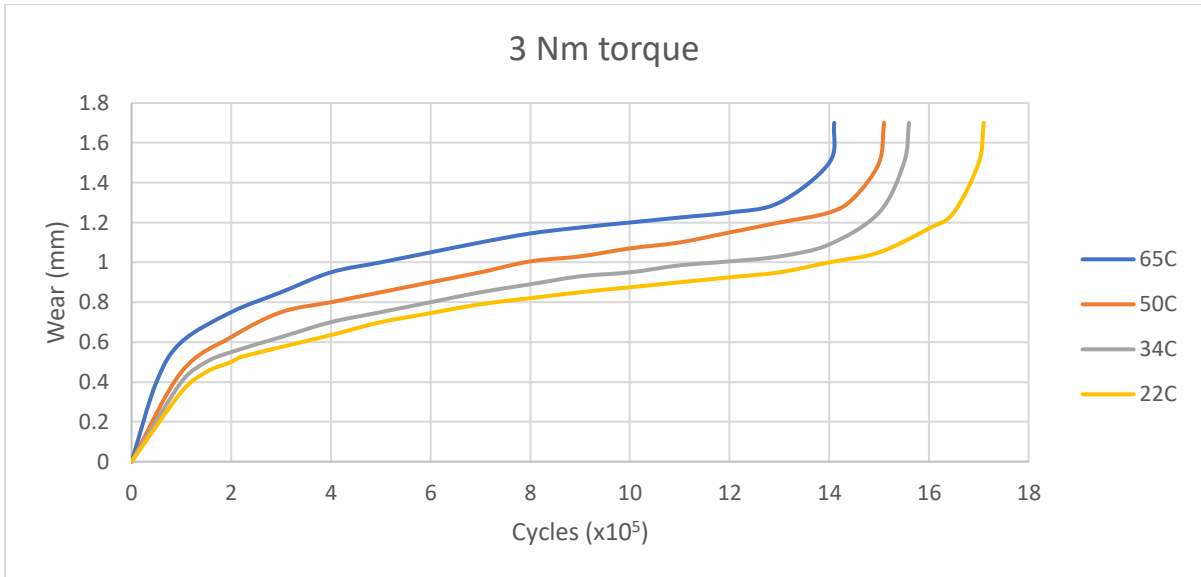
3 Nm torque

Fig 5.25 3 Nm wear curve comparisons for different mould temperatures.

The wear rates for this torque loading are shown in Fig 5.25.

3 Nm
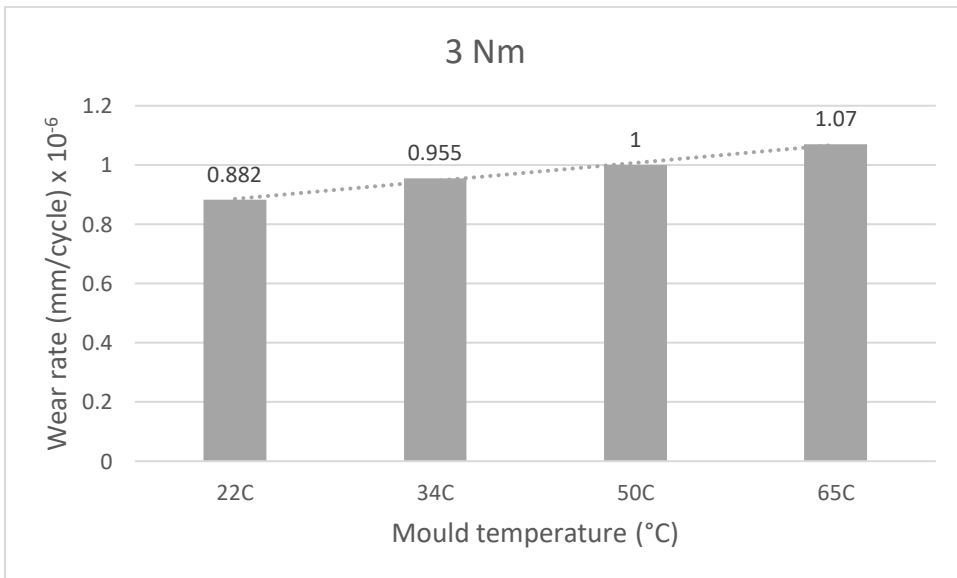
Fig 5.25 Wear rate dependency on mould temperature at 3 Nm, 1000 rpm

5.6.5.2 Visual appearance

At 3 Nm, the 65°C produced gears showed an increase in the number of cracked teeth which were completely detached from the gear at the pitch line, while the 22°C gears showed increased material flow which led to flaring. Fig 5.25 and Fig 5.26.

Fig 5.25 Detachment of teeth for 65°C gears at 3 Nm, 1000 rpm.
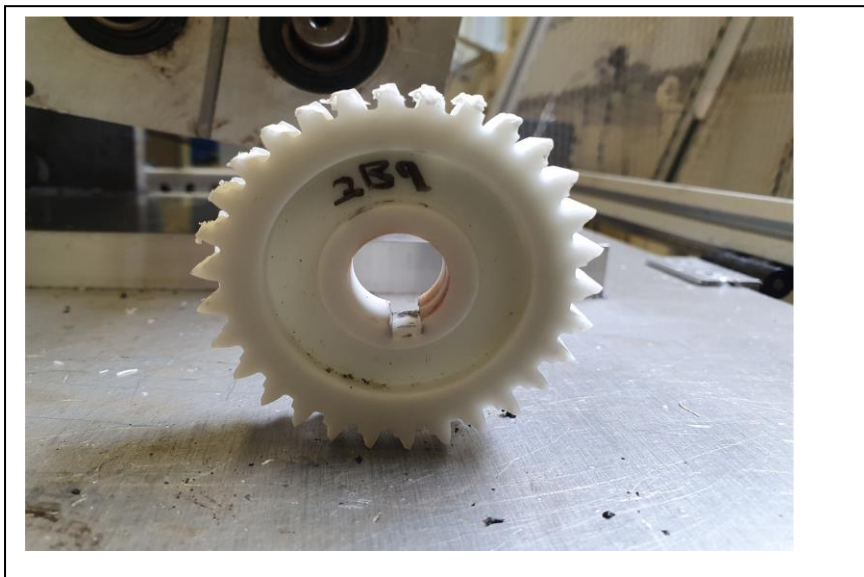
Fig 5.26 Failure of 22°C produced gear as result of increased material flow at 3 Nm, 1000 rpm.

5.6.5.3 SEM analysis

Fig 5.27 is an SEM image of a 22°C worn tooth surface. It shows how the material thins out as it flows from the pitch line towards the tooth tip.
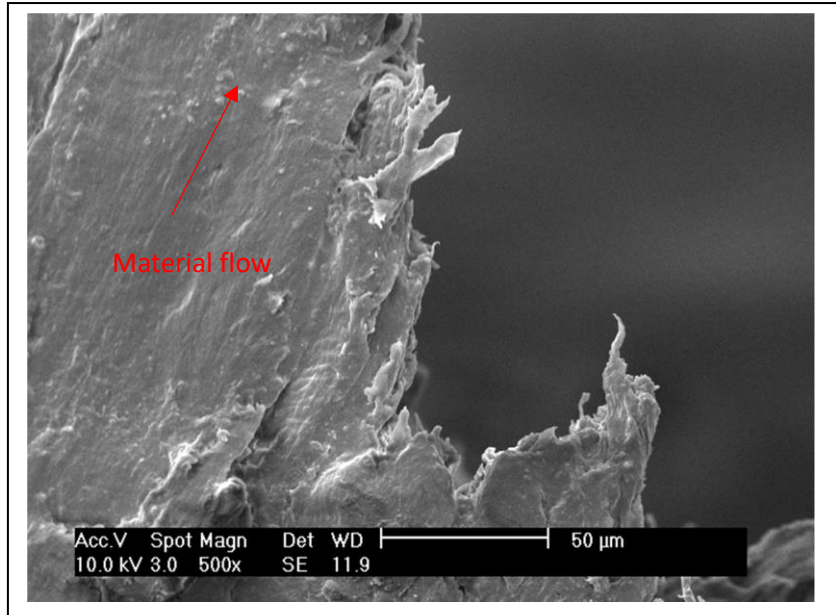
Fig 5.27 Tooth surface with material flares attached for 22°C gear.
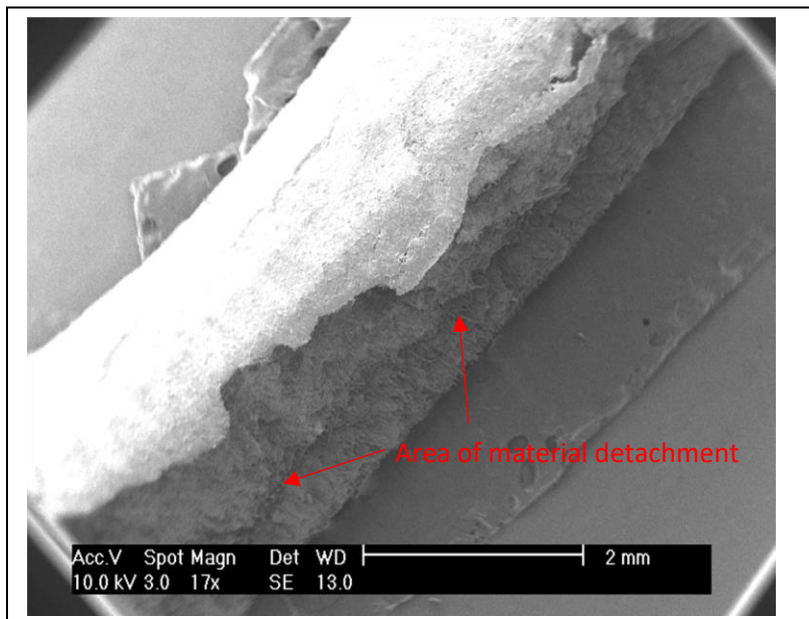
Fig 5.28 65°C broken tooth showing little flaring at point of detachment.

5.6.6 4 Nm torque at 1000 rpm

5.6.6.1 Wear curves

At 4 Nm, the wear curves for the 22°C, 34°C, and 50°C mould temperature setting show similar characteristics for all phases, Fig 5.29. What is interesting at this torque setting, however, is that after the initial running-in phase, the wear curve gradients for the transition wear phases are much less than those seen at lower torques, indicating lower wear rates. The final rapid wear phase exhibit exponential wear, as seen at 3 Nm.

The 65°C wear curve follows a unique path. The running-in phase duration lasts to around 0.2×10^6 cycles and is much steeper than at any other torque. Unlike the other wear curves, a state of linear wear is attained soon after. This lasts up to around 1.05×10^6 cycles. During this linear wear, the wear rate of the 65°C gears and that of the 50°C are equal between 0.75×10^6 cycles and 1.05×10^6 cycles.
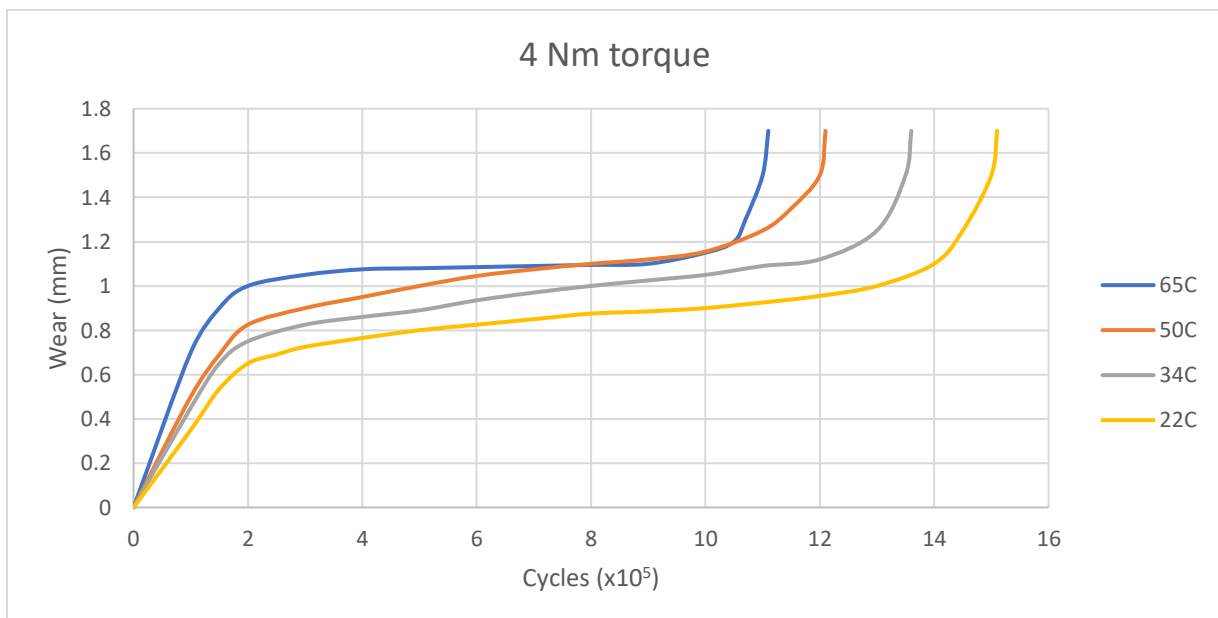
Fig 5.29 4Nm wear curve comparisons for different mould temperatures.

During the last wear phase, 65°C gears experience sudden failure as a result of tooth fracture at 1.1×10^6 cycles.

Failure for 50°C gears occurs at 1.2×10^6 cycles, for 34°C gears at 1.34×10^6, and for 22°C at 1.5×10^6.
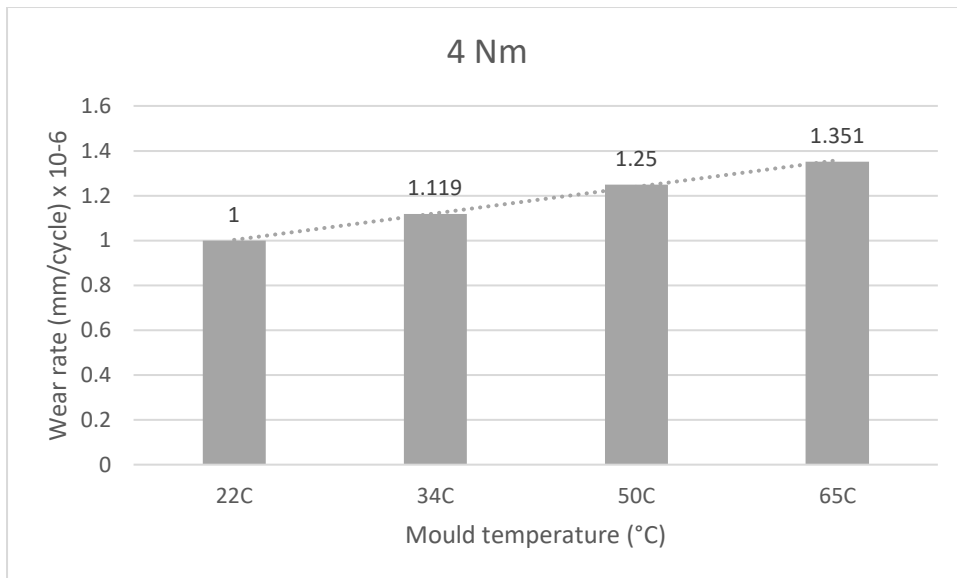
Fig 5.30 Wear rate dependency on mould temperature at 3 Nm, 1000 rpm.

5.6.6.2 Visual appearance for 4 Nm gears

Visual examination of the worn gears showed obvious patterns of failure. 65°C gears had missing teeth which had been fractured from the pitch line. Fig 5.31(a). The tips of the driving gear teeth were not as rounded as they were at 0.5 Nm, indicating that failure was sudden.

(a)   (b)
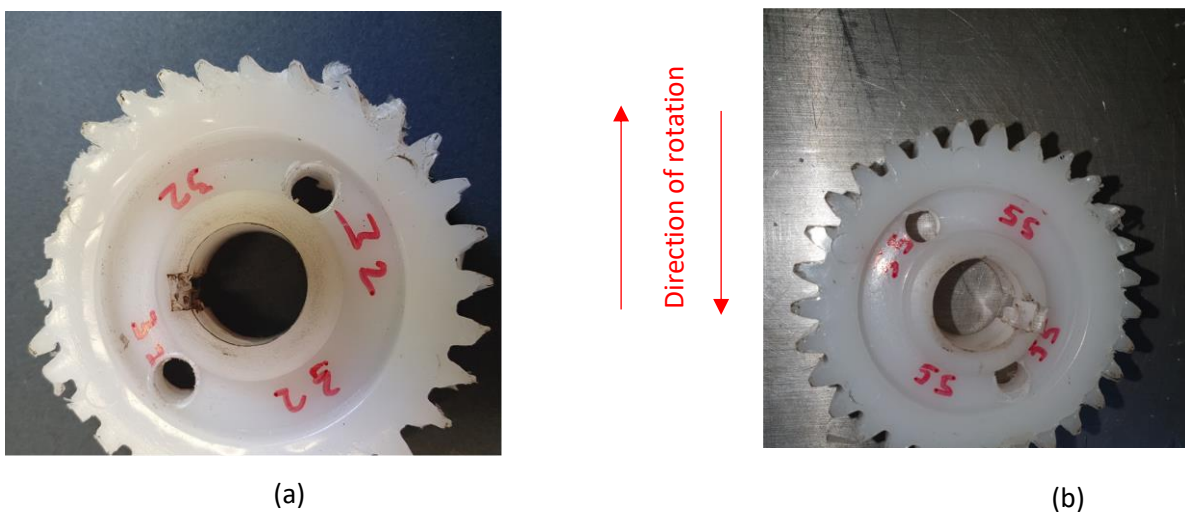
Fig 5.31 (a) Fracturing of teeth for driven gear at the pitch line for 65°C gear.
         (b) Worn 65°C driven gear.

22°C gear failure was through melting of teeth. Although no temperature measurements were taken, the reviewed literature [72, 104, 105, 106] has showed that an increase in load leads to an increase in gear teeth temperature, until a critical loading condition is reached where the material melting point is reached. The test rig was stopped at 1.3 x 10^6 cycles and the gears were examined.

Fig 5.32 Melting of gear teeth at width centre.

As shown in Fig 5.32, gear teeth were melted at the centre width, and melting material could be seen accumulating between gear teeth. This accumulating molten material, however, was not as noticeable at 1.5 x 10^6 when the gears failed. At failure, there were no broken teeth for 22°C produced gears.

(a)

(b)
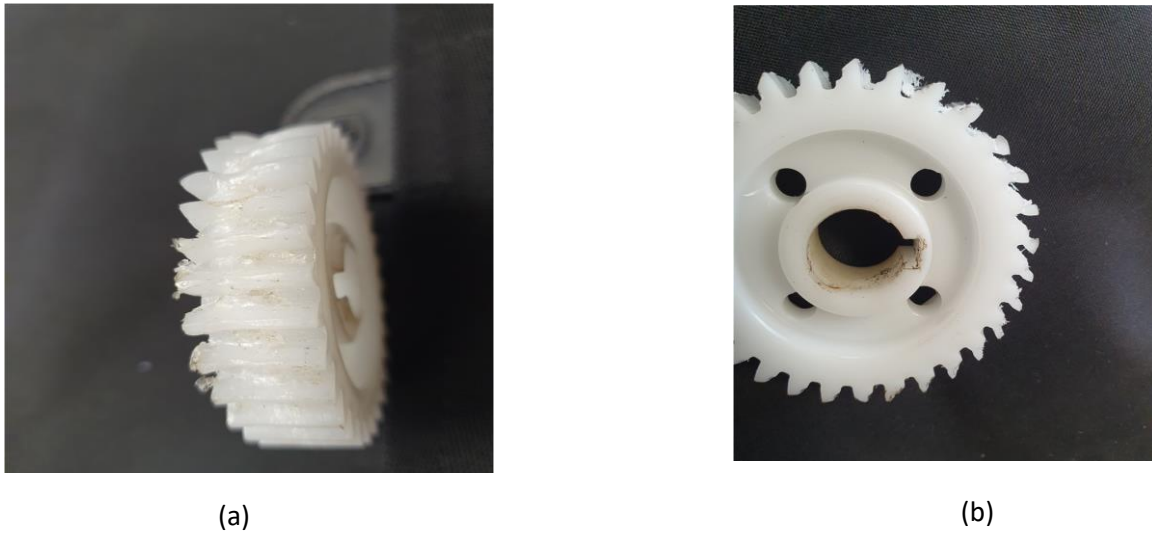
Fig 5.33 (a) and (b) Worn 22°C gears.

5.6.6.3 SEM analysis for 4 Nm gears

Topological examination of 22°C produced gears showed less material flow than that seen at lower torques. This was not expected as earlier increases in torque tended to increase material flow. Upon further analysis, it was clear that there was significant recrystallisation of melted material which did not show as material flow on examined failed gears. Fig 5.34.
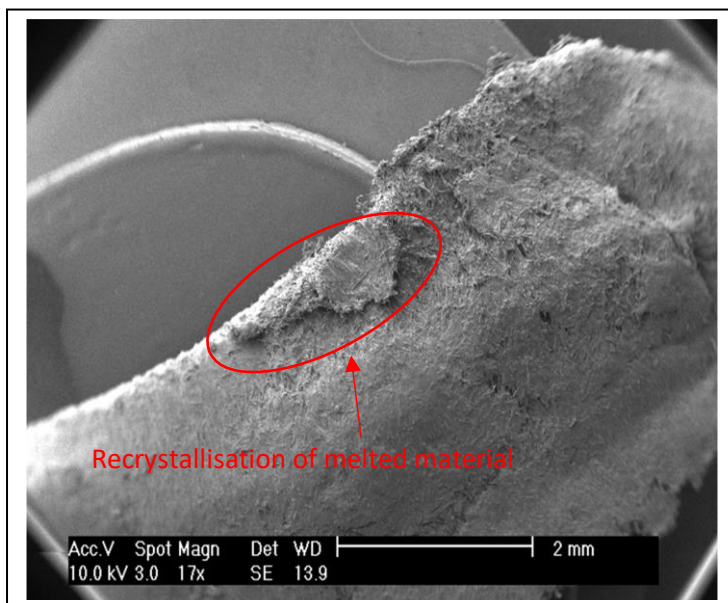
Fig 5.34 Recrystallisation of molten material.

Higher mould temperature gear teeth show failure as result of material separation as the teeth fracture at the pitch line. Fig 5.35.
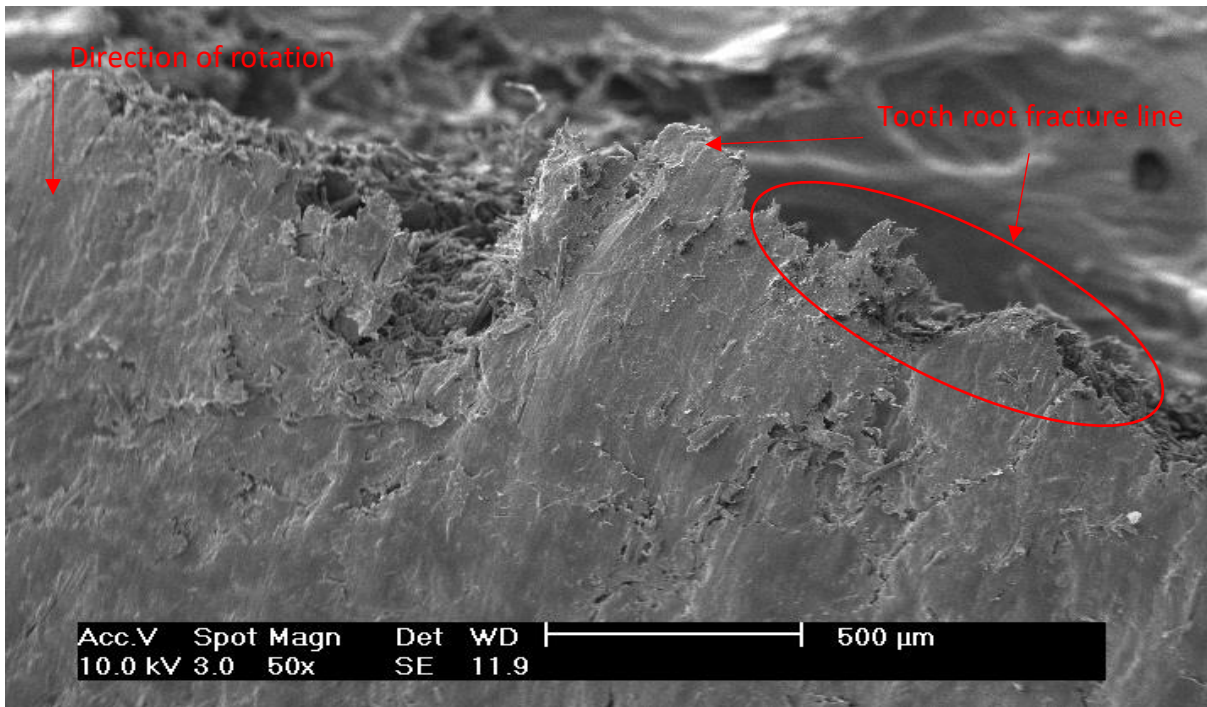
Fig 5.35. 65°C produced showing tooth fracture at root for driven gear.
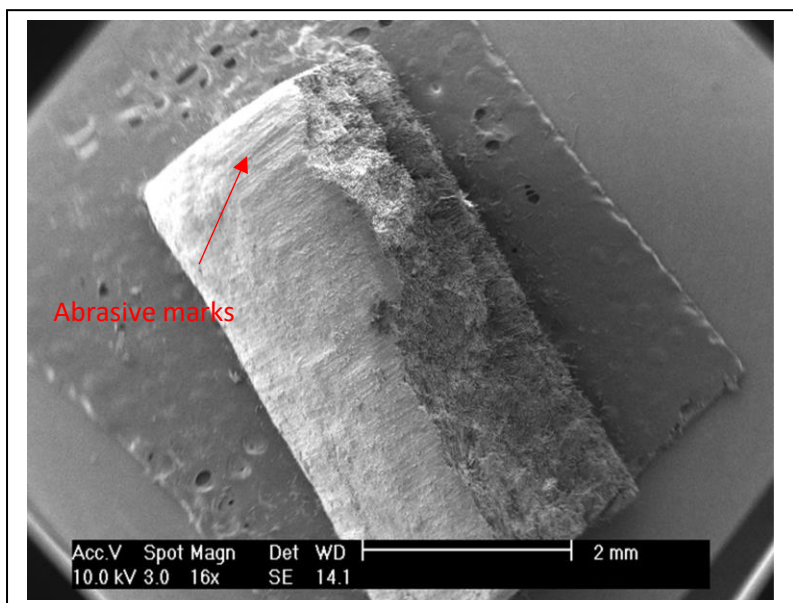
Fig 5.36 Abrasion marks on broken 65°C gear tooth.

5.6.6.4 Debris formation at 4 Nm

There was a slight reduction in the debris formed by the 22°C, and 34°C mould temperature gears compared to that produced at 3 Nm.

(a)

(b)
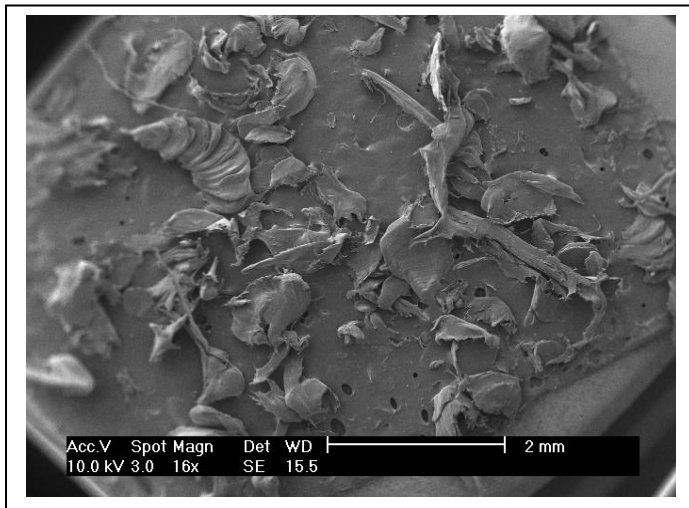
(c)

Fig 5.37 (a) Debris formation for 34°C gears at 1.1 x 10^6 cycles.
(b) Debris at gear failure.
(c) SEM image of debris at failure.

Interesting observations were noted for 65°C group, where the running-in and steady wear phases produced debris which was similar to the lower torque loads. The rapid wear phase produced less, but bigger debris. Broken gear teeth were also present.

(a)

(b)

Fig 5.38 (a) 65°C gear debris at 0.8 x 10^6 cycles.
  (b) Debris at failure.

5.6.7 4 Nm torque at 500 rpm

4 Nm torque loading tests were also done on HDPE gears at a rotational speed of 500 rpm. The wear curves are shown in Fig 5.39.
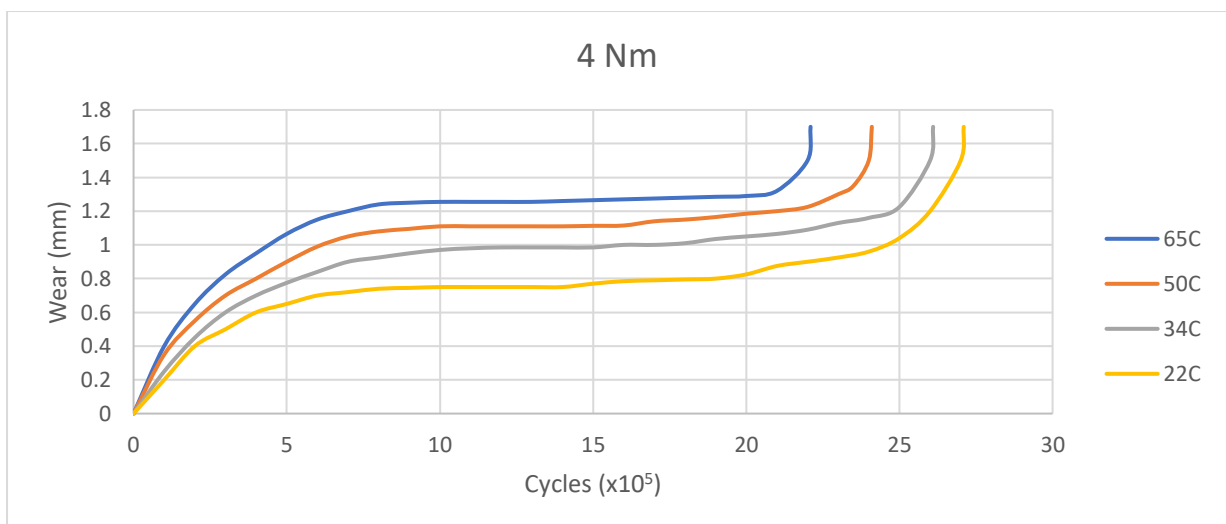
Fig 5.39 4 Nm wear curve comparisons for different mould temperatures at 500 rpm

A reduction of rotational from 1000 rpm to 500 rpm produces an increase in cycles to failure of 98% for the 65°C mould temperature gears, 92% for the 50°C, 79% for the 34°C and 80% for the 22°C.

The wear rates are shown in Fig 5.40.
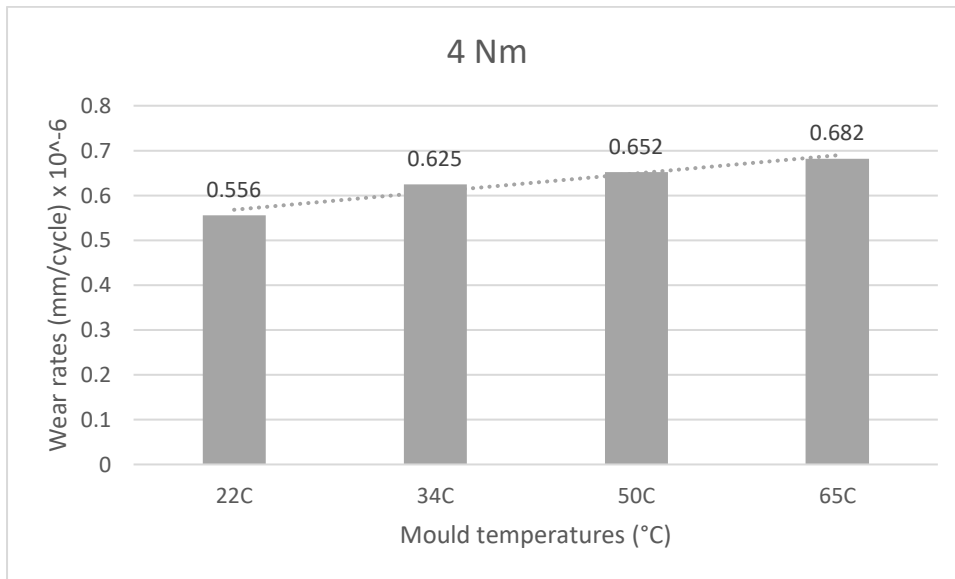
Fig 5.40 Wear rate dependency on mould temperature at 4 Nm, 500 rpm.

The visual appearance, SEM analysis, and debris formation at 500 rpm were very similar to those exhibited at 1000 rpm.

5.7 Summary

Several tests have been performed on HDPE gears, and the data presented in this chapter has shown that mould temperatures employed during the injection moulding process have effects on gear characteristics. Each mould temperature produces gears which respond differently to applied torques and rotational speeds.

The visual appearance of worn gears differs significantly according to mould temperatures. SEM analysis has shown that the mechanisms of wear was dependent on mould temperature, applied torque loadings, and on rotational speeds.

Debris formations were also shown to differ markedly in texture, colour, and size.

The discussion of these test results follows in the next chapter.

CHAPTER 6
DISCUSSION OF GEAR WEAR TEST RESULTS
_____

6.1 INTRODUCTION

The wear and performance results for HDPE gears produced at varying mould temperatures and subjected to different torque settings presented in chapter 5, are discussed in this chapter. Comparisons between the wear rates, mode of failure, and cycles to failure are then made.

6.2 Wear curves as a measure of wear rate

As mentioned in section 3.15, the calculation of wear rates as proposed by Friedrich et al [96], and presented in modified form in equation 3.23, requires the measurement of tooth wear depth (d) for a worn gear. This would be acceptable where tooth wear occurs from the dedendum into the addendum, thereby reducing tooth depth. The results of the present study have shown the following important observations which make the use of equation 3.23 inappropriate for use in the calculation of HDPE gear wear:

1. Depending on the mould temperature employed during the injection moulding process, the torque applied, and the rotational speed, HDPE gears have different modes of failure. Failure due to tooth fracture has been observed to occur while other teeth on the same gear are still exhibiting good tooth depth (d). Measurement of d on the unbroken tooth and inserting the value into equation 3.23, would produce an entirely different wear rate to that which would be obtained if measurement was taken from a point of fracture. Even if points of fracture were to be taken as d, this study has observed that fracture mainly occurs around the pitch line, and the value is unique for every fractured tooth on the same gear.
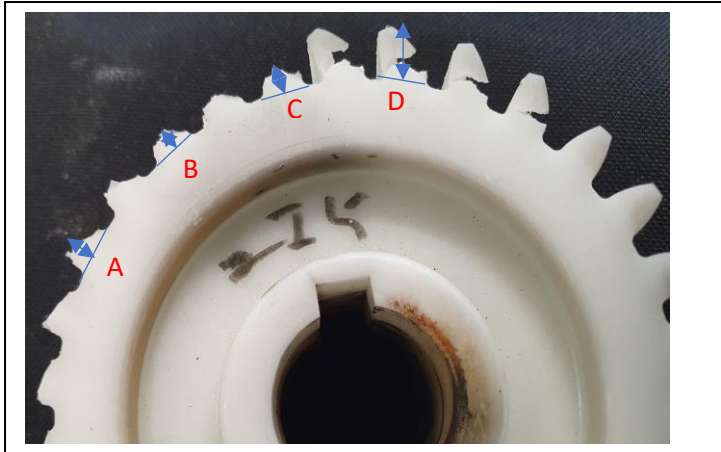
Fig 6.1 Measurement of d is different at point A, B, C, D.

2. Gear failure has been observed where tooth flanks have been bent in either the forward or rearward direction of rotation to such an extent that meshing contact is lost. The overall tooth depth of the unbent tooth would not have changed by any significant amount.

3. Melted material has been observed to accumulate around tooth roots. It would therefore be impossible to accurately measure d.

Using the output of the LVDT described in section 3.14 and plotting a continuous graph of displacement against cycles, enables the accurate calculation of wear at any given point by employing equation 3.22.

The wear graphs presented in chapter 5 show that each mould setting has a unique wear curve which is dependent on the torque applied, and rotation speed.

6.3 Mould temperature effects

6.3.1 Effects at 1000 rpm

6.3.2 0.5 Nm torque loading

As can be seen in Fig 5.1, at 0.5 Nm loading, lower mould temperatures produce higher wear rates. As the mould temperature increases, the wear rates decrease. Based on this observation, wear performance is a direct response to the level of crystallinity of the gears at this torque loading.

The lower mould temperatures cause lower crystallinity as discussed in chapter 4, which results in tooth flank flexing as the driving and driven gears come into mesh. This flexing causes the build-up of heat as a result of hysteresis and frictional forces. The wear curves show that a transition, instead of a linear wear phase, is attained between the running-in and rapid wear phases, indicating elevated wear rates for all mould settings due to continual tooth surface temperature rises, as identified by Mao et al [L20]. This continual rise in tooth surface temperature induces further material flow, until gear teeth strength is reduced to point of failure. This is referred to as plastic flow failure.

SEM analysis shows the accumulation of material and formation of distinct layers in some tooth surface regions due to the viscous flow of material for the lower mould temperature gears. This flow of material is referred to as plastic flow, and is a consequence of the yielding of surface or subsurface material. The direction of this plastic flow is dictated by whether the gear is the driver or is driven. As cycles continue to increase, these layers detach as course debris just below the rotating gears.

The higher crystallinity induced by higher mould temperatures gives the gears strength, but a reduction in toughness. Toughness describes the ability to handle impact forces [132]. The relationship between torque and impact force can best be described by equation 6.1:

$$F_t = \frac{2T}{d_p} \qquad\qquad (6.1)$$

Where F_t is the tangential force (impact force) which is operating at a tangent to the pitch circle in the transverse plane; d_p is the pitch circle diameter. The moment generated by the tangential force at pitch circle then equals the applied torque, T.

From equation 6.1, a low torque, T, results in a low tangential force, F_t (impact force), which can be handled by the higher crystallised gear teeth. The teeth are therefore less likely to fail through fracture, but through tooth surface wear. This explains why debris which is shiny, and has fine texture, accumulates at the base of the running gears as they wear. The SEM image of a worn 65°C produced gear in Fig 5.35 confirms the abrasion marks but no material flow or fractures. These findings are consistent with those of Russel et al [51], who carried out conformal tests on PA66 injection moulded discs and observed that increases in mould temperature increased strength due to an increase in crystallinity, but a reduction in impact resistance.

6.3.3 1 Nm torque loading

The wear curves for 1 Nm torque loading shown in Fig 5.14 indicate very little differences in performance between the different mould temperature groups, indicating that mould temperature has little effect at this torque.

The slight increase in wear for the lower mould temperature groups is caused by a slight increase in material flow due to a further rising of gear teeth surface temperatures, while that of the higher temperature groups are caused by an increase in tooth surface wear. The debris formations are similar to those seen at 0.5 Nm.

The final wear phase of the 22°C produced gear displays an interesting shift in failure behaviour. Failure is no longer sudden as a result of plastic flow, but is exponential in nature. SEM analysis shows a slight increase in material flow with a smoother layering. It is thought that the smoother layers are advantageous to gear teeth strength.

According to equation 6.1, a doubling of torque results in a four-fold increase in the tangential (impact) force experienced by each gear tooth. Examination of worn gears and debris, shows no broken teeth, indicating that the stretching of monomer bonds caused by induced tangential force, is still below the force needed to cause permanent separation.

6.3.4 2 Nm torque loading

A torque loading of 2 Nm induces a significant shift in the torque handling capacities of HDPE gears produced at different mould temperatures. The wear curves show that no mould temperature group passes through the linear wear phase. Wear continues to be relatively high even after the running-in period. It is thought that the higher torque induces rises in tooth surface temperatures due to the increased hysteresis, contact, and bending stresses. These increases in surface temperature lead to continual changes in gear teeth surface morphology due to the relatively low crystallinity formations caused by low mould temperatures, resulting in no steady wear state being attained.

Of particular interest for this torque loading is the fact that the lower mould temperature groups now have longer cycles to failure compared to the higher groups. This can be put down to the microstructural changes which the impact forces generated at 2 Nm are imposing on the material. The higher crystallinity induced by higher mould temperatures not only gives them increased strength, but causes them to be brittle.

SEM analysis shows that wear is concentrated at the pitch line. Fig 5.4. For 65°C produced gears, this wear is mainly caused by material removal which creates a crater working its way into the forward-facing surface of the driving tooth, and the rear facing surface for the driven tooth. As this wear progresses, less and less material remains supporting the tooth until they start to crack under load.
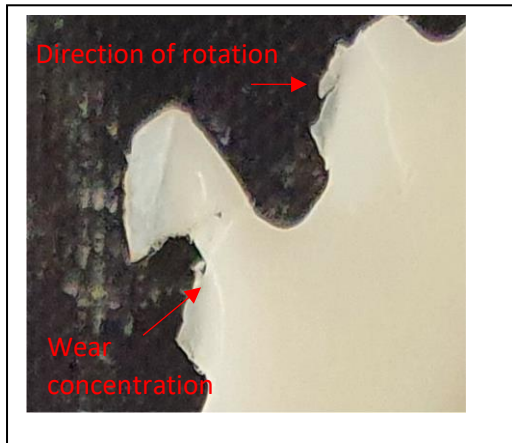
 Fig 6.2 Wear mechanism for 65°C driving tooth.

For 22°C gears, the increase in tooth surface heat caused by a higher torque increases material flow. As the surface temperature rises, the melting material sticks to the rotating tooth surfaces (adhesion) and momentarily acts as a lubricant before solidifying as a thin film on cooler tooth parts. These thin films of material are the flares seen in Fig 5.21.

6.3.5 3 Nm torque loading

There is a slight increase in wear at 3 Nm, but the mechanisms of the wear are similar to those at 2 Nm. The rate of adhesive wear for lower mould temperatures increases slightly, resulting in bigger sized debris forming at the base of the meshing gears. On the other hand, tooth fracture and detachment increase.

6.3.6 4 Nm torque loading

4 Nm was the highest torque setting tested on the gears. Although the mechanisms of failure for all temperature groups were very similar to those described for the 2 Nm and 3 Nm loadings, the progression of wear before failure shows distinct differences between the high and low temperature groups. Fig 6.3.
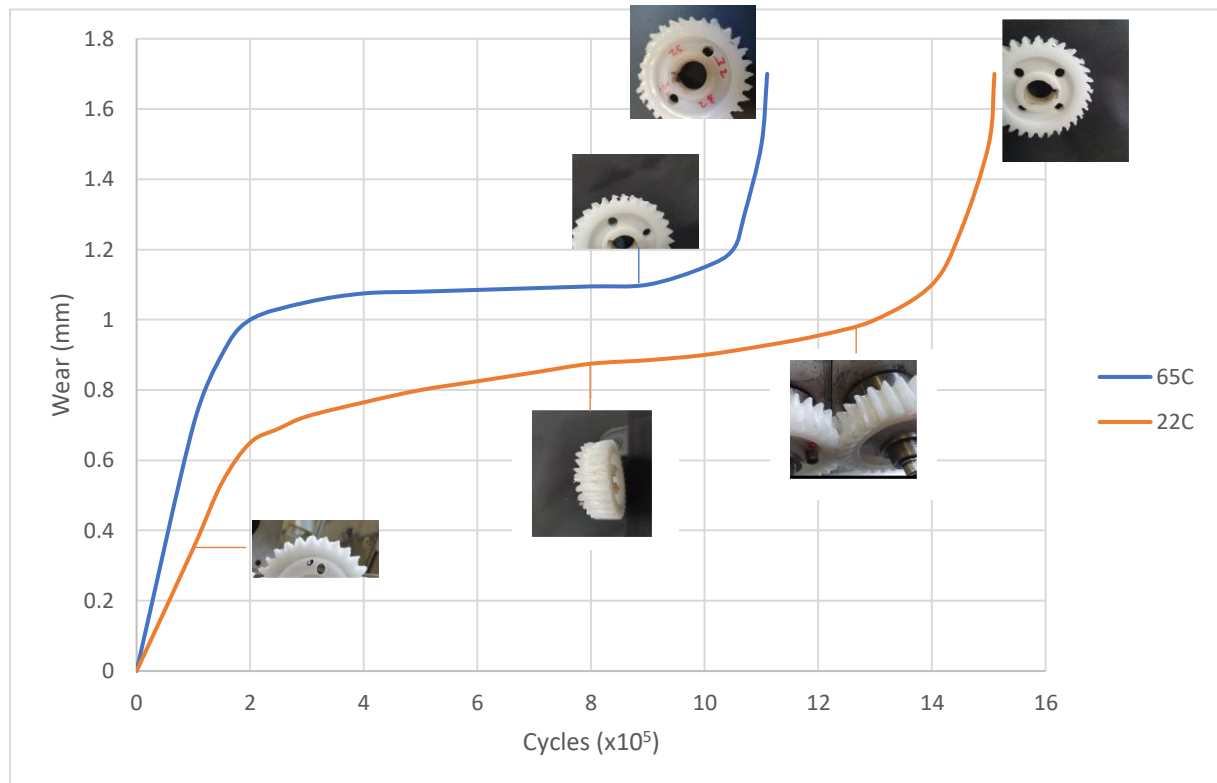
Fig 6.3 Wear progression for 65°C and 22°C produced gears at 4 Nm, 1000 rpm.

The running-in phase for the 65°C curve shows a gradient which is much steeper than the other groups. This is a phenomenon which was also observed by Apichartpattanasiri et al [64], whose work on injection moulded PA discs showed a much higher initial wear rate for higher mould temperatures, but which decreased with time. Unlike the other temperature groups, the 65°C curve has a steady wear phase. This implies that the rise in tooth surface temperature seen in the 22°C, 34°C, and 50°C groups is no longer a dominant contributor to morphological changes. It is believed that the higher crystallinity levels obtained through higher mould temperatures is responsible for this stability.

For the lower mould temperature groups, the thin film of material deposited on tooth flanks, and visible as flares, at 2 Nm and 3 Nm, were only noticeable during the initial running-in phase. Stopping

153

the test rig at 0.8 x 10^6 cycles and visually examining the gears showed molten material depositing below the pitch line. At failure, these deposits had filled the dedendum, effectively giving the impression that tooth wear had occurred at tooth root. The driving teeth flanks were bent backwards and those for the driven ones were pointing in the direction of rotation.

The 65°C mould temperature gears failed through the fracturing and detachment of teeth. Stopping the test rig at 0.9 x 10^6 cycles showed that rapid wear was initiated by the fracturing of a few teeth.

6.4 Debris formation

Examination of debris which collected below the running gears revealed important information regarding how material was removed from HDPE gears as wear occurred. An increase in cycles was accompanied by an increase in the amount of debris deposited.

The size and amount of the debris was dependent on two factors:

- The mould temperature group of the meshed gears
- The wear phase in which the gears were in

Gears produced at 65°C produced very fine debris compared to those produced at 22°C, but it was also observed that wear debris size tended to increase as the gears approached the final wear period, regardless of the production temperature. This phenomenon was also noted in the work done by Ghazali et al [93].

Most of the debris was deposited during the initial running-in phase and the final rapid wear phases.

6.5 Comparison of wear curves for 500 rpm and 1000 rpm

The wear curves presented in Fig 5.1 and Fig 5.9 show that rotational speeds have a greater effect on wear rates than step increment of torque between 0.5 Nm and 4 Nm. The cycles to failure for all temperature groups decrease as the speed is increased from 500 rpm to 1000 rpm. The cycles to failure for the 65°C, and 50°C mould temperature gears reduce by 31%, while those for 34°C reduce by 30%, and those for 22°C reduce by 33%.

The wear curves for 4 Nm presented in Fig 5.29 and Fig 5.39 show reductions in cycles to failure of 50% for 65°C mould temperature, 41% for 50°C, and 44% for both the 22°C and 34°C groups, as the rotational speed is increased from 500 rpm to 1000 rpm.

It is evident from these figures that increasing the rotational speed at higher torque loadings causes higher reductions in cycles to failure for all mould temperature groups.

5.6 Wear rate responses to varying mould temperatures and torque

The wear curves have shown that each mould temperature group has its own unique response to different torque loadings. Based on these unique responses, a Mould Temperature to Torque Reference Chart for HDPE as shown in Fig 6.4, is proposed.
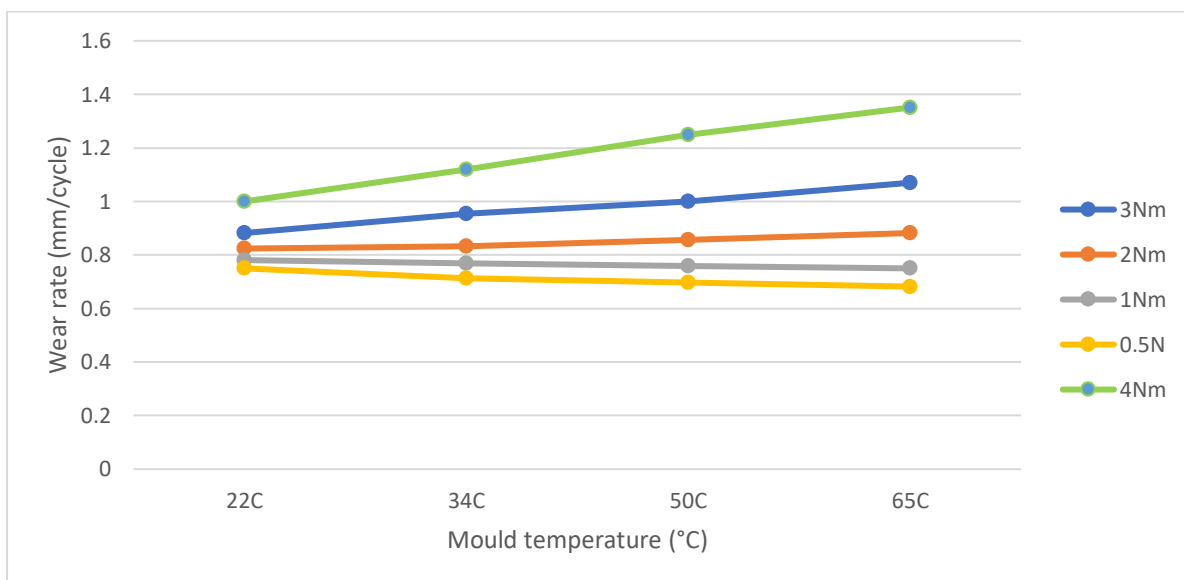
Fig 6.4 Mould Temperature to Torque Reference Chart for HDPE

From Fig 6.4, it can be seen that:

➢ At 0.5 Nm and 1 Nm, the wear rates decrease as mould temperature is increased

➢ At 2 Nm, 3 Nm, and 4 Nm, the wear rates increase with mould temperature

The rate of increase of wear rates increases at greater rates each time there is an increase in torque loading beyond 1 Nm.

This data shows that the selection of mould temperature should be based on the torque loadings which HDPE gears are to be subjected to. High mould temperatures are ideal for applications where low loads of below 1 Nm are applied, while low mould temperatures are ideal for applications where loads of 2 Nm to 4 Nm are experienced.

6.7 Summary

This chapter has discussed the effects which mould temperatures have on gear performance at different torque loadings. It has explained the mechanisms of failure for 0.5 Nm, 1 Nm, 2 Nm, 3 Nm, and 4 Nm, using results from wear curves, SEM analysis, and debris formations.

Each wear curve has shown a unique characteristic response to wear according to mould temperature, applied torque, and rotational speed. Based on these wear responses, a Mould Temperature to Torque reference Table for HDPE has been proposed.

SEM analysis has revealed that lower mould temperature gear teeth show distinct material flow which increases with applied torque, while higher mould temperature gears show wear as a result of material removal which is concentrated at the pitch line.

Debris formations have been shown to differ in texture, size and amount depending on the mould temperature employed during the injection moulding process, torque loading, and rotational speed.

Conclusions from these discussions are made in Chapter 7.

CHAPTER 7
CONCLUSIONS AND FUTURE WORK RECOMMENDATIONS

7.1 General conclusions

The wear behaviour of injection moulded HDPE gears produced at different mould temperatures has been extensively investigated using a uniquely designed test rig. Gears produced at the same mould temperature were meshed at different torque loadings and rotational speeds of 500 rpm and 1000 rpm, and their wear was continuously plotted against the number of cycles, until they failed. The resulting wear curves at different torque settings were compared for the different mould temperatures. It was observed that each mould temperature gear group resulted in different wear responses which were dependent on load and rotational speed. Based on these results, a Mould Temperature to Torque Reference Chart for HDPE was developed. This reference chart is of great importance to both gear manufacturers and those who match gear qualities with application use. The conclusions from the injection moulding process and the gear test rig results, are considered in the following sections.

7.2 Injection Moulding process

The gears were produced in-house using an Engel Victory 60T moulding machine. Melt temperature, injection volume, hold pressure, and hold time were identified from literature as having great influence on the quality of outputted products, and so were chosen for optimisation so that they did not become noise when the mould temperature was varied. Median values were chosen for all other input parameters. It was determined that injection volume had the least effect in shrinkage reduction of the gears within the high- and low-level settings. Slight deviation from the value range produced gears which were of low quality, with low injection volume produced gears showing deformities which were consistent with material deficiency, while high injection volume produced gears showing signs of flash.

Melt temperature showed only a slight improvement in shrinkage reduction compared to injection volume variations immediately after production. However, measurements which were taken 24 hours after production showed shrinkage of the gears had increased from 1.96% to 2.05%. This is a change of significance in applications where tight tolerances are critical. Melt temperature is usually the one input parameter which operators on the shop floor can easily change to improve viscosity and thereby physical appearance of products through the reduction of shear marks. The data gathered form this work shows a major drawback on such practices.

The hold pressure was the most effective input parameter in reducing shrinkage, provided the hold time was kept above the gate freeze time.

Shrinkage percentages of between 1.85% and 2.05% were recorded once optimised values were kept constant and mould temperature varied form a minimum of 22°C to a maximum of 65°C. These shrinkage rates compared well with the 1% to 4% shrinkage rates which the material manufacturers had listed. The changes in mass of the gears showed a 3% increase between the 22°C mould temperature produced gears, and those of the 65°C.

DSC analysis showed a change in the peak melting temperature from 136.1°C for the 22°C produced gears to 143°C for the 65°C produced gears. Exact crystallinity percentages were not calculated, but since the relationship between melting points and crystallinity for the same amorphous or semi-crystalline material is well proven, this upward shift in melting points of the gears, is an indication of increase in crystallinity. Of concern, however, was the discrepancy between the melt temperature shown by DSC of 140°C, compared to the stated manufacturer's range of between 180°C and 225°C. The Engel Victory 60T injection machine displayed melt temperatures which seemed to confirm the manufacturer's range of melt temperatures. These machine readings are what was used as reference temperatures for this research. This highlights the problem of manufacture self-certification without regulatory oversights by independent standardised rating standards.

7.3 Gear wear tests

Gear wear tests results have shown a clear link between mould temperature and performance. The data shows that the selection of mould temperature should be based on the torque loadings which the HDPE gears are to be subjected to. High mould temperatures are ideal for applications where low loads of below 1 Nm are to be experienced. Low mould temperatures are ideal for applications where loads of 2 Nm to 4 Nm are applied.

The failure mechanisms of HDPE gears are dependent on mould temperature, torque loading, and rotational speed. A doubling of rotational speed from 500 rpm to 1000 rpm resulted in a 30% reduction in the cycles to failure across all temperature groupings at low torque loadings. A 50% reduction was noticed at 4 Nm, indicating that the effects of increasing rotational speeds on wear increase as the torque is increased.

Wear is concentrated at the pitch line, regardless of any other fact examined. This is due to contact fatigue as identified by Hacman et al [90]. Lower mould temperature produced gears fail through tooth surface material flow. For the tested torque range, there were no tooth breakages observed for the 22°C, 34°C, and 50°C gears. The debris produced tended to be bigger in size, but less in amount. It also had a dull appearance.

Gears produced at 65°C mould temperature failed through tooth surface wear at lower torque loadings. The driving gear tooth flank tips were rounded, while those of the driven gear were more pointed. The debris produced had a very fine texture, and was shiny in appearance. At 3 Nm and 4 Nm, failure was through tooth fracture at the pitch line.

While the findings of this study agree with the work of Apichartpattanasiri et al [64], and Russel et al [51], who both carried out investigations into mould temperature effects on PA66, it seems to contradict the conclusions of Speke [52], whose work on amorphous polymers such as acrylonitrile butadiene styrene (ABS) and polycarbonate, found that higher mould temperatures produced better impact resistance and fatigue performance as a result of lower moulded-in stress. The most likely explanation to this apparent difference is the fact that Speke used high mould temperatures in combination with lower melt temperatures. The optimisation process during the injection moulding process of HDPE conducted in this study identified a high melt temperature in conjunction with a high mould temperature.

The higher cycles to failure at low torques shown by HDPE gears produced at higher mould temperatures indicate good wear resistance as a result of higher crystallisation rates. This performance advantage is lost at higher torques, where the higher mould-in stresses and brittleness identified by Speke come into play.

7.4 Recommendations for future work

The production of HDPE gears using injection moulding and the subsequent changes in performance has revealed some interesting new data and understanding of the link between manufacture and performance. This information is important as the focus on more energy efficient gearing increases in efforts to reduce the carbon footprint. However, there's still a lot more work to be done to gain an even greater depth of understanding. This requires time, finance, and more focus.

7.4.1 Injection moulding process

As has be identified by the reviewed literature there are over 200 input parameters in injection moulding which researchers have identified as having an influence on the final product. It is important that more factors are investigated to determine how each, and every input factor affects performance of polymer gears.

Diverse polymetric material analysis is an important area which needs further investigation. Unfilled polymers have a response to shrinkage and other microstructural changes which are different from those of reinforced polymers.

7.4.2 Gear testing and analysis

More in-depth DSC analysis needs to be carried out on the effects of mould temperatures and other input parameters. Time limitations have led to limited crystallinity analysis being done on samples.

Gear temperature changes need to be monitored during testing. This is important as it will give better understanding of temperature variations during the different wear phases.

REFERENCES

1. Lewis, M.J.T. (1993). *Gearing in the ancient world*. Endeavour, 17(3), pp.110–115. doi:10.1016/0160-9327(93)90099-o.

2. Derek, J. de S.P. (2010). *On the Origin of Clockwork, Perpetual Motion Devices, and the Compass.* 2nd ed. FQ Books

3. Radzevich, S.P. A Brief Overview on the Evolution of the Scientific Theory of Gearing: A Preliminary Discussion. *Proceedings of International Conference on Gears 2015*, October 5–7, Technische Universität München (TUM), Garching (near Munich), Germany, pp.1035-1046.

4. Lewis, W. (1910). Interchangeable Involute Gearing. *Proceedings of the Institution of Mechanical Engineers*. 79(1):1039-1066. doi:10.1243/PIME_PROC_1910_079_018_02

5. Savaria, V., Bridier, F. and Bocher, P. (n.d.). Predicting the effects of material properties gradient and residual stresses on the bending fatigue strength of induction hardened aeronautical gears. *International Journal of Fatigue*, 85, pp.70–85.

6. Senthilvelan, S. and Gnanamoorthy, R. (n.d.). *Effect of rotational speed on the performance of unreinforced and glass fiber reinforced Nylon 6 spur gears*. 3rd ed. [online] Materials & Design, pp.765–772. Available at: https://www.sciencedirect.com/science/article/pii/S0261306905003651 [Accessed: Jan 2022].

7. Materials for engineering. (n.d.). *polymer-find-use-in-engine-transmissions*. [online] Available at: www.materialsforengineeering.co.uk [Accessed 15 Jun. 2019].

8. Dengel, B. (2017). Plastic Gears Are The Future. [online] Machine Design. Available at: https://www.machinedesign.com/materials/article/21836156/plastic-gears-are-the-future [Accessed 8 Oct. 2019].

9. ASMT Compass. (2019). *Standard Classification System for Nylon Injection and Extrusion Materials (PA).* [online] Available at: https://www.astm.org/d4066-13r19.html [Accessed 1 Mar. 2020].

10. Mao, K., Langlois, P., Madhav, N., Greenwood, D. and Millson, M. (2019). A Comparative Study of Polymer Gears Made of Five Materials. In: *Lyon International Gear Conference 2018*. https://www.smartmt.com/wp-content/uploads/polymer-gears.pdf: Gear Technology.

11. Ashby, M.F. and Brechet, Y.J.M. (2003). Designing hybrid materials. *Elsevier,* [online] 51(19), pp.5801–5821. doi:https://doi.org/10.1016/S1359-6454(03)00441-5.

12. Singh, A.K., Singh, P.K. Polymer spur gears behaviors under different loading conditions: A review. *Proceedings of the Institution of Mechanical Engineers, Part J: Journal of Engineering Tribology*. 2018;232(2):210-228. doi:10.1177/1350650117711595

13. Bhandari, V.B. (2017). *Design of machine elements*. New Delhi: Mcgraw-Hill Education (India).

14. Khurmi, R.S. and Gupta, J.K. (2000). *Textbook of machine design for the students of UPSC (Engineering Services), etc. (in SI Units).* New Delhi: Eurasia.

15. Walton, D., Goodwin, A.J. *The wear of unlubricated metallic spur gears*. Wear 1998;222:103–13. doi: https://doi.org/10.1016/S0043-1648(98)00291-9.

16. Mao, K. (1993). *The performance of dry running non-metallic gears*. Doctoral dissertation, The University of Birmingham.

17. Adam, C.E. (1986). *Plastic gearing: Selection and application*. New York, Marcel Dekker, pp87

18. Mobley, R.K. (2001). *Plant Engineer's Handbook*. Elsevier

19. Kalawec, A. (2006). Comparative Analysis of Tooth-Root Strength Using ISO and AGMA Standards in Spur and Helical Gears With FEM-based Verification. *Journal of Mechanical Design*, 128(5), pp.1141–1158. doi:https://doi.org/10.1115/1.2214735.

20. Lewis, W. (1910). Interchangeable Involute Gearing. *Proceedings of the Institution of Mechanical Engineers*. 79(1):1039-1066. doi:10.1243/PIME_PROC_1910_079_018_02

21. Wright, N.A. and Kukureka, S.N. (2001). Wear testing and measurement techniques for polymer composite gears. *Wear*, [online] 251(1 - 12), pp.1567–1578. doi:https://doi.org/10.1016/S0043-1648(01)00793-1 ISSN 0043-1648.

22. Hertz, H., Jones, D.E., Schoth, G.A. (1896). *On the contact of elastic solids*. Macmillan.

23. Gupta, B., Choubey, A., Varde, G. (2012). Contact stress analysis of spur gears. *International Journal of Engineering Research and Technology*, Vol1, Issue 4.

24. Zhang, Y. and Finger, S. (2010). *Rapid Design through Virtual and Physical Prototyping*. [online] Available at:
https://www.cs.cmu.edu/~rapidproto/mechanisms/chpt7.html#HDR108A.

25. Ham, C. W., Crank E. J. and Rogers W. L. (1958). Mechanics of Machinery, McGraw-Hill.

26. Gowariker, V.R., Viswanathan, N.V., Sreedhar J. (1986). *Polymer Science*. Wiley, ISBN: 0470203226

27. Masuelli, M. A. (2013). Introduction of Fibre-Reinforced Polymers – Polymers and Composites: Concepts, Properties and Processes. In: *Fiber Reinforced Polymers - The Technology Applied for Concrete Repair*, IntechOpen, London. 10.5772/54629.

28. Crawford, R.J. (1998). *Plastics engineering*. 3rd ed. Jordan Hill, Oxford :butter worth heineman.

29. Callister, W. D. (2005). *Fundamentals of materials science and engineering: an integrated approach*. 2nd edition, John Wiley and Sons, ISBN: 0471470147 (hbk.).

30. Zhang, Z. and Friedrich, K. (2005). Effects of various fillers on the sliding wear of polymer composites, Composites Science and Technology. *ScienceDirect*, [online] 65(15 - 16), pp.2329–2343. doi:https://doi.org/10.1016/j.compscitech.2005.05.028 ISSN 0266-3538.

31. SABIC. (2016). *A guide to plastic gearing*. [online] Available at: https://www.sabic.com/assets/zh/Images/A%20Guide%20to%20Plastic%20Gearing%20-%20EN_tcm11-5340.pdf [Accessed 15 Jan. 2019].

32. Ku, H., Wang, H., Pattarachaiyakoop, N., Trada M. *A review on the tensile properties of natural fibre reinforced polymer composites*. Centre of Excellence in Engineering Fibre Composites and Faculty of Engineering, University of Southern Queensland.

33. Senthilvelan, Selvaraj & Gnanamoorthy, R. (2004). Damage Mechanisms in Injection Molded Unreinforced, Glass and Carbon Reinforced Nylon 66 Spur Gears. *Applied Composite Materials.* 11. 377-397. 10.1023/B:ACMA.0000045313.47841.4e.

34. Pogačnik, A. and Tavčar, J. (2015). An accelerated multilevel test and design procedure for polymer gears. *ScienceDirect*, [online] 65, pp.961–973. doi:https://doi.org/10.1016/j.matdes.2014.10.016, [Accessed 15 Jan. 2019]

35. Mohsenzadeh, R., Majidi, H., Soltanzadeh, M., Shelesh-Nezhad, K. (2019). Wear and failure of polyoxymethylene/calcium carbonate nanocomposite gears. *Proc Inst Mech Eng, Part J J Eng Tribol*, 811–20. https://doi.org/10.1177/1350650119867530.

36. Mao, K., Greenwood, D., Ramakrishnan, R., Goodship, V., Shrouti, C., Chetwynd, D., Langlois, P. (2019). The wear resistance improvement of fibre reinforced polymer composite gears. *Wear*, Volumes 426–427, Part B, Pages 1033-1039, https://doi.org/10.1016/j.wear.2018.12.043 [Accessed 2 Feb. 2020].

37. Nunna, S., Chandra, P.R., Shrivastava, S. and Jalan, A.K. (2014). A review on mechanical behavior of natural fiber based hybrid composites. *Journal of Reinforced Plastics and Composites*, [online] 31(11), pp759 – 769, doi:https://doi.org/10.1177/0731684412444325 [Accessed 2 Feb. 2019].

38. Joseph, P.V. (2002). Environmental effects on the degradation behaviour of sisal fibre reinforced polypropylene composites. *ScienceDirect*, [online] 62(10 -11), pp.1357–1372. doi:https://doi.org/10.1016/S0266-3538(02)00080-5.

39. Khoathane, M.C., Vorster, O.C., Sadiku, E.R. (2008). Hemp Fiber-Reinforced 1-Pentene/Polypropylene Copolymer: The Effect of Fiber Loading on the Mechanical and

Thermal Characteristics of the Composites. *Journal of Reinforced Plastics and Composites*. 27(14):1533-1544. doi:10.1177/0731684407086325

40. Sun, Z.Y., Han, H.S., Dai, G.C. (2010). Mechanical Properties of Injection-molded Natural Fiber-reinforced Polypropylene Composites: Formulation and Compounding Processes. *Journal of Reinforced Plastics and Composites*. 29(5):637-650. doi:10.1177/0731684408100264

41. Nishino, T., Hirao, K., Kotera, M., Nakamae, K., Inagaki, H. (2003). Kenaf reinforced biodegradable composite. *Compos Sci Technol*, 63, pp. 1281-1286

42. Krishnaprasad, R., Veena, N.R., Maria, H.J. et al. (2009). Mechanical and Thermal Properties of Bamboo Microfibril Reinforced Polyhydroxybutyrate Biocomposites. *J Polym Environ 17*, 109. https://doi.org/10.1007/s10924-009-0127-x

43. Han, G., Lei, Y., Wu, Q., Kojima, Y., Suzuki, S. (2008) Bamboo-fiber filled high density polyethylene composites: effect of coupling treatment and nanoclay. *J Polym Environ 16*, pp. 123-130

44. Espert, A., Vilaplana, F., Karlsson, S. (2004). Comparison of water absorption in natural cellulosic fibres from wood and one-year crops in polypropylene composites and its influence on their mechanical properties. Compos Part A: *Appl Sci Manuf*, 35: 1267–1276.

45. Adekunle, K., Cho, S.W., Patzelt, C., Blomfeldt, T., Skrifvars, M. (2011). Impact and flexural properties of flax fabrics and Lyocell fiber-reinforced bio-based thermoset. *Journal of Reinforced Plastics and Composites*, 30, pp. 685-697

46. Alawar, A., Hamed, A.M. and Al-Kaabi, K. (2009). Characterization of treated date palm tree fiber as composite reinforcement. *ScienceDirect*, [online] 40(7), pp.601–606. doi:https://doi.org/10.1016/j.compositesb.2009.04.018.

47. Saba, N., Paridah, M.T., Jawaid, M. (2015). Mechanical properties of kenaf fibre reinforced polymer composite: A review. *Construction and Building Materials*, Volume 76, Pages 87-96, ISSN 0950-0618, https://doi.org/10.1016/j.conbuildmat.2014.11.043.

48. Callister, W. D. (2000). *Materials science and engineering: an introduction*. 5th edition, Wiley, ISBN: 0471150223 (hbk.)

49. Fei, N.C., Mehat, N.M. and Kamaruddin, S. (2013). Practical Applications of Taguchi Method for Optimization of Processing Parameters for Plastic Injection Moulding: A Retrospective Review. *International Scholarly Research Notices*, 2013. doi:https://doi.org/10.1155/2013/462174 Article ID 462174.

50. Agrawal, A.R., Pandelidis, I.O., Pecht, M. (1982). *Injection Molding Process Control – A Review.* Department of Mechanical Engineering, University of Maryland, SRC TR 86-28

51. Russel, D.P., Beaumont, P.W.R. (1980). Structure and properties of injection-moulded nylon 6. Part 1. Structure and morphology of nylon 6. *Journal of Material Science 15*, pp197-207

52. Speke, M. (2011). *The importance of Melt and Mold Temperature*. [online] Plastics Technology. Available at: https://www.ptonline.com [Accessed 17 Feb. 2019].

53. O'Connor, P. (2001). *Test Engineering: A Concise Guide to Cost-Effective Design, Development and Manufacture (Quality and Reliability Engineering Series*). USA: John Wiley & Sons Inc.

54. Polymer Training & Innovation Centre. (2018). Injection Moulding Appreciation Manual. *City of Wolverhampton College.*

55. Bryce, D.M. (1997). *Plastic Injection Molding: Material Selection and Product Design Fundamentals*. Fundamental of Injection Molding ed. Society Manufacturing Engineers.

56. Ishikawa, K. (1968). *Guide to Quality Control*. Tokyo: JUSE.

57. Thiriez, A., Gutowski, T. (2006). An environmental analysis of injection molding. *In Proceedings of the 2006 IEEE International Symposium on Electronics and the Environment*. pp. 195-200, IEEE.

58. Kelly, A.L., Woodhead, M., Coates, P.D. (2001). Comparison of injection moulding machine performance. *SPE Annual Technical Conference (ANTEC),* Paper #238

59. Insights. (2020). *Robotics in Injection Moulding*. [online] Available at: https://www.rnaautomation.com/insight/robotics-in-injection-moulding/ [Accessed 24 Jan. 2021].

60. Bozdana, A.T., Eyercilu. (2002). Development of an expert system for the determination of injection moulding parameters of thermoplastic materials: EX-PIMM. *Journal of Materials Processing Technology*, vol. 128, no. 1–3, pp. 113–122.

61. Chang, T.C., Faison, E. (2001). Shrinkage behavior and optimization of injection molded parts studied by the Taguchi method. *Polymer Engineering and Science*, vol. 41, no. 5, pp. 703–710.

62. Bozzelli, J. (2016). *Unraveling the Mysteries of Melt Temperature.* [online] Plastic Technology. Available at: https://www.ptonline.com/articles/unraveling-the-mysteries-of-melt-temperature [Accessed 1 Mar. 2019].

63. Cartledge, H.C.Y., Braillie, C.A. (1999). Studies of microstructural and mechanical properties of   nylon/glass composite: Part 1. The effect of thermal processing on crystallinity, transcrystallinity and crystal phases. *Journal of Material Science*. Vol 34, Issue 2, Pg5099-5111

64. Apichartpattanasiri, S., Hay, N., Kukureka, S.N. (2001). A study of the tribological behaviour of polymide 66 with varying injection-moulding parameters. Vol 251, Issue 1-12, pg 1557-1566, School of Metallurgy & Materials, *The University of Birmingham*

65. Woodward, A. E. (1995). *Understanding Polymer Morphology*. Hanser Publishers, Munich.

66. Dominick, V., Rosato, Donald, V. and MarIene, G. (2000). *Injection molding handbook*. 3rd ed. New York: Springer Science+Business Media.

67. Zhuang, Z., Li, Y., Qi, D., Zhao, C., Na, H. (2017). Novel polymeric humidity sensors based on sulfonated poly (ether ether ketone)s: Influence of sulfonation degree on sensing properties. *Sensors and Actuators B*: Chemical, 10.1016/j.snb.2016.09.179, 242, (801-809).

68. Johannaber, F. (1983). *Injection molding machines: a user's guide*. John Waley & Sons.

69. Bright, P. F., Crowson, R. J., Folkes, M. J. (1978). A study of the effect of injection speed on fibre orientation in simple mouldings of short glass fibre-filled polypropylene. [online] *Journal of Materials Science,* vol. 13, pp. 2497-2498, [Accessed 02 Feb 2019].

70. Pötsch, G., Michaeli, W. (1995). Injection molding: an introduction. Hanser Pub Inc.

71. Pontes A. J, Neves N. M, Velosa J. C, Faria A. R, Pouzada A.S. Glass fibre contents of PP plates and their properties: Part I: Shrinkage and changes in time. [online]*, Key Engineering Materials*, vol. 230-232, pp. 52-55, [Accessed 5 Feb 2019].

72. Pye, A. (2018). *Injection Moulding: The role of backpressure*. [online] Available at: www.knowledge.ulprospector.com [Accessed 15 Jan. 2020].

73. Nunn, R., E (1975). *SCREW PLASTICATING IN THE INJECTION MOULDING OF THERMOPLASTICS*. [Thesis] Available at: https://spiral.imperial.ac.uk/bitstream/10044/1/21104/2/Nunn-RE-1975-PhD-Thesis.pdf.

74. Agrawal, A.R. (1987). Injection-molding process control—A review. *Polymer Engineering and Science*, [online] 27(18), pp.1345–1357. Available at: https://4spepublications.onlinelibrary.wiley.com/doi/abs/10.1002/pen.760271802 [Accessed Jun. 2019].

75. Polymerdatabase. (2019). *Stress-Strain Behaviour of Polymers*. [online] Available at: https://polymerdatabase.com/polymer%20physics/Stress-Strain%20Behavior.html [Accessed Jul. 2020].

76. Standard B, ISO B. Calculation of load capacity of spur and helical gears—. ISO 2006;6336:1996.

77. Walton, D., Shi, Y.W. (1989). A comparison of Ratings for Plastic Gears. Proceedings of the Institution of Mechanical Engineers, Part C, *Journal of Mechanical Engineering Science*

78. Karimpour, M., Dearn, K.D. and Walton, D. (2010). A kinematic analysis of meshing polymer gear teeth. *Journal of Materials: Design and Application*, [online] 224(3). Available at: https://journals.sagepub.com/doi/10.1243/14644207JMDA315 [Accessed Jun. 2020].

79. Breeds, A.R., Kukureka, S.N., Mao, K., Walton, D. and Hooke, C.J. (1993). Wear behaviour of acetal gear pairs. *Wear*, 166(1), pp.85–91. doi:https://doi.org/10.1016/0043-1648(93)90282-Q.

80. Hackmann H, Strickle E. Polyamides as gear materials. Konstruktion, 18(3), 1966

81. Walton, D., Hooke, C.J. and Mao, K. (1992). A new look at testing and rating non-metallic gears. *3rd World Congress on Gearing and Power Transmissions*, Paris.

82. Mao, K., Li, W., Hooke, C.J. and Walton, D. (n.d.). Friction and wear behaviour of acetal and nylon gears. *Wear*, 267(1 - 4), pp.639–645. doi:https://doi.org/10.1016/j.wear.2008.10.005.

83. Zhang, Z. (2003). Artificial neural networks applied to polymer composites. *Composite Science and Technology*, Vol 63, Issue 14

84. Mckeen, L. (2021). *The effects of Long Term thermal Exposure on Plastics and Elastomers*. 2nd Edition, William Andrew Publishing, p35-64

85. Gouno, E. (2007). Optimum step-stress for temperature accelerated life testing. *Quality and Reliability Engineering International,* 23 (8), pp. 915-924

86. Charki, A. (2011). Robustness evaluation using highly accelerated life testing. *International Journal of Advanced Manufacturing Technology*, 56 (9–12), pp. 1253-1261

87. Gouno, E. (2007). Optimum step-stress for temperature accelerated life testing. *Quality and Reliability Engineering International.* 23(8), pp.915-924.

88. Kurokawa, M., Uchiyama, Y., Iwai, T., Nagai, S. (2003). Performance of plastic gear made of carbon fiber reinforced polyamide 12. *Wear*, Volume 254, Issues 5–6, Pages 468-473.

89. Vaziri, M., Spurr, R.T., and Stott, F.H. (1988). Investigation of the wear of Polymeric Materials. *Wear* 122.

90. Hacman, H. and Strickle, E. (1968). Design of nylon gears. *SPE Annual Technology Conference*, Vol 26.

91. Terashima, K., Tsukamoto, N., Nishida, N. and Shi, J. (1986). Development of Plastic Gear for Power Transmission : Abnormal Wear on the Tooth Root and Tooth Fracture near Pitch Point. *The Japan Society of Mechanical Engineers*, 29(251), pp249-255. doi:https://doi.org/10.1299/jsme1958.29.1598.

92. Marshek, K.M., Chan, P.K.C. (1977). Wear damage to plastic worms and gears. *Wear,* 44: 405–409.

93. Ghazali, M.J., Rainforth, W.M., Jones H. (2005). Dry sliding wear behaviour of some wrought, rapidly solidified powder metallurgy aluminium alloys. *Wear* 259, pp490–500.

94. Bellow, D.G. and Viswanath, N.S. (1993). An analysis of the wear of polymers. *Wear*, 162 - 164, pp.1048–1053. doi:https://doi.org/10.1016/0043-1648(93)90121-2.

95. Hooke, C.J et al. (1993). Measurement and prediction of the surface temperature in polymer gears and its relationship to gear wear. *Journal of Tribology*, ASME 115 p119-124

96. Friedrich, K. (1986). Friction and Wear of Polymer Composites. *Elsevier Scientific Publisher*, Amsterdam.

97. Wood, A.K et al. (2010). The Relative Performance of Spur Gears Manufactured from Steel and PEEK. *International Conference on Gears*, Technical University of Munich.

98. Takahashi, M., Itagaki, T., Takahashi, H., Koide, T. (2014). Lifetime and meshing teeth temperature of plastic crossed helical gear: case of grease lubrication. *International Gear Conference 2014*: 26th–28th August 2014, Lyon, Chandos Publishing, pp148-157, https://doi.org/10.1533/9781782421955.148.

99. Duhovnik, J. (2016). *The effect of the teeth profile shape on polymer gear pair properties*. Published paper, Faculty of Mechanical Engineering, University of Ljubljana.

100. Rhee, S.K. (1970). *Wear Equations for polymers sliding against metal surfaces.* The Bendix Corp Research laboratories, Southfield, Mich.

101. Hoskins, T.J., Dearn, K.D., Chen, Y.K. and Kukureka, S.N. (2014). The wear of PEEK in rolling–sliding contact – Simulation of polymer gear applications. *Wear*, 309(1-2), pp.32–42. doi:https://doi.org/10.1016/j.wear.2013.09.014.

102. Melick, H. (2007). Tooth-Bending Effects in Plastic Spur Gears. *Gear Technology*. [online] Available at: https://www.geartechnology.com/ext/resources/issues/0907x/plastic.pdf [Accessed 24 Jun. 2019].

103. Donald, G., Bellow, N.S. (1993). *An analysis of the wear of polymers*. University of Alberta, Department of Mechanical Engineering, Edmonton.

104. Kalin, M et al. (2017). The dominant effect of temperature on the fatigue behaviour of polymer gears. *Elsevie*r, Vol 376-374, Laboratory for Tribology and Interface Nanotechnology, Faculty of Mechanical Engineering, University of Ljubljana.

105. Mao, K. (2007). *A numerical method for polymer Composite gear flash temperature prediction*. Mechanical Engineering, School of Engineering and Design, Brunel University.

106. Hooke, C.J., Mao, K., Walton, D., Breeds, A.R., Kukureka, S.N. (1993). Measurement and prediction of the surface temperature in polymer gears and its relationship to gear wear. *Journal of Tribology ASME*, 115(1), p119-124. https://doi.org/10.1115/1.2920964.

107. Nakamae, K., Nishino, T., Shimizu, Y. and Hata, K. (1990). Temperature dependence of the elastic modulus of crystalline regions of polyoxymethylene. *ScienceDirect*, 31(10), pp.1909–1918. doi:https://doi.org/10.1016/0032-3861(90)90016-R.

108. Jabbour, T., Asmar, G., Abdulwahab, M., Nasr, J. (2021). Real contact ratio and tooth bending stress calculation for plastic/plastic and plastic/steel spur gears, *Mechanics & Industry*, 22(30), https://doi.org/10.1051/meca/2021029.

109. Imrek, H. (2009). Performance improvement method for Nylon 6 spur gears. *Tribology International*, [online] 42(3), pp.503–510. Available at: https://www.sciencedirect.com/science/article/pii/S0301679X08001941 [Accessed 12 Mar. 2020].

110. Düzcükoğlu, H. (2009). PA 66 spur gear durability improvement with tooth width modification. *Material and Design*, 30(4), pp.1060–1067. doi:https://doi.org/10.1016/j.matdes.2008.06.037.

111. Koffi, D., Bravo, A., Toubal, L. (2016). Optimized use of cooling holes to decrease the amount of thermal damage on a plastic gear tooth. *Advances in Mechanical Engineering*, https://doi.org/10.1177/1687814016638824

112. Bringas, J.E. (2004). *Handbook of Comparative World Steel Standards*: 5th Edition, ASTM International.

113. Engel Technical manual. [online], http://files.globalprecision.co.uk/Templates%20&%20Docs/Machine%20Specs/90T%20Engel/Engel%2090T%20Manual/EN-OM_machine_V1.12_CC200.PDF

114. Goldsberry, C. (2018). *Scientific tests prove HDPE can be recycled at least 10 times.* [online] Plastics today. Available at: https://www.plasticstoday.com/packaging/scientific-tests-prove-hdpe-can-be-recycled-least-10-times [Accessed 12 Dec. 2019].

115. Product Catalogue: (2018). *High Density Polyethylene*. [online] Molgroup Chemicals. Available at: https://www.molgroupchemicals.com/userfiles/catalog/2018april/MOL_Termkkatal-gus_HDPE_2018_EN_96_dpi.pdf [Accessed 15 Jan. 2019].

116. Box, Joan Fisher. (1980). R. A. Fisher and the Design of Experiments, 1922-1926. *The American Statistician*, vol. 34, no. 1, pp. 1–7. JSTOR, https://doi.org/10.2307/2682986. Accessed 24 Jan. 2020.

117. Rao, R.S., Kumar, C.G., Prakasham, R.S., Hobbs, P.J. (2008). The Taguchi methodology as a statistical tool for biotechnological applications: a critical appraisal. *Biotechnology Journal*, vol. 3, no. 4, pp510–523.

118. Mehat, N.M., Kamaruddin, S. (2011). Investigating the effects of injection molding parameters on the mechanical properties of recycled plastic parts using the Taguchi method. *Materials and Manufacturing Processes*, vol. 26(2), pp202–209.

119. Bharti, P.K., Khan, M.I., Singh, H. (2011). Six sigma approach for quality management in plastic injection molding process: a case study and review. *International Journal of Applied Engineering Research*, vol. 6(3), pp303–314.

120. Jansen, K.M.B., Van Dijk, D.J. and Husselman, M.H. (2004). Effect of processing conditions on shrinkage in injection molding. *Polymer Engineering and Science*, 38(5), pp.838–846. doi:https://doi.org/10.1002/pen.10249.

121. Wagner, M. (2009). *Thermal Analysis in Practice*. Mettler Toledo.

122. Mettler Toledo. (2009). *Thermal Analysis in Practice: Collected Applications*. www.mt.com

123. Croppe, A.B. (2003). *The failure mode analysis of plastic gears*. PhD thesis, University of Birmingham.

124. Mao, K., Chetwynd, D.G. and Millson, M. (2020). A new method for testing polymer gear wear rate and performance. *Polymer Testing*, 82. doi:https://doi.org/10.1016/j.polymertesting.2019.106323.

125. Zedong, H. (2017). *Wear and Thermal-mechanical Performance of Polyacetal Gears*. Theses, University of Warwick.

126. Alharbi. (2018). *Mechanical contact behaviour*. Theses, University of Warwick.

127. BS 6168. (1987). *Specification for non-metallic spur gears*. British Standards Institution, London.

128. Bain, M.F., Janicki, S.L., Ulmer, A.S., Thomas, L.S. (1992). Mold shrinkage: Not a single data point. *Proceedings of 50th annual meeting of the Society of Plastics Engineers*, Detroit.

129. Wang, K.K. and Han, S. (2013). Shrinkage Prediction for Slowly-Crystallizing Thermoplastic Polymers in Injection Molding. *International Polymer Processing*. doi:https://doi.org/10.3139/217.970228.

130. Mamat, A., Trochu. F., Sanschagrin, B. (1995). Shrinkage analysis of injection polypropylene parts. *Polymer Engineering Science*, vol. 35(19), pp1511-1520.

131. Ronkay, F., Molnar, B., Nagy, D et al. (202). Melting temperature versus crystallinity: new way for identification and analysis of multiple endotherms of poly(ethylene terephthalate). *Journal of Polymer Research*, vol 27(372).

132. Kono, S. (2002). *Increase in power density of plastic gears for automotive applications.* PhD Thesis, University of Birmingham.

133. Merah, N., Saghir, F., Khan, Z., Bazoune, A. (2006). Effect of temperature on tensile properties of HDPE pipe material. *Plastics, Rubber and Composites,* 35:5, 226-230, DOI:10.1179/174328906X103178